

CORRECTED VERSION

(19) World Intellectual Property Organization  
International Bureau  
(43) International Publication Date  
16 January 2020 (16.01.2020)



(10) International Publication Number  
WO 2020/013902 A9

- (51) International Patent Classification: G06F 3/041 (2006.01)
- (21) International Application Number: PCT/US2019/029079
- (22) International Filing Date: 25 April 2019 (25.04.2019)
- (25) Filing Language: English
- (26) Publication Language: English
- (30) Priority Data: 62/662,349 25 April 2018 (25.04.2018) US
- (71) Applicant: THE REGENTS OF THE UNIVERSITY OF CALIFORNIA [US/US]; 1111 Franklin Street, Twelfth Floor, Oakland, California 94607-5200 (US).
- (72) Inventors: PEI, Qibing; UCLA Materials Science and Engineering Dept., 410 Westwood Plaza., Los Angeles, California 90095-1595 (US). QIU, Yu; 3290 Sawtelle Blvd., Apt. 207, Los Angeles, California 90066 (US).
- (74) Agent: SERAPIGLIA, Gerard B.; GATES & COOPER LLP, 6060 Center Drive, Suite 830, Los Angeles, California 90045 (US).
- (81) Designated States (unless otherwise indicated, for every kind of national protection available): AE, AG, AL, AM, AO, AT, AU, AZ, BA, BB, BG, BH, BN, BR, BW, BY, BZ, CA, CH, CL, CN, CO, CR, CU, CZ, DE, DJ, DK, DM, DO,

(54) Title: REFRESHABLE TACTILE DISPLAY USING BISTABLE ELECTROACTIVE POLYMER AND DEFORMABLE SERPENTINE ELECTRODE

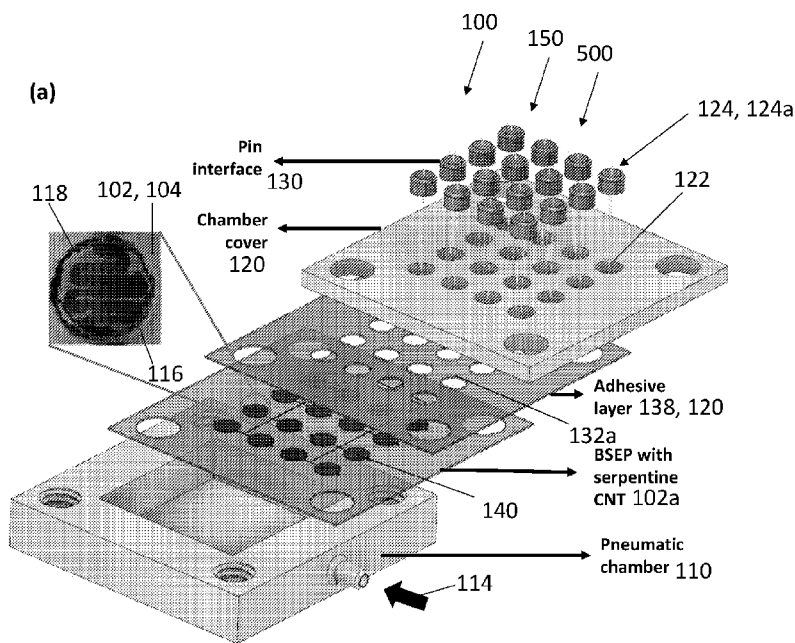


FIG. 1A

(57) Abstract: A refreshable tactile display using a bistable electroactive polymer with a stretchable serpentine Joule heating electrode. A portable refreshable tactile display with Braille standard resolution has been demonstrated. The steep modulus change of BSEP over a narrow temperature range achieves a device with high blocking force of over 50g and large displacement of 0.7mm. A "P3R" fabrication process of Prestretch-Pattern-Protect-Release is effective to form a S-CNT electrode in the wrinkled surface layer with high compliancy and resistance-consistence up to 188% area strain. The electrode can soften the BSEP film at 30 V in less than 1 s. The simple architecture of the tactile display ensures an easy and low-cost fabrication. The demonstrated refreshable tactile display should find a wide range of applications in recreation, entertainment, robotics, health care, and so on.

WO 2020/013902 A9

DZ, EC, EE, EG, ES, FI, GB, GD, GE, GH, GM, GT, HN, HR, HU, ID, IL, IN, IR, IS, JO, JP, KE, KG, KH, KN, KP, KR, KW, KZ, LA, LC, LK, LR, LS, LU, LY, MA, MD, ME, MG, MK, MN, MW, MX, MY, MZ, NA, NG, NI, NO, NZ, OM, PA, PE, PG, PH, PL, PT, QA, RO, RS, RU, RW, SA, SC, SD, SE, SG, SK, SL, SM, ST, SV, SY, TH, TJ, TM, TN, TR, TT, TZ, UA, UG, US, UZ, VC, VN, ZA, ZM, ZW.

**(84) Designated States** (*unless otherwise indicated, for every kind of regional protection available*): ARIPO (BW, GH, GM, KE, LR, LS, MW, MZ, NA, RW, SD, SL, ST, SZ, TZ, UG, ZM, ZW), Eurasian (AM, AZ, BY, KG, KZ, RU, TJ, TM), European (AL, AT, BE, BG, CH, CY, CZ, DE, DK, EE, ES, FI, FR, GB, GR, HR, HU, IE, IS, IT, LT, LU, LV, MC, MK, MT, NL, NO, PL, PT, RO, RS, SE, SI, SK, SM, TR), OAPI (BF, BJ, CF, CG, CI, CM, GA, GN, GQ, GW, KM, ML, MR, NE, SN, TD, TG).

**Declarations under Rule 4.17:**

— *of inventorship (Rule 4.17(iv))*

**Published:**

- *without international search report and to be republished upon receipt of that report (Rule 48.2(g))*
- *with information concerning authorization of rectification of an obvious mistake under Rule 91.3 (b) (Rule 48.2(i))*

**(48) Date of publication of this corrected version:**

13 February 2020 (13.02.2020)

**(15) Information about Correction:**

see Notice of 13 February 2020 (13.02.2020)

REFRESHABLE TACTILE DISPLAY USING BISTABLE  
ELECTROACTIVE POLYMER AND DEFORMABLE SERPENTINE  
ELECTRODE

CROSS REFERENCE TO RELATED APPLICATIONS

This application claims the benefit under 35 U.S.C. Section 119(e) of co-pending and commonly-assigned U.S. Provisional Patent Application Serial No 62/662,349 filed on April 25, 2018, by Qibing Pei and Yu Qiu entitled “REFRESHABLE TACTILE DISPLAY USING BISTABLE ELECTROACTIVE POLYMER AND DEFORMABLE SERPENTINE ELECTRODE”, (2018-449-1); which application is incorporated by reference herein.

STATEMENT REGARDING

FEDERALLY SPONSORED RESEARCH AND DEVELOPMENT

This invention was made with government support under Grant Numbers 1638163 and 1700829, awarded by the National Science Foundation. The Government has certain rights in the invention.

TECHNICAL FIELD

The present invention relates to tactile displays and methods of fabricating the same.

BACKGROUND OF THE INVENTION

(Note: This application references a number of different publications as indicated throughout the specification by one or more reference numbers in brackets, e.g., [x]. A list of these different publications ordered according to these reference numbers can be

found below in the section entitled “References.” Each of these publications is incorporated by reference herein.)

The interests in developing tactile interactive devices have been growing exponentially in recent years thanks to the increasing demands in a wide range of areas from virtual surgery training in medical technology [1-3], haptic controller of virtual reality (VR) headset in entertainment [4,5], and telemanipulation in robotic controls [6,7]. Tactile communication is also indispensable for people who are visually impaired [8]. Unlike audible and visual means, which are restricted to specific body parts, the sense of touch covers the entire body. Thus, by adding the sense of touch, the quality and amount of information one can gain from a machine will be substantially enriched. The most widely studied tactile displays are those that provide normal indentation to user’s fingertips by vertically moving miniature pins to reproduce shape, pattern, or textures. Despite the growing needs, there is only a handful of tactile display products available on the market due to critical technological barriers. In particular, there is a need for a suitable actuation mechanism that (1) can produce large deformations with sufficiently high blocking force, (2) can be packaged at high pixel resolution, (3) has a compact form factor and is light weight, and (4) can be produced at low costs [9].

Most of the tactile devices suffer from bulky actuator structures. Piezoelectric bimorph tactile displays exhibit a high blocking force in a wide frequency range [10,11]. Unfortunately, these devices are large and bulky due to the encumbrance of the cantilevers. Tactile shape displays using RC servomotors [12] have large displacement and appropriate actuator density but are bulky (76mm × 76mm × 119mm) and inconvenient for day to day operation. Shape memory alloy (SMA) [13] have also been implemented in previous tactile displays. The requirement for extensive heating and cooling steps limits the utility of the device, and raises manufacturing costs. Phase changing materials that exhibit volume change over melting [14] or boiling [15] point were developed as refreshable Braille cells. These devices, which require a miniature Joule

heating electrode and a thermally insulated chamber for each dot, have complex architecture and usually exert small stroke and force.

In recent years, dielectric elastomer actuators (DEA) have emerged as a promising compact tactile display technology [16, 17]. Their light weight, high actuator density, and high stroke range, offers the same performance as previous technologies but in much more compact form factors. However, the translation of the DEA technology to the marketplace has been sluggish, due to the high driving voltages which could cause static shocks or even injury. Attempts by researchers to incorporate insulating layers to seal the DEA generally lowered the actuation performance and increased the fabrication complexity [18-21]. We reported an alternative approach to fabricating a refreshable Braille display using a bistable electroactive polymer (BSEP) as an electroactive transistor [22]. The shape memory property of the BSEP allowed for separation of high voltage elements from operators, but the device used an external heater, and the resulting stroke was small. While mitigated in these designs, the concerns for high voltage were not entirely eliminated.

In comparison to the electric stimuli, pneumatic tactile devices are usually more stable and can provide higher force feedback. However, most pneumatic devices either have complex structures which require individual air streams for each actuator [23] or require electrostatic microvalves for each dot [24]. Scaling up the number of actuators while maintaining compact form factor is challenging. Recently, Besse et al. [25] reported a 32 by 24 actuator pneumatic flexible active skin based on a shape memory polymer (SMP). Each actuator has a diameter of 3 mm, and is placed on a 4-mm pitch. The device was demonstrated as active camouflage and tactile display with a stroke of 0.4mm. The pitch and the stroke do not match the requirements for Braille text which are typically 2.5 mm and 0.5-0.6 mm respectively.

What is needed then, are superior actuation mechanisms for tactile displays. Embodiments of the present invention satisfy this need.

### SUMMARY OF THE INVENTION

A refreshable tactile display according to one or more examples illustrated herein comprises primarily of three parts (1) a polymer membrane with stretchable conductive layer in serpentine patterns, (2) a fluidic pressure chamber connected to a fluidic pressure source, and (3) a rigid membrane comprising one or more through holes. In various examples, each through hole on the rigid membrane defines a tactile pixel area, and aligns with the conductive layer.

In one or more examples, the polymer membrane is relatively rigid at ambient temperature, possesses a tensile modulus in the range of 100 MPa to 10 GPa, and turns into a soft and stretchable elastomer at elevated temperature (e.g., above a transition temperature) with a modulus in the range of 10 kPa to 10 MPa. In various examples, the transition temperature of the polymer membrane is higher than 40°C but lower than 70°C.

In one or more examples, the conductive layer is deposited on the polymer membrane by printing, spraying, or casting, and can be heated due to a voltage between two separated points on the conductive layer.

In one or more examples, the fluidic pressure comprises pneumatic pressure caused by compressed gas, a pneumatic pump, or compressed vapor due to liquid evaporation. In one or more further examples, the fluidic pressure comprises liquidous pressure caused by compressed liquid, a liquid pump, or liquid volume change due to phase change or temperature change.

In various examples, the rigid membrane is laminated to the polymer membrane.

The refreshable tactile display starts with a relatively flat surface and then can be electrically controlled to soften the polymer membrane at one or multiple pixel areas by applying voltage on the conductive layer to generate Joule heat. The softened areas of the polymer membrane are then deformed by the fluidic pressure source. The deformation of the polymer membrane is out of plane such that part of the tactile pixel surface is raised above

the plane of the polymer membrane. The deformation can be maintained at ambient temperature, and can be recovered by raising temperature at the deformed area to above the softening temperature of the polymer membrane.

In one example, a 4x4 portable refreshable tactile display with Braille standard resolution has been demonstrated using a polymer membrane comprising BS80-AA5. The steep modulus change of the BS80-AA5 over a narrow temperature range achieves the device with high blocking force of over 50g and large displacement of 0.7mm. The “P3R” fabrication process of Prestretch-Pattern-Protect-Release is effective to form a highly compliant serpentine-patterned CNT (S-CNT) electrode in wrinkled topography with resistance-consistence up to 188% area strain. The electrode can soften the BSEP film at 30 V in less than 1s. This patterning process is also applicable for larger surface area with more taxels, while keep in compact form factor. The simple architecture of the tactile display ensures an easy and low-cost fabrication.

The display can be embodied in many ways including, but not limited to, the following.

1. A refreshable tactile display unit comprising:
  - a) a polymer membrane comprising a polymer which is relatively rigid at an ambient temperature and in a rubbery state at an elevated temperature, wherein a rigid-to-soft transition of the polymer occurs within a temperature range narrower than 10 °C;
  - b) a fluidic pressure chamber, wherein the fluidic pressure chamber applies fluidic pressure, generated from a fluidic pressure source, to the polymer membrane;
  - d) a conductive layer including one or more heating elements coupled to the polymer membrane; and
  - e) a rigid membrane comprising one or more through holes, wherein:  
the polymer membrane deforms through the one or more through holes in response to:

one or more of the heating elements heating the polymer membrane to the elevated temperature so as to form a softened polymer membrane in the rubbery state, and

the fluidic pressure source applying the fluidic pressure to the softened polymer membrane so as to deform the polymer membrane.

2. The unit of claim 1, wherein the polymer is the bistable electroactive polymer (BSEP) comprising a combination of stearyl acrylate (SA), urethane diacrylate (UDA), acrylic acid (AA), trimethylolpropane triacrylate (TMPTA), 2,2-Dimethoxy-2-phenylacetophenone (DMPA), and benzophenone (BP).

3. The unit of claim 1, wherein the polymer is the bistable electroactive polymer (BSEP) comprising 80 parts of stearyl acrylate (SA) by weight, 20 parts of UDA by weight, 5 parts of acrylic acid (AA) by weight, 1.5 parts of trimethylolpropane triacrylate (TMPTA) by weight, 0.25 parts of 2,2-Dimethoxy-2-phenylacetophenone (DMPA) by weight, and 0.125 parts of benzophenone (BP) by weight.

4. The unit of clause 1, wherein the polymer is a bistable electroactive polymer (BSEP) comprising 40-80 parts of stearyl acrylate (SA) by weight, 20-60 parts of UDA by weight, 5-15 parts of acrylic acid (AA) by weight, 0.25-1.5 parts of trimethylolpropane triacrylate (TMPTA) by weight, 0.125-0.75 parts of 2,2-Dimethoxy-2-phenylacetophenone (DMPA) by weight, and 0.0075-0.2 parts of benzophenone (BP) by weight.

5. The unit of clause 1, wherein the polymer is a bistable electroactive polymer (BSEP) comprising a combination of tert-butyl acrylate (TBA), urethane



diacrylate (UDA), ethoxylated trimethylolpropane triacrylate (ETMPTA), and 2,2-Dimethoxy-2- phenylacetophenone (DMPA).

6. The unit of clause 1, wherein the polymer is a bistable electroactive polymer (BSEP) comprising 90-110 parts of tert-butyl acrylate (TBA) by weight, 5-25 parts urethane diacrylate (UDA) by weight, 1-5 parts ethoxylated trimethylolpropane triacrylate (ETMPTA) by weight, and 0.25-1.5 parts 2,2-Dimethoxy-2-phenylacetophenone (DMPA) by weight.

7. The unit of any of the clauses 1-6, wherein the polymer membrane:  
has a tensile modulus greater than 100 megapascals (MPa) but less than 10 gigapascals (GPa) at the ambient temperature; and  
has a tensile modulus of greater than 10 kPa but less than 10 MPa at the elevated temperature.

8. The unit of any of the clauses 1-7, wherein the polymer membrane has a rigid-to-soft transition temperature higher than 40°C but lower than 70°C.

9. The unit of any of the clauses 1-8, wherein the fluidic pressure comprises pneumatic pressure caused by compressed gas, a pneumatic pump, or compressed vapor due to liquid evaporation.

10. The unit of any of the clauses 1-8, wherein the fluidic pressure comprises liquidous pressure caused by compressed liquid, a liquid pump, or a liquid volume change due to a phase change or a temperature change.

11. The unit of any of the clauses 1-10, wherein the fluidic pressure chamber is rigid.
12. The unit of any of the clauses 1-10, wherein the fluidic pressure chamber is flexible.
13. The unit of any of the clauses 1-12, wherein the conductive layer is a coating on the polymer membrane.
14. The unit of any of the clauses 1-13, wherein the conductive layer is deposited by printing, spraying, or casting.
15. The unit of any of the clauses 1-14, wherein the conductive layer is heated when a voltage is applied between two separated points on the conductive layer.
16. The unit of any of the clauses 1-15, wherein each of the heating elements comprises a serpentine pattern.
17. The unit of any of the clauses 1-16, wherein each of the through holes defines a tactile pixel area and is aligned with a heating element in the conductive layer so that the heating element provides local heating of the polymer membrane.
18. The unit of any of the clauses 1-17, wherein the rigid membrane is laminated on the polymer membrane.
19. A refreshable tactile display, comprising:

a plurality of tactile pixels each controlled by softening a surface area of a polymer membrane, wherein the polymer membrane is relatively rigid at ambient temperature and in a softened state at an elevated temperature;

a conductive layer including a plurality of heating elements, each of the heating elements coupled to a different one of the surface areas of the polymer membrane; and

a rigid membrane comprising through holes, each of the through holes aligned with one of the heating elements, wherein:

the softening of the polymer membrane is controlled by applying a voltage across one or more of the heating elements, so as to heat one or more of the surface areas of the polymer membrane to the elevated temperature and into the softened state;

the one or more surface areas in the softened state are deformed out of a plane of the polymer membrane into a deformed state by a fluidic pressure generated using a fluidic pressure source, such that part of the tactile pixel coupled to the surface area associated with the tactile pixel is raised above a plane including the through holes;

the deformed state is maintained at the ambient temperature; and

deformation in the deformed state is recovered by raising a temperature of the one or more surface areas in the deformed state to above a softening temperature at which the polymer membrane softens.

20. The refreshable tactile display of clause 19, wherein the polymer membrane:

comprises a phase changing polymer exhibiting a tensile modulus change by at least two orders of magnitude in a temperature range of less than 10°C;

possesses a tensile modulus of at least 100 MPa at room temperature to provide a high blocking force, and

becomes rubbery with tensile modulus less than 1 MPa at the elevated temperature; and

has a thickness greater than 10  $\mu\text{m}$ .

21. The refreshable tactile display of clauses 19 or 20, wherein:

the conductive layer comprises one or more conductive materials selected from the group of single walled carbon nanotube, multiwalled carbon nanotube, graphite powder, graphene, metal nanowires, metal nanoparticles, thin coating of a metal or alloy, thin conducting polymer coating, conducting polymer nanofibers,

each heating element covers one of the surface areas comprising a circular area with diameter larger than 0.1 mm but less than 10 mm,

each heating element aligns with one of the through holes, comprising a circular through hole, on the rigid membrane,

the rigid membrane comprises a chamber cover for a fluidic pressure chamber connected to the fluidic pressure source, the fluidic pressure chamber transferring or applying the fluidic pressure to the polymer membrane.

22. The display of clause 21, wherein the carbon nanotubes are embedded in a polymer layer.

23. The display of any of the clauses 19-22, wherein each of the heating elements comprise a serpentine pattern.

24. The display of any of the clauses 19-22, wherein the tactile pixels have a relatively flat surface.

25. The display of clause 19, wherein the polymer membrane comprises a combination of stearyl acrylate (SA), urethane diacrylate (UDA), acrylic acid (AA),

trimethylolpropane triacrylate (TMPTA), 2,2-Dimethoxy-2- phenylacetophenone (DMPA), and benzophenone (BP).

26. The display or unit of any of the clauses 1-25, wherein deformation of the polymer membrane actuates one or more pixels by displacing one or more pins in the one or more through holes.

27. The display or unit of any of the clauses 1-26, wherein Joule heating of the conductive layer softens the polymer membrane.

28. The display or unit of any of the clauses 1-27, wherein the polymer layer and the conductive layer form a interpenetrating composite (the polymer layer and the conductive layer interpenetrate).

29. A method of making the refreshable tactile display, comprising:

a) stretching a softened polymer membrane and maintaining deformation of the softened polymer membrane when the polymer membrane is cooled to ambient temperature;

b) spraying a dispersion of carbon nanotubes (CNTs) in a solvent onto the deformed rigid polymer membrane through a shadow mask which has one or more serpentine shaped cutout pattern(s), so as to form a carbon nanotube coating on the deformed rigid polymer membrane;

c) spraying a solution comprising a polymer or polymer precursor on top of the carbon nanotube coating; and

d) ) releasing the deformation of the stretched polymer membrane at elevated temperature, and cooling down to ambient temperature.

30. A method of making a refreshable tactile display, comprising:
- forming a coating of carbon nanotubes on a release substrate;
  - patterning the coating into serpentine shapes by laser ablation;
  - applying a polymer precursor layer over the coating;
  - curing the polymer precursor layer, forming a cured polymer layer; and
  - separating the cured polymer layer from the release substrate.

31. A bistable electroactive polymer, comprising a combination of stearyl acrylate (SA), urethane diacrylate (UDA), acrylic acid (AA), trimethylolpropane triacrylate (TMPTA), 2,2-Dimethoxy-2- phenylacetophenone (DMPA), and benzophenone (BP).

32. A bistable electroactive polymer (BSEP) comprising a combination of tert-butyl acrylate (TBA), urethane diacrylate (UDA), ethoxylated trimethylolpropane triacrylate (ETMPTA), and 2,2-Dimethoxy-2- phenylacetophenone (DMPA).

#### BRIEF DESCRIPTION OF THE DRAWINGS

Referring now to the drawings in which like reference numbers represent corresponding parts throughout:

FIGS. 1A-1D. A compact tactile display according to one or more embodiments of the present invention. FIG. 1A is a Schematic of the layered structure of a 4x4 pixel array. FIG. 1B is a cross sectional view of the working mechanism. The taxels, with Braille size (I), are individually actuated by softening (50°C) and deforming the BSEP in the corresponding area (II). The deformation is then maintained without any energy input when the BSEP film cools below 40°C (III). The original shape is recovered by reheating the BSEP (IV). FIG. 1C illustrates demonstration of a 4x4 tactile display showing “U”, “C”, “L”, “A”. FIG. 1D shows photographs of a 4x4 tactile display in the flat state (left)

and all actuated state (right). Both states are stable without any external energy input. The scale bar represents 2mm.

FIG. 2A. Schematic illustration of the fabrication process of the BSEP film with a serpentine carbon nanotube (CNT) Joule heating electrode. (I) Prestretch: the BSEP film is prestretched biaxially at elevated temperature and then cooled down. (II) Pattern: a carbon nanotube solution is spray coated on the prestretched BSEP through a shadow mask. (III) Protect: A monomer (UDA) solution is spray-coated on the CNT electrode and cured, forming a CNT-poly(UDA) interpenetrating composite. (IV) Release: the prestrain is released by softening the BSEP film.

FIG. 2B. Optical microscopic images of the BSEP active layer with (above) and without (bottom) the poly(UDA) layer. The scale bar represents 0.1mm.

FIG. 2C. Schematic illustration of shape memory mechanism of phase changing BSEP.

FIG. 2D. Chemical structures of monomers and initiators used for the synthesis of BS80-AA5.

FIGs. 3A-3D. Mechanical properties of BS80-AA5. FIG. 3A shows the sharp change of storage modulus and loss factor with respect to temperature. FIG. 3B shows cyclic tensile loading-unloading tests of BS80-AA5 under different stretch ratio with strain rate of 0.01/s. FIG. 3C shows measured (symbols) and simulated (dashed curves) blocking force required to completely press down an actuated BS80-AA5 taxel with different displacement. The thickness of the un-deformed BSEP films ranges from 40 $\mu$ m to 170 $\mu$ m. FIG. 3D shows a rigid BSEP taxel with 90 $\mu$ m thick BSEP capable of deforming a user's fingertip (upper left) and supporting a 25g mini stapler (down left), and a schematic illustration of measured blocking force (right).

FIG. 3E(i)-(iii). Shape memory demonstration of a BS80-AA5 film in its original shape (i), deformed with 100% linear strain via a heating-stretching-cooling procedure

(ii), and recovered to original shape (iii). All shapes are rigid and free-standing. The scale bar represents 1 cm.

FIG. 3F. Tensile stress-strain response of two different BSEP films (BS80-AA5 and BS80) at 50°C.

FIG. 3G. Measured (symbols) and simulated (dashed curves) internal air pressure needed to actuate a softened BSEP taxel to different heights. The thickness of the BSEP films ranges from 40 $\mu$ m to 170 $\mu$ m.

FIG. 3H Tensile test comparison of poly(UDA), BS80-AA5, and BS80-AA5/poly(UDA) composite. The composite film was made by spraying and curing a thin layer of poly(UDA) (5  $\mu$ m) on a 90  $\mu$ m BS80-AA5.

FIG. 3I. Storage modulus measurements of the three materials at room temperature (RT) and 50 °C high temperature (HT).

FIG. 4A-4E. Performance of S-CNT Joule heating electrode. FIG. 4A shows relative resistance variation of a serpentine CNT electrode under different area expansion. FIG. 4B shows lifetime test on a serpentine CNT Joule heating electrode with 100% area expansion deforming and releasing cycle at a frequency of 0.8Hz for over 100,000 cycles. The insets show the serpentine CNT electrode retaining the continuous electrode line (up left and up right, scale bar 0.2mm) and stable heating (down left and down right, scale bar 1mm) after the cycling test. FIG. 4C is a comparison of heating performance of important stretchable Joule heating films with respect to heating rate, stretchability, and resistance consistency. Heating rates of the literature films were calculated from reported temperature versus time curve under the highest voltage provided. If not specified in the literature, stretchability was defined as the stretch ratio when the resistance increases by 20%. The resistance consistency was obtained by initial resistance over the resistance after a stretch-release cycle. FIG. 4D is a demonstration of a one-cell Braille device showing “U” “C” “L” “A” in Braille characters with infrared images of the corresponding S-CNT Joule heating electrode shown to the left. The scale bars are 2mm.



FIG. 4E shows testing of the adhesion of CNT on different BSEP films (BS80-AA5 and BS80) using Kapton™ tape.

FIG. 5A-5E. Illustration (FIG. 5A, FIG. 5B) and simulated (FIG. 5C, FIG. 5D) results of current density distribution in serpentine shaped and round shaped electrodes. The widths of the red dotted lines in FIG. 5A and FIG. 5B indicate relative current density. FIG. 5E Transient temperature responses of the electrodes at 30 V. Insets in FIG. 5E are infrared camera images of the heated electrode areas. The scale bar is 2 mm.

FIG. 6A. Temperature profiles of S-CNT electrode under different voltage supplied. Downward arrows indicate when heating voltage is removed. The “Softening” line indicate the temperature above which the polymer is soft, and the “Stiffening” line indicates the temperature below which the polymer is stiff.

FIG. 6B. Raised height and temperature of a taxel as a function of time during a bistable actuation.

FIG. 7A. Flowchart illustrating methods of making a tactile display according to embodiments of the present invention.

FIG. 7B. Flowchart illustrating another method of making a tactile display according to embodiments of the present invention.

FIG. 7C. Flowchart illustrating yet another method of making a tactile display according to embodiments of the present invention.

FIGs. 8A-8B. Schematic illustration of the proposed PolyPad, a Braille electronic reader packaged as a (FIG. 8A) smartphone or (FIG. 8B) tablet case, to respectively display 5\*15 and 10\*30 Braille cells. The side panels on the phone case fold behind the Braille display to stay within the silhouette of the smartphone. The pump is placed on the right-side panel and protrudes 0.5 cm from the surface of the case when folded. The tablet case folds by extending and folding the three-piece triangular structure, which supports the tablet, onto the Braille display. The pump is placed on the center of the three

support panels, and a similar 0.5 cm protrusion will be present when in the folded configuration.

FIG. 9A. Schematic of the actuation of a BSEP polymer. The BSEP can be actuated to any rigid shape intermediate between A and D reversibly and repeatedly. FIG. 9B. Modulus change with temperature of 5 different BSEP polymer compositions.

FIG. 10A-10C. Schematic of a Braille PolyPad (not to scale). FIG. 10A shows layered structure of a  $4 \times 10$  Braille cell display. FIG. 10B is a cross sectional view of the working mechanism (I). The taxels are individually actuated in the active areas (II). The deformation is then maintained without any energy input at ambient temperature (III). The original shape is recovered by reheating the BSEP (IV). FIG. 10C is a photograph of a commercial miniature pump measuring  $3.75 \times 1.78 \times 0.5$  cm.

FIGs. 11A-11D. Demonstration of a phone screen sized tactile PolyPad ( $23 \times 44$  taxels) showing "UCLA" (FIG. 11A), chemical structure of benzene (FIG. 11B), and a complex map of UCLA School of Engineering (FIG. 11C) that is based on the visual map (FIG. 11D) from Google Maps.

FIG. 12A A raised BSEP dot that can support finger pressing without deformation.

FIG. 12B Cyclic tensile loading-unloading behaviors of a softened BSEP film.

FIG. 13A Storage modulus of the BS80 (black curve) and a VSP polymer (blue curve) with empirically projected narrower phase-changing temperature range. FIG. 13B. Schematic of the molecular structure of the new polymer, where A and B are homopolymer chains of stearyacrylate and butylacrylate, respectively, and X are crosslinking sites.

FIG. 14A Optical image of a serpentine-shaped CNT electrode embedded in the surface layer of a BSEP film, and infrared image of the electrode area under Joule heating.

FIG. 14B Relative resistance variation of the serpentine CNT electrode under different area expansion.

FIG. 14C Lifetime test on the serpentine heating electrode with repeated 100% area expansion at 0.8 Hz for 100,000 cycles.

FIG. 15. Schematic of the compliant Joule heating electrodes for a Braille cell.

FIG. 16A Schematic of a Braille cell based on a rigid, 3D printed pneumatic chamber.

FIG. 16B. Optical (in gray background) and infrared (in purple background) images of a Braille cell. The pins are decorated black for easy viewing.

FIG. 17A. Heating voltage (red line) and voltage for pneumatic pump (blue line).

FIG. 17B. A picture of a PCB to drive a  $4 \times 10$  Braille cell array line by line.

FIG. 18A. Data sharing architecture. FIG. 18B Parallel display architecture. SPM: serial-to-parallel module.

## DETAILED DESCRIPTION OF THE INVENTION

### TECHNICAL DESCRIPTION

In the detailed description of the invention, references may be made to the accompanying drawings which form a part hereof, and in which is shown by way of illustration specific embodiments in which the invention may be practiced. It is to be understood that other embodiments may be utilized, and structural changes may be made without departing from the scope of the present invention. A number of different publications are also referenced herein as indicated throughout the specification. A list of these different publications can be found below in the section entitled "REFERENCES". All publications, patents, and patent applications cited herein are hereby incorporated by reference in their entirety for all purposes.

Unless otherwise defined, all terms of art, notations and other scientific terms or terminology used herein are intended to have the meanings commonly understood by those

of skill in the art to which this invention pertains. In some cases, terms with commonly understood meanings are defined herein for clarity and/or for ready reference, and the inclusion of such definitions herein should not necessarily be construed to represent a substantial difference over what is generally understood in the art. Many of the techniques and procedures described or referenced herein are generally well understood and commonly employed using conventional methodology by those skilled in the art. As appropriate, procedures involving the use of commercially available kits and reagents are generally carried out in accordance with manufacturer defined protocols and/or parameters unless otherwise noted.

#### A. Example Tactile Device

##### 1. Design and operation

FIG. 1A and FIG. 1B illustrate a refreshable tactile display unit 100 comprising a polymer membrane 102 comprising a polymer 104 which is relatively rigid 106 at an ambient temperature and in a rubbery state 108 at an elevated temperature, wherein a rigid-to-soft transition of the polymer occurs within a temperature range narrower than 10 °C; a fluidic pressure chamber 110, wherein the fluidic pressure chamber applies fluidic pressure 112, generated from a fluidic pressure source 114, to the polymer membrane 102; d) a conductive layer 116 including one or more heating elements 118 coupled to the polymer membrane; and a rigid membrane 120 comprising one or more through holes 122. The polymer membrane deforms through the one or more through holes in response to: one or more of the heating elements heating the polymer membrane to the elevated temperature so as to form a softened polymer membrane in the rubbery state, and the fluidic pressure source applying the fluidic pressure to the softened polymer membrane so as to deform the polymer membrane. Membrane 102a may include conductive layer 116 combined with polymer membrane 102.

FIG. 1A and FIG. 1B further illustrate a plurality of tactile pixels 124 or pins 124a each controlled by softening a surface area 126 of the polymer membrane. FIG. 1B illustrates the polymer membrane is relatively rigid (in a rigid state 128) at ambient temperature and in a softened state 130 at an elevated temperature.

FIG. 1B and FIG. 1C show the one or more surface areas 126 in the softened state 130 are deformed out of a plane 132 of the polymer membrane into a deformed state 134 by the fluidic pressure generated using the fluidic pressure source, such that the tactile pixel 124 or part of the tactile pixel 124 coupled to the surface area 126 associated with the tactile pixel is raised above a plane 136 or thickness of the rigid membrane including the through holes 122. The deformed state 134 is maintained at the ambient temperature; and deformation 134a in the deformed state 134 is recovered by raising a temperature of the one or more surface areas 126 in the deformed state 134 to above a softening temperature at which the polymer membrane softens.

FIG. 1D (left) shows the 4 x 4 tactile display in the “OFF” state when the BSEP film was not deformed and the surface of the display was flat. FIG. 1D (right) image shows that all the taxels were actuated with a stroke of 0.7 mm. Both two states are stable without any external energy input.

The demonstrated tactile device illustrated in FIG. 1A contains a 4 by 4 tactile pixel (taxel) matrix 150 with outer size of 17mm x 17mm x 3mm. Each taxel has 1.5 mm diameter with 2.5 mm distance between the centers of two adjacent taxels (designed according to Braille standard). As illustrated in FIG. 1A and FIG. 1B, the device primarily comprises of two parts: a pneumatic system and a thin BSEP active film that can be thermally controlled to soften locally. The pneumatic system constitutes a pneumatic chamber and a miniature pump to provide pressurized air for actuation. The specific BSEP polymer used is a phase changing polymer that exhibits stiffness change of three orders of magnitude in a narrow temperature range of less than 10°C [26]. At room temperature, the BSEP possesses a modulus of several hundred MPa, and behaves as a rigid plastic, capable

of providing a blocking force as high as 50 g. Above its transition temperature, the polymer becomes soft and stretchable with its modulus decreasing to 0.1 MPa. The BSEP active film has a thickness of about 90  $\mu\text{m}$ . A matrix of highly compliant single-walled carbon nanotube (CNT) Joule heating electrodes patterned in serpentine shape (S-CNT) is formed on the upper surface of the BSEP film. The thermal stability, mechanical compliancy, and chemical resistance of CNTs made it an ideal choice as the Joule heating electrode [27,28]. The BSEP with S-CNT electrode is attached on the chamber to seal it. The rigid chamber cover is then mounted using an adhesive tape or adhesive layer 138 and 4 corner screws. The circular openings 132a on the adhesive tape and the openings or holes 122 in the chamber cover align with the S-CNT electrode areas, each defining a taxel area 140. A pin 124a with a flange on one end to prevent the pin from dropping out of the taxel cell is placed in each taxel. The protruding surface 142 of the pin is the tactile interface of the taxel. As each taxel has an independent S-CNT Joule heating electrode, the modulus of the BSEP can be administered locally, enabling individual taxel control of the display panel. By synchronizing the pneumatic pressure and thermal stimuli, the BSEP can be locally softened and deformed, thereby raising individual pins by 0.7 mm in height (FIG. 1D) and presenting unique configurations to the end user. Upon cooling, the BSEP rigidifies, which takes less than 2 s, no external energy input is then needed. In FIG. 1C, the 4 x 4 tactile display shows “U” “C” “L” “A” on the device, demonstrating the precise control of individual dots. The display can be quickly refreshed by reheating the deformed taxels without applying any pneumatic pressure.

## 2. Example serpentine-patterned carbon nanotube (S-CNT) electrode fabrication

The core component in the pneumatic tactile display is the BSEP film with stretchable Joule heating electrode. To obtain high stretchability, we developed a “P3R” fabrication process: Prestretch-Pattern- Protect-Release (FIG. 2A). The method starts with

prestretching a softened BSEP film biaxially by 100% x 100%. The prestretched film maintains the stable shape after it cools down. A dispersion solution of CNTs in an isopropyl alcohol and water mixture solvent is then sprayed on the prestretched BSEP through a shadow mask. The mask has a serpentine shaped cutout pattern formed by laser ablation. Next, a solution of urethane diacrylate (UDA) monomer in toluene is sprayed on top of the CNT-coated BSEP film. Because of its low viscosity, the UDA solution infiltrates into the CNT network, forming an ultra-thin CNT- Poly(UDA) interpenetrating composite electrode after the UDA layer is cured. As the CNT network is embedded into the poly(UDA) layer, physical translation of CNTs is largely prevented during the deformation of the BSEP film. Moreover, since the UDA monomer is also one of the comonomers to form the BSEP, the poly(UDA) layer strongly bonds the BSEP film. When the resulting poly(UDA)/CNT/BSEP composite structure is heated above the BSEP's  $T_m$  to release the prestretch in the BSEP layer, the BSEP matrix along with the S-CNT electrode shrinks 100% x 100% biaxially, while the poly(UDA) layer wrinkles up (FIG. 2B). The wrinkled topography is shown as a "greasy" surface in the upper microscopic image, whereas the flat surface of the CNT/BSEP electrode prepared without the poly(UDA) shows a "dry" surface. Note that the "greasy" surface resulted from the surface unevenness that blurs the optical image and imparts the S-CNT electrode with high stretchability. This "P3R" method and the serpentine shaped pattern of the CNT layer afford an active BSEP film with a highly compliant and stretchable Joule heating electrode.

### 3. Example BSEP compositions and structures

Variable stiffness material has been an actively researched subject for decades because the ability of muscle to adjust its modulus is responsible for the adaptability and dexterity of animals. Shape memory polymers (SMP), which exhibit a modulus change by a few hundred-fold during glass transition [29], can be programmed to different rigid shapes via stretching at elevated temperatures. Glass transition typically spans in a broad

temperature range of over 20 °C [22] which limit the utility of these materials. For applications involving human tactile interaction [25], the SMP needs to remain rigid up to around 37°C to prevent incidental shape changes. The actuation would be conducted above the polymer's glass transition temperature ( $T_g$ ), or more than 20°C above body temperature which could induce tissue damage. This limitation is addressed in embodiments described herein with a phase changing BSEP polymer comprising a stearyl acrylate (SA) moiety in the polymer that can reversibly crystallize and melt within a narrow temperature range (FIG. 2C) [26]. The phase change occurs within 10°C and induces a modulus change of nearly 1000-fold.

FIG. 2C illustrates an example BSEP material is a variable stiffness polymer comprising nanometer-size crystalline aggregates in a chemically crosslinked polymer matrix. The shape memory property is obtained by reversible crystal melting (phase-changing), resulting in a material with large modulus change between the rigid and rubbery states during temperature cycles. Below its transition temperature, the soft side chains (SA moieties) from different polymer backbones pack closely to form crystalline aggregates which stiffen the material. Above the melting temperature ( $T_m$ ) of the crystalline aggregates, the polymer becomes rubbery and can be programmed into different shapes. Such deformation may be preserved by cooling down the temperature below  $T_m$  as the crystalline aggregates of SA moieties reform. And the shape can be recovered by reheating the polymer above  $T_m$ .

In one or more examples of a BSEP based tactile actuator, large blocking force, low actuation (pneumatic) pressure, and high mechanical toughness are the main aspects that needed to be considered. Stearyl acrylate (SA) has a long alkyl chain that can crystallize at room temperature. The reversibly crystallizing and melting of SA moieties provide the variable stiffness property. Urethane diacrylate (UDA) is an oligomer comprising flexible polyether diol segments. UDA was selected as long chain crosslinker to enhance elongation at break and improve the toughness. Trimethylolpropane triacrylate (TMPTA), which is a



trifunctional acrylic monomer, was used as small molecule crosslinker to provide the network baseline. Such small molecule crosslinker can stiffen the polymer at larger strains, thus increase the tensile strength. Acrylic acid (AA) was added to introduce hydrogen bonds to the polymer system, which can help increase the modulus change, mechanical toughness, and electrode bonding. 2,2-Dimethoxy-2-phenylacetophenone (DMPA) and benzophenone (BP) were synergistically used as co-initiators to achieve complete bulk and surface curing in thin films.

The compounds used to synthesize the phase changing BSEP are shown in FIG. 2D, and the synthetic details are found in the experimental section. To obtain the optimal overall performance for tactile display application, the BSEP was formulated to contain 80 parts of SA (by weight), 20 parts of UDA, 5 parts of acrylic acid (AA), 1.5 parts of TMPTA, 0.25 part of DMPA, and 0.125 part of BP, and the polymer is labeled as BS80-AA5. Adding the small amount of acrylic acid was found to help increase the modulus change, mechanical toughness, and electrode bonding.

#### 4. Characterization of an example BSEP (BS80-AA5)

FIG. 3E demonstrates the shape memory property. A strip made from BS80-AA5 was attached on two pieces of Kapton™ tape at the ends. The initial distance between two tapes was 1.5 cm. At 50 °C, the softened BS80-AA5 was stretched to 3 cm with a linear strain of 100%. The film was then cooled down in air to “lock” the deformation. The deformed film was free-standing with a fixation rate close to 100%. The original shape can be recovered by heating the strip again above the transition temperature, and the recovery rate is 100%.

Stiffness change is critical for BS80-AA5 to maintain the actuated shape. The hydrogen bonds from the carboxylic acid group in AA helped increase the difference in modulus between room temperature and elevated temperature. At room temperature, the carboxylic acid groups form double hydrogen bonding dimers which help increase the

stiffness [30]. With increasing temperature, the strength of hydrogen bonds decreases, thus won't have much effect on the modulus of softened BSEP. Dynamic mechanical analysis of the BSEP polymer was conducted at a temperature ramping rate of 2 °C/min from 25 to 55 °C and a mechanical loading frequency of 1Hz. FIG. 3A shows that BS80-AA5 possesses a steep stiffness change of 3000 times from about 300 MPa to about 0.1 MPa. The transition occurs from 40 °C to 47 °C. Once the transition is completed, the storage modulus remains constant with further increasing temperature. The ultralow modulus of only 0.1 MPa in the rubbery state is resulted from the presence of large amount of molten stearyl chains which serve as plasticizers to the polymer. The substantial modulus switching leads to high shape memory property (FIG. 3E(i)-(iii)). In fact, the fixation rate and recovery rate of BS80-AA5 are both close to 100%.

An essential requirement for the refreshable tactile display is the reversibility and repeatability of the taxel actuation over many cycles. The elasticity of BS80-AA5 in the rubbery state was thus characterized. The loss factor of the softened BS80-AA5 is around 0.05 (FIG. 3A), which indicates very low viscoelasticity and thus fast response speed. Cyclic tensile tests were also carried out at 50 °C with a strain rate of 0.01 s<sup>-1</sup>. The tests consisted of three loading-unloading loops with strain successively up to 50%, 100%, and 150%, respectively, in three separate tests. The resulting stress-strain curves are shown in FIG. 3B where the loading and unloading curves completely overlap, suggesting that the material behaves elastically with minimal hysteresis, thereby agreeing with the low loss factor measured in dynamic mechanical analysis. Another important requirement for BS80-AA5 to resist fracture during stretching is high toughness. The hydrogen bonds from acrylic acid act as reversible crosslinks to enhance the toughness. Physical crosslinks have been identified as an essential element to toughen soft gel [31–33]. The non-permanent crosslinks can break and re-form to overcome stress concentration and dramatically enhance crack propagation resistance. The comparison of toughness between BS80-AA5 and BS80 (without acrylic acid) was characterized via uniaxial tensile test at 50 °C (degrees

Celsius) with a stretching rate of 0.1 mm/s (FIG. 3F). The BS80-AA5 has a maximum elongation of 320% with a normal tensile strength of 8 MPa and true tensile strength calculated to be 34 MPa. Without the toughening effect from acrylic acid, BS80 ruptured at 191% strain with a tensile strength of only 0.26 MPa (true stress calculated to be 0.76 MPa). The high tensile strength of BS80-AA5 is important for the polymer to resist against fracture. Meanwhile, the stress to obtain up to 200% strain is low, i.e., the softened BS80-AA5 is highly compliant, and large deformation could be obtained with low pneumatic pressure. The air pressure needed to actuate a taxel to different heights was measured and the results are shown in FIG. 3G. For a 90  $\mu\text{m}$  thick BSEP film, the pressure to generate an out-of-plane displacement of 0.7 mm (minimum displacement requirement for Braille is 0.5 mm [34]) is only 160 mmHg.

In the rigid state of the BSEP polymer, the crystalline aggregates of the SA moieties act as hard segments in the polymer, resulting in a storage modulus of 340 MPa. The taxels are thus expected to be able to resist large forces applied to the raised dots. The blocking force, or force required to press down the raised dots to completely overcome the original vertical displacement, was measured for taxels in which the BSEP polymer had originally been actuated into various raised height. Note that raised height of 0.75 mm means the BSEP film was actuated to a half-dome shape with an area expansion of 100%. The results are shown in FIG. 3C for BS80-AA5 films with pre-deformation thickness ranging from 40  $\mu\text{m}$  to 170  $\mu\text{m}$ . ANSYS Finite Element Analysis (FEA) was also performed to simulate the blocking force of the taxels based on Yeoh's 3rd hyperelastic model. The FEA simulation results match the experimental data quite well. More information about FEA simulations can be found in the attached appendix. For the taxel display panel device we fabricated, the BSEP film with un-deformed thickness of 90  $\mu\text{m}$  was used. The rigid taxels with displacement of 0.5 mm have a blocking force of 50 g, which is much greater than the 15 g requirement in typical tactile devices [34]. An actuated BS80-AA5 dot is capable of

supporting vigorous tapping and rubbing from a user's finger without deforming, suggesting that the rigid BSEP actuator is strong enough for repetitive heavy touches.

#### 5. Example Serpentine CNT Joule heating electrode fabrication

Mechanical impedance of the Joule heating electrode coated on the BSEP film can alter the actuated strain (raised height) and uniformity (shape of the raised dome structure). It is essential to develop a heating electrode that is both highly compliant and stretchable. In recent years, great efforts have been made to develop stretchable conductors for the next generation of flexible and wearable electronics that can conform to movable and arbitrarily shaped surfaces [35–37]. Much of these reported stretchable conductors are too stiff for the present application. We selected carbon nanotube as the Joule heating electrode material thanks to the nanotubes' large length-to-diameter aspect ratio that form highly porous percolation networks and high thermal and environmental stability. The Joule heating would require a thick coating of CNT to obtain low surface resistance for low-voltage heating, but a thick coating would induce significant mechanical impedance [27] and may delaminate from the polymer matrix. Moreover, with such high resolution, where the closest distance between two adjacent taxels is only 1 mm, it is essential for the Joule heating electrodes to receive uniform and precise heating to prevent crosstalk. To overcome these issues, the "P3R" fabrication process: Prestretch-Pattern-Protect-Release was employed to obtain simultaneously low surface resistance, low mechanical impedance, and high stretchability.

The carbon nanotubes (P3-SWNT, Carbon Solutions, Inc) we used for the electrode are specifically tailored for dispersion in solvents, and contain 6% carboxylic acid groups (SWNT-COOH) [43]. The SWNT-COOH bonds to BS80-AA5 strongly through the hydrogen bonding interactions between carboxylic acid groups. FIG. 4E demonstrates the CNT electrode on a BS80-AA5 film capable of surviving multiple tape peeling tests. A Kapton<sup>TM</sup> tape with a high peeling strength of 46 oz/in was used to check if the CNT could

be removed during peeling. After several peeling processes, the resistance and the color of the CNT electrode on BS80-AA5 didn't change at all, suggesting strong bonding between CNT and BS80-AA5. In comparison, the CNT electrode(s) similarly formed on a BS80 film were almost completely transferred to the tape after one test, and lost surface conductivity.

FIG. 5A illustrates the softening of the polymer membrane is controlled by applying a voltage (V) 500 across one or more of the heating elements 118 (e.g. across electrodes 502), so as to heat one or more of the surface areas 126 of the polymer membrane to the elevated temperature and into the softened state.

The heating process is the most critical step in the operation of the tactile display device. To achieve high- efficiency heating with low mechanical impedance, we fabricated the CNTs into a serpentine shape. The serpentine architecture has been explored by a number of groups as an effective approach to impart large stretchability to electrodes [38–42]. As a Joule heating electrode, a more important characteristic is uniform and rapid heating. With applied voltage, the charge carriers will be restricted within the winding path of the serpentine pattern, resulting in uniform heating over the taxel area. On the other hand, for the round shaped pattern, the charge carriers tend to travel the shortest distance, causing the heat mainly being distributed along the equatorial area (FIG. 5A). In our device, the resistance of one S-CNT was kept at around 30-40 k $\Omega$  to ensure low voltage ( $\sim$  30 V) activation for the device. As shown in FIG. 5B, the time needed for serpentine shaped electrode to reach 45 °C, which is the temperature to soften BS80-AA5, is less than 1s, while it will take more than 5 seconds (s) for the round shaped electrode (with same resistance) to reach 40°C. The unique winding path of S-CNT increases the heating efficiency, resulting in rapid and uniform heating in a very short time. The short heating phase also prevents excess heat dissipation. Moreover, the serpentine pattern is also very effective to retain the compliancy of the Joule heating electrode. Under the same electrode loading per unit area, the storage modulus of the poly(UDA)/CNT/BS80-AA5 films where

the CNT electrode is either blanket-coated or serpentine patterned are 1.9 MPa and 0.36 MPa, respectively, at 50 °C. Both moduli are higher than that of the bare BS80-AA5 film which is 0.13 MPa at 50 °C. Note that PUA layer has higher stiffness compared to BS80-AA5, which also contributes in the modulus increase. High compliancy of the S-CNT electrode is essential for the low air pressure actuation.

#### 6. Characterization of the Example Serpentine CNT Joule heating electrode

Joule heating characteristics of the S-CNT electrode under different voltages were also investigated, and the results are shown in FIG. 6A. FIG. 6A shows the time evolution of temperature increase and decrease for the serpentine CNT electrode under different voltage input. The temperature increased rapidly with time and reached a relative saturated plateau. The plateau increased with the input power. In most cases, the taxel can reach the softening line, which is 47 °C, within a few seconds. The cooling process takes longer because of the temperature overshooting. For the proposed taxel, 40 °C is the temperature to stiffen the material, so the cooling time usually takes less than 2 s. Thus, the electrode exhibits high heating rate, with minimal energy consumption considering the high resistance of the S-CNT electrode. As the BS80-AA5 stiffens below 40°C, the cooling step only requires about 2 seconds to reach completion. In addition, the pneumatic pump assists in heat dissipation further driving down the duration of the cooling step. Thus, a taxel actuation cycle requires about 3 seconds for completion. After one second, the Joule heating can be turned off, while the pneumatic pump is turned on. Because of the elastic nature of the BS80-AA5 film, once the pump is on, the pin interface is lifted immediately. Then the pump can be turned off in 2 seconds when the film has cooled down.

To ensure stable heating during actuation, the resistance of the Joule heating electrode needs to remain constant. In our device, to latch a 0.7mm displacement, the BSEP active layer needs to expand about 100% area strain to form a half spherical dome. In other words, the Joule heating electrode needs to be compliant enough to be stretched at least

100% area strain without much restriction to the polymer matrix, while maintaining a constant resistance to allow for consistent heating steps. FIG. 4A shows the normalized resistance of a braille sized S-CNT electrode on BS80-AA5 in response to area expansion on a diaphragm. The resistance stays almost constant with area strain up to about 200%, and increases dramatically with further increase strain. Such behavior is reasonable because of the “Prestretch-Release” process from the “4P3R” fabrication process mentioned above. In the “Prestretch” part, the BSEP film is prestretched to about 100% x 100% biaxial strain. The following “Releasing” process causes the CNT coating embedded in the P(UDA) layer to wrinkle with the P(UDA) layer. Subsequent stretching translates into flattening of the wrinkles without substantial elongation within the CNT coating and thus ensures a relatively constant resistance until the wrinkles have been flattened and further stretching leads to elongation within the S-CNT coating. To obtain high stretchability and durability of the S-CNT electrode, interpenetration of the CNT network with in the protecting P(UDA) layer is important to prevent the carbon nanotubes from translational movement during repetitive deforming-recovering cycles.

Cyclic stretching test was also carried out on one taxel. Under induced area strain of 100%, which will exert a displacement over 0.7 mm, the resistance and Joule heating characteristics remain stable for over 100,000 repetitive cycles at a frequency of 0.8 Hz (FIG. 4B). The upper insets show optical microscope images of a continuous electrode line of the S-CNT electrode before and after the 100,000 cycles of lifetime test. Uniform and precise heating was observed from the infrared thermal images of the electrode after the test (lower insets). FIG. 4C compares heating rate, stretchability, and resistance consistency of S-CNT electrode with other reported compliant and stretchable Joule heating films that can generate uniform heat across the surface. The main efforts of contemporary research activities on stretchable heaters are focused on low dimensional carbon materials (filled symbols) [44–47], metal nanowires: silver based (open symbols) [48–52] and copper based (half-filled symbols) [53–56], and conductive polymers (half-filled pentagon) [57]. The S-

CNT electrode can simultaneously perform fast heating rate (31°C/s), large stretchability (188% linear strain), and high resistance consistency (98.9%), which can be very challenging for most other reported Joule heating electrodes to fulfill all three-performance metrics at the same time. FIG. 4D demonstrates a Braille cell device using the S-CNT-BSEP system, which shows “U” “C” “L” “A” in Braille characters. The insets are the corresponding infrared images of working S-CNT Joule heating electrodes. The heating is precise and uniform without any crosstalk between adjacent dots.

FIG. 4E shows the adhesion tests of an example CNT electrode on BSEP substrates. Same amount of CNT solution was sprayed on BS80-AA5 and BS80 respectively through a shadow mask. The resulting CNT/BS80-AA5 and CNT/BS80 has the same initial resistance. Two pieces of Kapton™ tape with peeling strength of 46 oz/in were attached firmly on top of CNT/BSEPs. The tapes were then peeled off, and the resistance of the electrodes were measured subsequently. The results show a constant resistance of CNT/BS80-AA5 after 3 repetitive tape-peel tests, while CNT/BS80 lost surface conductivity after one test as almost all the CNT has transferred to the tape. The results demonstrate the strong bonding between CNT and BS80-AA5, and such strong bonding is because of the hydrogen bond interaction between acrylic acid and SWNT-COOH.

#### 7. Example Thermal and pneumatic control sequence

FIG. 6B demonstrates an example thermal and pneumatic control sequence of a taxel. The actuation cycle starts with the BS80-AA5 membrane at room temperature and in an OFF state. The interface surface is flat. The taxel area of BS80-AA5 is heated up by S-CNT Joule heating electrode for 1 s. Then the pneumatic pump is turned on with the S-CNT electrode voltage removed at the same time. The softened BSEP area is deformed out-of-plane by the pneumatic pressure, which props up the pin interface. The taxel is allowed to cool for 2 s before the pump is turned off. The raised pin's height is measured to be around 0.7 mm and remains relative stable after removal of the internal pneumatic pressure. The



raised pin falls back to the original position when the deformed BS80-AA5 is softened by the Joule heating electrode and recovers to flat.

B. Experimental methods for fabrication of the example tactile device described in section A

1. Materials

Urethane diacrylate (UDA) (catalog name: CN9021) was obtained from SARTOMER and used as received. Stearyl acrylate (SA), trimethylolpropane triacrylate (TMPTA), acrylic acid (AA), 2,2-Dimethoxy-2- phenylacetophenone (DMPA), benzophenone (BP), and isopropyl alcohol (IPA) were purchased from Sigma-Aldrich and used as received. Single-walled carbon nanotubes (P3-SWNT) were purchased from Carbon Solutions, Inc.

UDA is a urethane diacrylate oligomer comprising a flexible polyether diol segment and an aliphatic diisocyanate segment. In one or more examples, the homopolymer, poly(UDA), has a large elongation at break of 495%, a tensile strength of 0.93 MPa, and a modestly low modulus of 0.66 MPa at room temperature and 0.19 MPa at 50 °C. In one or more examples, the resulting BS80-AA5/poly(UDA) composite film has higher maximum elongation of 357% and tensile strength of 8.05 MPa compare to pristine BS80-AA5, and despite the strengthening effect from poly(UDA), the stress-strain behavior of the two films are very similar at strain smaller than 200%. Thus, in one or more examples, poly(UDA) won't have much mechanical effect on the BSEP film during operation of the device. In the example illustrated At room temperature, because of the lower modulus of poly(UDA), the storage modulus of the composite film is lower (320 MPa) compared to that of BS80-AA5 (344 MPa). In the rubbery state, the composite possesses a slightly higher modulus of 0.16 MPa compare to 0.13 MPa of BS80-AA5.

## 2. BS80-AA5 thin film fabrication:

The prepolymer solution was made by mixing 80 parts of SA (by weight), 20 parts of UDA, 5 parts of AA, 1.5 parts of TMPTA, 0.25 part of DMPA, and 0.125 part of BP at 50°C. The prepolymer solution was then injected between a pair of glass slides on a hot plate with two strips of tape as spacer. The thickness of the liquid layer was defined by the thickness of the spacer. Next, the prepolymer was cured through a UV curing conveyor equipped with a Fusion 300S type “H” UV curing bulb for about 3min. Then the film can be gently peeled off the glass slide after it cooled down to room temperature.

The CNT dispersion solution was made by mixing 5 mg of P3-SWNT powder, 1 ml water, and 20 ml IPA. The mixture was bath sonicated for 90 minutes (min) to get a stable dispersion. Large aggregates were then disposed using centrifuge at 8500rpm for 10min. The resulting supernatant is then ready for spray coating.

The stretchable S-CNT electrode was obtained by first prestretching the softened BSEP film by 100% × 100% biaxially. Then a shadow mask with serpentine pattern cutout was attached to the prestretched rigid BSEP. The prepared CNT dispersion solution was sprayed on BSEP through the mask using an airbrush at an air pressure of 30 pounds per square inch (psi). Next, a solution of UDA in toluene (10vol%) was sprayed and cured on top of the entire film without the mask. Finally, the film recovered to its original size by heating and releasing the prestretch.

The tensile stress-strain response of softened BS80-AA5 and BS80 were measured at 50 °C using DMA. The tensile strength is 8MPa for BS80-AA5 and 0.26MPa for BS80, while the elongation at break is 320% and 191% for BS80-AA5 and BS80 respectively. The improved toughness of BS80-AA5 is due to the reversible crosslinks introduced by acrylic acid.

### 3. Device assembly

The resulting film of BSEP with S-CNT was attached to the chamber cover with a double-sided Kapton™ tape as adhesive layer in between. The double-sided tape was cut with openings that align with the S-CNT matrix. The whole device could be assembled by screwing the chamber cover with the pneumatic chamber.

### 4. Finite element analysis simulation:

Finite element analysis (FEA) was carried out to study the mechanical performances of BS80-AA5 thin film. By taking advantage of mathematical approximation, FEA could simplify the complex physical analysis process to the overall consideration of every discrete, small, simple but interactional element in the system. Through comparing the experimental results and the simulated results, a more accurate perception could be obtained. To better understand the actuation performances, a computer simulation based on ANSYS FEA software was performed. Like most elastomers, softened BSEP is essentially incompressible. The strain energy function  $W$ , which is the energy preserved in material per unit volume, is defined as:

$$W = \sum_{i=1}^N C_{i0} (\lambda_1 - 3)^i \quad (5)$$

Where:

W = The strain energy density, which is strain per unit volume;

5

N = A positive deciding the number of terms in the above function (N=1 for Yeoh's 1<sup>st</sup> model, N=2 for

Yeoh's 2<sup>nd</sup> model and N=3 for Yeoh's 3<sup>rd</sup> model);

10  $r_1$  = The first invariant of the deviatoric strain;

$C_{ij}$  = Material constants, describing the shear behavior of the material;

By fitting the strain energy density function with the experimental uniaxial stress-strain curve through nonlinear least square optimization technique, Yeoh's 3<sup>rd</sup> hyperelastic model was selected to tailor the mechanical properties of softened BS80-AA5. Thus, the strain energy density function W was determined as:

15

$$W = 75060(r_1 - 3) + 22284(r_1 - 3)^2 - 908.2(r_1 - 3)^3$$

20

The constants in this nonlinear elastic model were derived from the strain-stress curve measured from the experimental uniaxial tensile test. Solid 185, a three-dimensional eight-node element type, was used to mesh the model. For the solver control of the FEA process, the large deflection option was on to take the nonlinear effect in for consideration. The model was set according to the international Braille standard. For the reported 4 × 4 tactile display, a layer of BS80-AA5 was first created on the bottom, on top of which a rigid PMMA substrate with through holes that correspond with the taxel areas was glued. In this way, areas other than the taxels are all constrained by the PMMA board as fixed support to prevent any deformation.

25

To demonstrate the actuation, ANSYS finite element model was carried out to simulate the internal pneumatic pressure needed to actuate a taxel to different heights. The tests were conducted on BS80-AA5 film with thickness ranging from 40 μm to 170 μm. The

simulated results match the experimental data quite well. The pneumatic pressure to generate a stroke of 0.7 mm is 100 mmHg for 40  $\mu\text{m}$  BSEP and 160 mmHg for 90  $\mu\text{m}$  BSEP. For the 170  $\mu\text{m}$  BSEP, the stroke with 160 mmHg pressure is only 0.3 mm. In one or more examples, the thinner the BSEP film is, the lower pressure is required to actuate the taxel to the same  
5 height. However, in one or more examples, if the BSEP is too thin, the taxel may not be able to provide enough blocking force to the end user. Thus, in one or more examples, 90  $\mu\text{m}$  BSEP was chosen to fabricate the tactile display. Please note that 160 mmHg is not high pressure, as a latex balloon in its 2/3 capacity has a pressure of 810 mmHg.

To demonstrate the heating performance, ANSYS finite element analysis was also  
10 carried out to simulate the current density distribution in serpentine shaped and round shaped electrode (FIG. 5C and FIG. 5D). Both models are established according to the setup of one taxel. The resistivity of SWCNT ( $10^{-7} \Omega\cdot\text{m}$ ) and the mesh size of 0.02 mm were applied to the two models. 30 V was set as the activation voltage during the simulation. The serpentine shaped and round shaped electrode were divided into 6578 elements and 3103 elements  
15 respectively to analyze their steady-state electric conduction. Based on the simulation results, the serpentine shaped CNT has a more uniform distribution of current density within the electrode area, which should serve better as heating electrode.

The experimental results of the heating performance of serpentine shaped CNT and round shaped CNT are also corresponding with the simulation. With same resistance (50  
20  $\text{k}\Omega$ ) and voltage supply (30 V), the serpentine shaped electrode exhibits higher and more locally defined heating spots. For the S-CNT, the time needed to reach 50  $^{\circ}\text{C}$ , which is the temperature to soften BS80-AA5, is less than 1 second (s) whereas round shaped electrode is unable to reach the required temperature even after 5 seconds of applied voltage. The infrared thermal images (ICI 9320P) of the serpentine shaped electrode illustrates these  
25 advantages. That is because that during the lengthy heating process of round shaped electrode, more and more heat dissipates through air and surrounding materials, crosstalk of adjacent taxels could happen with such high-density array. As for the serpentine shaped CNT, the unique winding path increases the heating efficiency and results in rapid heating in a very short time.

### C. Process steps

FIG. 7 is a flowchart illustrating a method of fabricating a refreshable tactile display unit.

5 Block 700 represents providing a polymer (e.g., polymer membrane) which is relatively rigid at ambient temperature and rubbery at an elevated temperature (e.g., above a transition temperature).

In one or more examples, the polymer/polymer membrane is the bistable electroactive polymer (BSEP) comprising combination of stearyl acrylate (SA), urethane diacrylate  
10 (UDA), acrylic acid (AA), trimethylolpropane triacrylate (TMPTA), 2,2-Dimethoxy-2-phenylacetophenone (DMPA), and benzophenone (BP).

In one or more examples, the polymer/polymer membrane is the bistable electroactive polymer (BSEP) comprising 80 parts of stearyl acrylate (SA) by weight, 20 parts of UDA by weight, 5 parts of acrylic acid (AA) by weight, 1.5 parts of trimethylolpropane triacrylate  
15 (TMPTA) by weight, 0.25 parts of 2,2-Dimethoxy-2-phenylacetophenone (DMPA) by weight, and 0.125 parts of benzophenone (BP) by weight.

In one or more embodiments, the polymer/polymer membrane is the bistable electroactive polymer (BSEP) comprising 40-80 parts of stearyl acrylate (SA) by weight, 20-  
20 60 parts of UDA by weight, 5-15 parts of acrylic acid (AA) by weight, 0.25-1.5 parts of trimethylolpropane triacrylate (TMPTA) by weight, 0.125-0.75 parts of 2,2-Dimethoxy-2-phenylacetophenone (DMPA) by weight, and 0.0075-0.2 parts of benzophenone (BP) by weight.

In one or more embodiments, the polymer/polymer membrane is the bistable electroactive polymer (BSEP) comprising a combination of tert-butyl acrylate (TBA),  
25 urethane diacrylate (UDA), ethoxylated trimethylolpropane triacrylate (ETMPTA), and 2,2-Dimethoxy-2-phenylacetophenone (DMPA).

In one or more embodiments, the polymer/polymer membrane is the bistable electroactive polymer (BSEP) comprising 90-110 parts of tert-butyl acrylate (TBA) by weight, 5-25 parts urethane diacrylate (UDA) by weight, 1-5 parts ethoxylated  
30 trimethylolpropane triacrylate (ETMPTA) by weight, and 0.25-1.5 parts 2,2-Dimethoxy-2-phenylacetophenone (DMPA) by weight.

In one or more embodiments, the components (e.g., TBA, UDA, ETMPTA, DMPA, SA, AA, and/or TMPTA) of the BSEP examples provided herein are polymerized together through chemical bonds to form a massive polymer network.

In one or more examples, the bistable electroactive polymer is a polymer exhibiting SMP and electrical actuation in the rubbery state. In one or more examples, the display described herein does not utilize the electrical actuation property of the BSEP.

In one or more embodiments, the BSEP is a phase changing polymer changing modulus using a different mechanism as compared to an ordinary SMP.

In one or more examples, the polymer membrane has a tensile modulus greater than 100 MPa but less than 10 GPa at the ambient temperature and has a tensile modulus of greater than 10 kPa but less than 10 MPa at the elevated temperature. In one or more examples, the polymer membrane possesses a tensile modulus of at least 100 MPa at room temperature to provide a high blocking force and becomes rubbery with tensile modulus less than 1MPa at the elevated temperature to become deformable and stretchable. In one or more examples, the polymer membrane comprises a phase changing polymer exhibiting a tensile modulus change by at least two orders of magnitude in a temperature range of less than 10 °C. In one or more examples, the polymer membrane has the transition temperature comprising a rigid-to-soft transition temperature higher than 40 °C but lower than 70 °C.

In one or more examples, the polymer membrane has a thickness greater than 10 μm. Block 702 represents coupling a conductive layer including one or more heating elements (e.g., Joule heating elements) to the polymer membrane. In one or more examples, the step comprises coupling a conductive layer, including one or more serpentine patterns, to the polymer membrane.

In one or more examples, the conductive layer is a coating on the polymer membrane. In one or more examples, the conductive layer is deposited by printing, spraying, or casting.

In one or more examples, the conductive layer can be deposited into serpentine patterns.

In one or more examples, the conductive layer is heated when a voltage is applied between two separated points on the conductive layer.

In one or more examples, the conductive layer comprises carbon nanotubes (e.g., single walled carbon nanotubes). The carbon nanotubes can be embedded in a polymer layer, for example.

In one or more examples, the conductive layer comprises silver nanowires. The silver nanowires can be embedded in a polymer layer, for example.

Block 704 represents connecting a fluidic pressure chamber to the polymer membrane and a fluidic pressure source. The fluidic pressure chamber can apply/transfer fluidic pressure (generated in the fluidic pressure source) to the polymer membrane so as to deform the polymer membrane. The fluidic pressure chamber can be rigid or flexible.

In one or more examples, the fluidic pressure comprises pneumatic pressure caused by compressed gas, a pneumatic pump, or compressed vapor due to liquid evaporation.

In one or more examples, the fluidic pressure comprises liquidous pressure caused by compressed liquid, a liquid pump, or a liquid volume change due to a phase change or a temperature change.

Block 706 represents connecting a rigid membrane including one or more through holes. The polymer membrane deforms through the one or more through holes, or actuates a pin in each of the through holes, in response to (1) the conductive layer heating the polymer membrane to the elevated temperature (so as to form a softened polymer membrane which is rubbery/in a rubbery state), and (2) the fluidic pressure source applying the fluidic pressure to the softened polymer membrane. Each of the through holes may define a tactile pixel area and be aligned with a heating element (e.g., serpentine pattern) in the conductive layer so that the heating element can provide local heating of the polymer membrane.

In one or more examples, the rigid membrane is laminated on the polymer membrane.

Block 708 represents the end result, a refreshable tactile display, e.g., as illustrated in FIG. 1.

In one or more examples, the refreshable tactile display comprises a matrix of tactile pixels each controlled by softening a surface area of a polymer membrane at one or more pixel areas, wherein the polymer membrane is relatively rigid at ambient temperature and rubbery at an elevated temperature; a conductive layer including a matrix of heating elements (e.g., serpentine patterns), each of the heating elements coupled to a different one of the surface areas of the polymer membrane; and a rigid membrane comprising through holes,



each of the through holes aligned above one of the heating elements (e.g., one of the serpentine patterns). The softening of the polymer membrane is controlled by applying a voltage across the conductive layer (or across one or more of the heating elements), so as to heat one or more of the surface areas of the polymer membrane to the elevated temperature and into a softened state. As illustrated herein, the one or more surface areas in the softened state are deformed out of a plane of the polymer membrane into a deformed state by the fluidic pressure applied from a fluidic pressure source, such that part of the tactile pixel coupled to one of the surface areas is raised above a plane including the through holes. In one or more examples, the deformed state is maintained at the ambient temperature and deformation in the deformed state is recovered by raising a temperature of the one or more surface areas (deformed areas) to above a softening temperature at which the polymer membrane softens.

In one or more examples, each serpentine pattern or heating element covers one of the surface areas comprising a circular area with diameter larger than 0.1 mm but less than 10 mm, and each serpentine pattern aligns with one of the through holes, comprising a circular through hole, on the rigid membrane. In one or more examples, the rigid membrane comprises a chamber cover for a fluidic pressure chamber connected to the fluidic pressure source, so that the fluidic pressure chamber may transfer or apply the fluidic pressure to the polymer membrane.

FIG. 7A and 7B illustrate, in one or more examples, the method of making the refreshable tactile display comprises (a) stretching the softened polymer membrane and maintaining deformation of the softened and/or stretched polymer membrane when the polymer membrane is cooled to ambient temperature (e.g., as represented in the providing step 700 or step 710); (b) applying/spraying a dispersion of carbon nanotubes (CNTs) in a solvent onto the deformed rigid polymer membrane through a shadow mask which has one or more serpentine shaped cutout pattern(s), so as to form a carbon nanotube coating on the deformed rigid polymer membrane (e.g., as represented in the coupling step 702 or step 712); (c) spraying or applying a solution comprising a polymer or polymer precursor on top of the carbon nanotube coating (e.g., as represented in step 700 or step 714); and (d) releasing the deformation of the stretched polymer membrane at elevated temperature (Block 716), and cooling down to ambient temperature (Block 718), so as to form the display 500.

FIG. 7A and 7C illustrate, in one or more further examples, the method of making a refreshable tactile display comprises (a) forming a coating of carbon nanotubes on a release substrate (Block 720); (b) patterning the coating into serpentine shapes, e.g., by laser ablation (Block 722); (c) applying a polymer precursor layer over the coating (Block 724);  
5 (d) curing the polymer precursor layer, forming a cured polymer layer (Block 726); and (e) separating the cured polymer layer from the release substrate (Block 728), so as to form the display 500.

#### D. Example Display Panel

10 FIG. 8 illustrates an electronic display technology (e.g., PolyPad) for Braille text and graphics. The proposed display panel comprises an array of tactile pixels (taxels) electronically actuated to various raised heights (e.g., up to 0.6 mm) from the surface and maintain form until triggered to relax. In one example, the display 500 may be thin and packaged as a smartphone or tablet case as an attachment of the mobile devices. Most of the  
15 mobile devices are Braille ready. In one example, once folded, the display fits within the silhouette of the smartphone, e.g., with a total thickness of ~ 1 cm and weighing ~150 grams and/or such that the folded device has an outside envelope of ~80 × 160 × 10 mm. Thus, in one or more examples, the device has one or more of the following characteristics: foldable, lighter weight, more content, and lower cost than conventional devices, benefiting a majority  
20 of current Braille users and possibly promoting Braille literacy rate through their enhanced functionality and user friendliness.

FIG. 9A and FIG. 9B illustrate operation of an example BSEP transducer for use in the display, the BSEP comprised of nanometer-size crystalline aggregates in a chemically crosslinked polymer matrix; the reversible phase-change results in a large modulus change  
25 from rigid to rubbery states during temperature cycles. The storage modulus of the polymer at room temperature is on the order of 100 MPa, similar to a tough plastic and sufficient to serve as Braille dots. Above the phase-change temperature ( $T_m$ ), the polymer becomes rubbery with a storage modulus ~0.2 MPa (state B), and it can be either electrically actuated or mechanically deformed (state C). The  $T_m$  itself is tunable around 40°C, as shown in the  
30 modulus charts in FIG. 9B. The polymer also demonstrates shape memory properties with fixation rate and recovery rate both close to 100%; thus, it can be systematically actuated to undergo large, rigid-to-rigid deformation (A to D).

In one or more examples, the Braille dots can be actuated with displacement of around 0.6 mm by applying 100 V/ $\mu$ m electric field to the softened BSEP membrane. The use of such a device in real-life application can be challenging due to the high driving voltage, about 4 kV (as high-V, low-power switching circuits may be currently unavailable).  
5 In addition, the insulation requirements for the high V bus lines between dots (pixels) limits the display resolution. Finally, controlling the temperature change in the actuation cycle requires Joule heating electrodes that are highly compliant to avoid restricting the expanding BSEP film all the while sustaining repeated large-strain deformation without significant loss of conductivity. FIG. 10 illustrates an example transducer technology (comprising taxel  
10 architecture and actuation mechanism) for the display that can overcome these challenges, exploiting the variable stiffness of the BSEP polymer which is thus also called a variable stiffness polymer (VSP). In the example, a compliant and stretchable serpentine-shaped silver nanowire (AgNW) Joule heating electrode is used to modulate the stiffness of the VSP. A pneumatic pressure change supplied by a miniature-sized pump expands the VSP film to  
15 raise Braille pins. A flexible printed circuit board (PCB) is placed on the VSP film and aligned with the AgNW electrodes. Circular openings in the PCB allow the out-of-plane (diaphragm) deformation of the VSP films in the active taxel areas. The outer most sheet – the chamber cover – contains pins that interface with the user’s fingertips.

In one or more examples, the taxel architecture enables a PolyPad panel comprising 5  
20  $\times$  15 Braille cells, wherein each cell is made up of  $3 \times 2$  Braille dots set to display alphanumeric letters and numbers (0 to 9). In one or more examples, 3D printing techniques can be used fabricate the pneumatic chamber, pins, and other essential parts of the display device. In one or more further examples, a low-voltage (e.g., 12 V), high-current driving circuit can be fabricated to display Braille texts and refresh the contents.

25 FIG. 11 illustrates an example taxel architecture comprising a multiline tactile device with compact form factor that can display graphical information. FIG. 11 illustrates that a multiline display with a size of a smart phone screen can convert visual information into tactile patterns, including English letters, molecular structures, and maps.

30 D1. Example: Improving the VSP polymer for operational efficiency and robustness  
The BSEP polymer BS80 shown in FIG. 12A exhibits a modulus of  $>100$  MPa at

ambient temperatures, which is important to maintain a large supporting force and its shape (FIG. 12A). Above 45 °C, it becomes a soft rubber with reversible, large-strain deformation (Fig. 12B). As the core active material, it is essential for BS80 to have steep modulus variation and high tensile strength at both the rigid and rubbery states to ensure high supporting force and durability during repeated use and incidental impacts. The preliminary BS80 is a random copolymer of stearyl acrylate (SA) and butylacrylate at an 80:20 weight ratio. A small amount of trifunctional acrylate monomer was added for chemical crosslinking. The randomly distributed crystalline size of SA moieties in rigid BS80 has resulted in modulus inconsistency below the transition temperature (FIG. 13, black curve), which affects the supporting force of the Braille dot. The synthesis of controllable polymer structure can be investigated and modified to make the BSEPs with more predictable modulus change and higher toughness.

Further improvement can expand the modulus plateau below the transition temperature such that below 42 °C the modulus remains above 100 MPa, maintaining the shape of the raised Braille dots and providing large supporting force even in hot weather (Fig. 13B, blue curve), e.g., by synthesizing a triblock copolymer comprised of two SA homopolymer chains linked by a butylacrylate homopolymer chain (Fig. 13B) via anionic living or atom transfer radical polymerization. The homopolymer chains in the resulting VSP polymer will have controllable chain length and narrow chain length distribution (polydispersity <1.1) [23]. The stearyl groups in this new VSP may be more closely assembled than those in the BS80, and thus can crystallize more rapidly below its melting temperature, which determines the polymer's  $T_m$ . The resulting nanocrystallites may have a more uniform size distribution, and the softening of the BSEP may be suppressed until approaching the  $T_m$ , leading to steep modulus change in a narrow phase-changing temperature range shown by the blue curve in Fig. 13A. The modulus of the BSEP at the rigid state may be tuned by the weight ratio of poly(SA) blocks to poly(butylacrylate) blocks. The crosslinking groups at the polymer chain ends (X in Fig. 13B) may be introduced to affect chemical crosslinking and prevent viscous flow in the softened state. This chemical crosslinking has at least two interesting features. First, the modulus above  $T_m$  is determined by the chemical crosslink density and thus remains relatively flat with further increasing temperature. This constant modulus eases the control of the actuation strain. Second, the

modulus in the rubbery state is controllable by adjusting the concentration of the X group. Low modulus in the soft state is essential for low pressure actuation and low energy consumption. However, the polymer must retain high toughness to prevent material rupture.

Other examples of polymer include Kraton™, which is synthesized by anionic living polymerization and known for high tensile strength. Similar ABA-type triblock copolymers exhibiting supersoft modulus but low tensile strength have also been synthesized by atom transfer radical polymerization [24, 25] and may also be used.

a. Modifying the polymerization conditions to increase the chain lengths in the triblock copolymer. The reaction is sensitive to moisture and protonic acid impurities. Thus, all monomers will be carefully purified before use. The inhibitors added in the monomers to prolong storage lifetime will be removed with flash chromatography. Furthermore, experimental conditions, such as the reaction temperature and duration, may be systematically adjusted to maximize the polymer chain.

15

b. Introducing reversible crosslinks to enhance toughness

Physical crosslinks such as hydrogen bonds have been identified as essential elements in enhancing the toughness of soft gels [26, 28, 34]. The non-permanent crosslinks can break and re-form to overcome stress concentration and dramatically restrict crack propagation. In our preliminary study modifying the BS80 polymer, a random copolymer synthesized via free radical polymerization, adding acrylic acid significantly enhanced the polymer's tensile strength (FIG. 3F). At 5% acrylic acid loading, the tensile strength reaches 8 MPa. The true tensile strength is calculated to be 34 MPa, which is in the range of polyurethane [28] at 42 MPa and PDMS-silica composite [29] at 27 MPa. Without the toughening effect from acrylic acid, the BSEP ruptured at 191% strain with a tensile strength of only 0.26 MPa (true stress calculated to be 0.76 MPa). To adapt this approach for the ABA triblock copolymer BSEP, the acrylic acid can be studied as a hydrogen bond forming co-monomer. In one or more examples, the amount of acrylic acid and acrylamide may be varied between 0 and 10 weight%. The tensile strength, as well as the storage modulus and loss factor of the resulting polymers may be characterized to obtain the structure-property relationship which may be used to guide optimization of overall performance (e.g., using statistical evaluation)..

30

Improved BSEP according to embodiments described herein are enabling technology of the PolyPad device. In one or more examples, the target VSP material may have a  $T_m$  of ~43 °C, such that the modulus of the polymer exceeds 100 MPa at temperatures up to 42 °C, high enough to avoid accidental softening due to environmental heat. The modulus at 45 °C and higher may be at least three orders of magnitude lower, enabling pneumatic raising of the Braille dots by a low-cost compact pneumatic pump. In one or more examples, decreasing the temperature range required to accomplish this stiffness variation to 3 °C reduces power consumption by 50%. The VSP film at the soft state may have a true tensile strength greater than 10 MPa to resist tearing and puncture, and other types of mechanical bumps that would be expected in typical usage in the field. In one or more examples, the film can be biaxially stretched by 100% area expansion for 200,000 cycles without measurable fatigue to meet the application requirement. The estimated 200,000-cycle of operation assumes a device lifetime of 3 years, in which an average user flips 300 pages per day. In one or more examples, to mitigate against chain-growth polymerization being hindered by the presence of acrylic acid, acrylamide, another commonly used monomer containing hydrogen bonds can be used.

D2. Example: Improving the Joule heating electrode for fast heating and low cost fabrication in the display

Temperature controls the modulus change of the VSP. A compliant electrode coated on the VSP provides localized Joule heating to efficiently regulate the transition while also compensating for heat dissipation. We have developed a composite electrode technology for stretchable electronic devices in which CNTs and/or AgNWs are embedded in the surface layer of the substrate, providing high surface conductivity without significantly impeding the deformability of the polymer substrate [59-62]. Electrode resistance is constant at up to ~30% strain, but larger strain induces significant resistance increases, lowering the heating power from a given driving voltage. Serpentine-architecture electrodes have been explored as an effective approach to impart large stretchability to metal films [63-67]. We combined these two approaches and fabricated serpentine shaped CNT electrodes embedded in the surface layer of BSEP films (FIG 14A). The serpentine ribbon was formed by spray coating through a shadow mask. This electrode can heat to 70 °C in 2 seconds at 30 V, with constant electrode resistance at up to 180% area expansion and for 100,000 cycles at 100% area

expansion. This is very promising or useful for the application in a display. Further improvements may include (1) significantly lowering the electrode resistance in order to increase the heating rate and thus the refresh speed of the PolyPad devices, (2) lowering the resistance allowing the Joule heating to be done at 12 V enabling use of store-bought, inexpensive, and compact switching circuits; and (3) improved pattern resolution and, by extension, fabrication yield.

The electrical power equals  $(V)^2/R$ , where  $V$  is the driving voltage and  $R$  is the load resistance. Reducing the voltage from 30 V to 12 V requires lowering the load resistance from 50 k $\Omega$  to 8 k $\Omega$  to maintain the electrical power. This is obtainable by increasing the thickness of the CNT layer by a factor of 6.25, but the layer would become more rigid and impede the expansion of the VSP film [68]. As such, in one or more examples, a much more conductive material than CNT (e.g., silver nanowires) can be instead be used to form the serpentine-shaped Joule heating electrode. Our work has led to AgNW coating with a sheet resistance as low as 10  $\Omega$ /sq, with high optical transparency and mechanical compliancy [59, 69]. The AgNWs has also demonstrated effective and stable heating up to 200 °C. When a uniform coating of AgNWs is transferred into an elastomer substrate, the resulting composite electrode can be stretched to 50% strain repeatedly and reversibly [69, 70]. However, the resistance at 50% strain is three times that at zero strain, partly due to elongated shape and partly due to other factors, including sliding among nanowires. In one or more examples, the AgNW coating may be patterned into a serpentine-shaped ribbon to better accommodate large macroscopic strains while maintaining small strains within the ribbon (FIG. 15). In one or more examples, nanowire (e.g., Ag nanowire) ribbons can be patterned by laser ablation, e.g., with one or more of the following dimensions: 50  $\mu$ m wide AgNW ribbons with 10  $\Omega$ /sq, total length of the ribbon of 15 mm for each 1.5 mm diameter Braille dot, and length-to-width ratio of the ribbon of 15 mm/50  $\mu$ m or 300. For such dimensions, the resistance is 10  $\Omega$   $\times$  300 or 3 k $\Omega$ , much lower than the 8 k $\Omega$  required to lower the driving voltage from 30 to 12 V. The heating rate is thus increased by at least 166% (heating rate increases superlinearly with input electrical power as heat dissipation loss is reduced with faster heating). It is estimated that the heating time to raise the temperature of the VSP film to >45 °C can be controlled to within 0.5 s via the new compliant AgNW electrode.

The combination of highly conductive AgNW network and the stretchable serpentine patterning may lead to Joule heating electrodes with low voltage activation (12 V), high stretchability (>100% area strain), and fast refresh speed (~1 s). The heating speed can be improved to 0.5 s. The cooling speed could also be improved to <0.5 s with the stiffness variation of the VSP film being completed within a temperature range spanning only 3 °C. Therefore, the refresh speed can be shortened to ~1 s as compared to ~5 s at present.

A potential problem is increased resistance after repeated heating and stretching cycles of the AgNW based heaters. We have proven that CNT serpentine electrodes are capable of stable resistance performance across 100,000 cycles at 100% area expansion. A risk mitigation is to increase the sheet resistance of the AgNW coating to below 10 Ω/sq, such that the ribbon could be made thinner to lower the local strain in the ribbon. Techniques that we have separately developed to improve the thermal stability of the AgNW network<sup>45</sup> may also be introduced as necessary to ensure that the resistance increase after 200,000 heating cycles is no more than 20%.

15

### D3. Example Assembling driving circuit and fabricating proof-of-concept PolyPad devices

FIG. 16 illustrates an example Braille cell that can be used in a Polypad device. The cell is actuated to display in sequence the letters “U”, “C”, “L”, and “A” in Braille. This Braille cell is a convenient platform to evaluate the VSP polymer, the compliant Joule heating electrode, and to articulate the layered structure of the taxel panel. FIG. 10 illustrates the general architecture of the taxel array scaled up to  $4 \times 10$  cells. In one or more examples of a smartphone device embodiment (FIG. 8), a panel comprising  $5 \times 15$  cells may be used to cover the smartphone screen area. With a total of  $5 \times 15 \times 6$  or 350 Braille pins that need to be independently controlled to display and refresh Braille contents, designing a rapid-switching, compact and energy efficient driving circuit is an important aspect.

FIG. 17A illustrates an example operational scheme for the Braille display based on an BSEP film: when the corresponding heating voltage is turned on, it takes ~ 2 seconds to heat and soften the BSEP film in the Braille dot areas. Midway during heating the air pump is activated to raise the softened dots. The heating voltage is then powered off, and the pump stays on for another 2 seconds until the VSP has stiffened. The raised dots retain their shapes

30



until the next refresh cycle. The actuation voltages are 30 V for heating and 5 V for pumping. FIG. 17B illustrates an example integrated circuit fabricated on a compact printed circuit board (PCB) to supply 30 V inputs to the Joule heating electrodes to individually switch the Braille dots on a PolyPad panel. The prototype PCB is  $150 \times 70 \times 1.6$  mm, and was designed to control the actuation of a  $4 \times 10$  Braille cell matrix. During operation, the Braille content displays from the beginning of the first line. It requires about 4 seconds to display each line, and a total time of 16 seconds for the control panel to finish displaying one page. This preliminary work demonstrates the technical feasibility. In another example, the PCB can be designed to control  $5 \times 15$  cells with compact size, faster refresh speed, and high power efficiency.

Line-scanning technique was used in the preliminary PCB to control the actuation of each line, meaning that the four lines share the same 8-bit data signals from the microprocessor control unit (MCU) as shown in FIG. 18A. By doing that, the number of I/O ports of MCU was largely reduced for small-size structure. However, the display time to actuate the whole page increased accordingly. A more efficient architecture for the  $5 \times 15$  Braille cell array, as shown in FIG. 13B, can be used to parallelly display 5 lines. In this architecture, data are parallelly collected in the serial-to-parallel modules and distributed to the five lines. By doing this, it only takes  $2 \mu\text{s}$  more time to finish data generation for the whole page display in each refresh process as compared to refreshing a single line in the previous design. This approach reduces refresh of PolyPad Braille content from 16 to 4 seconds, while maintaining the compact form factor of the PCB. Use of the improved VSP film and compliant AgNW electrode illustrated herein, respectively, can potentially shorten screen refresh time to  $\sim 1$  second (s).

Electrical contacts between the bus lines in the PCB board and the Joule heating electrodes can be made by proper alignment, as illustrated in FIG. 15. A silver nanoparticle paste minimizing contact resistance will be screen printed on the contact ends of the Joule heating electrodes before tassel panel assembly.

An exemplary device may further include a smartphone application (e.g., the iOS APP) and communication (firmware and electronics) between the APP and the tactile display. The APP captures content from three types of sources. The most direct source is pre-loaded reading materials such as books. Another source is an internet browser, where text

from web pages can be obtained by a HTML parser. Finally, the APP can capture displayed images, then recognize handwritten characters using Optimal Character Recognition (OCR) algorithm or run image classification to generate captions using an artificial intelligence (AI) server in the Cloud. The APP then translates the contents from the above sources into Braille text, and communicates with or drives the tactile display via Bluetooth, e.g., which consumes about 2.5 milliwatts (mW) with around 10 meters range.

In one or more examples, the power consumption of the PolyPad is mainly for heating, pumping, refreshing and communicating. In various examples, the PCB and the Bluetooth together consume about 40 mW (peak power is 50 mW) during operation, and heating and the pneumatic pump consume a peak power of approximately 0.7 W total, giving a total peak power consumption of the PolyPad of about 0.8 W. Under such exemplary conditions, equipped with a typical phone battery (~3000 mAh), the device can work for around 5 hours after each full charge if a user refreshes the pages rapidly. Under normal use, the usage time is more than 2 days without need of recharging.

In one or more examples, the thickness of the Braille display panel is determined by the PCB board, the pneumatic pump, and the battery. The PCB can be fabricated on a metal thin sheet for compactness and enhanced mechanical properties, for example. A commercial micro air pump,  $3.75 \times 1.78 \times 0.5 \text{ cm}^3$ , designed for medical application producing 30 kPa pressure and 4.7 mL/s flow rate, can drive the softened VSP film, for example. A typical ~3000 mAh lithium battery is  $11 \times 5 \times 0.3 \text{ cm}^3$ . Using such components, the overall thickness of the PolyPad device embodiment is ~ 1 cm, thicker than a typical iPhone cases, but still comfortably fitting in a user's pocket. Total device weight is ~ 150 grams, slightly lighter than an iPhone X.

Adhesive layers can also be selected (e.g., as available at 3M<sup>®</sup>) and air-releasing microchannels may be created to obtain the optimal tradeoff for rapid expansion of the VSP film when the pump is on, and rapid release (via leakage) of the air pressure when the pump is turned off. The results can be administered with the internal pneumatic pressure to guarantee the Braille dots rapidly raise during actuation and rapidly return during refreshing.

In one or more examples, a fabrication process includes: (1) large area coating of the VSP polymer by doctor blade coating in a clean environment for highly uniform films; (2) AgNW electrode deposition using Meyer rod techniques and patterning using a laser scribe;

and (3) assembly and alignment of the components. Raised Braille pin heights with respect to applied pneumatic pressure, supporting force on the pin, and cycle lifetime of the device can be characterized and modified according to application. In one or more examples, materials and textures of the pin top surface can be selected for optimal tactile reading.

5 To adapt the above design for the fabrication of a tactile graphic display panel comprising  $23 \times 44$  pins, the same pin-to-pin center distance of 2.5 mm can be maintained. The taxels are uniformly distributed over the smartphone screen area. An exemplary PCB board can include buslines vertically interconnected electrode (VIE) such that the buslines do not occupy the taxel surface area. In one or more examples, a circuit can be designed to  
10 enable the control of 3 discrete states of the pump: OFF, 50% and 100% pressure, to correspond to the flat, half-raised, and fully raised Braille pin heights. In one or more examples, the dimensions and power consumption of the graphic panel is comparable to the Braille-only panel.

PolyPad durability and ruggedness can be comparable to other consumer electronics  
15 made for continuous use in active environments, such as cell phones and biomedical devices, due to use of analagous materials, component designs, and manufacturing processes.

#### Example embodiments

A display or unit according to one or more embodiments described herein include, but  
20 is not limited to, the following examples.

1. A refreshable tactile display unit comprising:

a) a polymer (104) membrane (102a) comprising a polymer (104) which is relatively rigid (106) at an ambient temperature and in a rubbery state (130, 134) (108) at an elevated temperature, wherein a rigid (106)-to-soft transition of the polymer (104) occurs within a  
25 temperature range narrower than  $10^\circ\text{C}$  (degrees Celsius);

b) a fluidic pressure chamber (110), wherein the fluidic pressure chamber (110) applies fluidic pressure (112), generated from a fluidic pressure source (114), to the polymer (104) membrane (102a);

d) a conductive layer (116) including one or more heating elements (118) coupled to  
30 the polymer (104) membrane (102a); and

e) a rigid (106) membrane (102a) comprising one or more through holes (122)holes (122), wherein:

the polymer (104) membrane (102a) deforms through the one or more through holes (122)holes (122) in response to:

5 one or more of the heating elements (118) heating the polymer (104) membrane (102a) to the elevated temperature so as to form a softened polymer (104) membrane (102a) in the rubbery state (130, 134) (108), and

the fluidic pressure source (114) applying (100) the fluidic pressure (112) to the softened polymer (104) membrane (102a) so as to deform the polymer (104) membrane  
10 (102a).

2. The unit of embodiment 1, wherein the polymer (104) is the bistable electroactive polymer (104) (BSEP) comprising a combination of stearyl acrylate (SA), urethane diacrylate (UDA), acrylic acid (AA), trimethylolpropane triacrylate (TMPTA), 2,2-  
15 Dimethoxy-2- phenylacetophenone (DMPA), and benzophenone (BP).

3. The unit of embodiment 1, wherein the polymer (104) is the bistable electroactive polymer (104) (BSEP) comprising 80 parts (2) of stearyl acrylate (SA) by weight, 20 parts (2) of UDA by weight, 5 parts (2) of acrylic acid (AA) by weight, 1.5 parts  
20 (2) of trimethylolpropane triacrylate (TMPTA) by weight, 0.25 parts (2) of 2,2-Dimethoxy-2- phenylacetophenone (DMPA) by weight, and 0.125 parts (2) of benzophenone (BP) by weight.

4. The unit of embodiment 1, wherein the polymer (104) is a bistable  
25 electroactive polymer (104) (BSEP) comprising 40-80 parts (2) of stearyl acrylate (SA) by weight, 20-60 parts (2) of UDA by weight, 5-15 parts (2) of acrylic acid (AA) by weight, 0.25-1.5 parts (2) of trimethylolpropane triacrylate (TMPTA) by weight, 0.125-0.75 parts (2) of 2,2-Dimethoxy-2- phenylacetophenone (DMPA) by weight, and 0.0075-0.2 parts (2) of benzophenone (BP) by weight.

30

5. The unit of embodiment 1, wherein the polymer (104) is a bistable electroactive polymer (104) (BSEP) comprising a combination of tert-butyl acrylate (TBA), urethane diacrylate (UDA), ethoxylated trimethylolpropane triacrylate (ETMPTA), and 2,2-Dimethoxy-2- phenylacetophenone (DMPA).

5

6. The unit of embodiment 1, wherein the polymer (104) is a bistable electroactive polymer (104) (BSEP) comprising 90-110 parts (2) of tert-butyl acrylate (TBA) by weight, 5-25 parts (2) urethane diacrylate (UDA) by weight, 1-5 parts (2) ethoxylated trimethylolpropane triacrylate (ETMPTA) by weight, and 0.25-1.5 parts (2) 2,2-Dimethoxy-  
10 2- phenylacetophenone (DMPA) by weight.

7. The unit of any of the embodiments 1-6, wherein the polymer (104) membrane (102a):

15 has a tensile modulus greater than 100 megapascals (MPa) but less than 10 gigapascals (GPa) at the ambient temperature; and

has a tensile modulus of greater than 10 kPa but less than 10 MPa at the elevated temperature.

8. The unit of any of the embodiments 1-7, wherein the polymer (104) membrane (102a) has a rigid (106)-to-soft transition temperature higher than 40°C but lower than 70°C.

9. The unit of any of the embodiments 1-8, wherein the fluidic pressure (112) comprises pneumatic pressure caused by compressed gas, a pneumatic pump, or compressed  
25 vapor due to liquid evaporation.

10. The unit of any of the embodiments 1-8, wherein the fluidic pressure (112) comprises liquidous pressure caused by compressed liquid, a liquid pump, or a liquid volume change due to a phase change or a temperature change.

30

11. The unit of any of the embodiments 1-10, wherein the fluidic pressure (112) chamber (114) is rigid (106).

12. The unit of any of the embodiments 1-10, wherein the fluidic pressure (112) chamber (114) is flexible.

13. The unit of any of the embodiments 1-12, wherein the conductive layer (116) is a coating on the polymer (104) membrane (102a).

14. The unit of any of the embodiments 1-13, wherein the conductive layer (116) is deposited by printing, spraying, or casting.

15. The unit of any of the embodiments 1-14, wherein the conductive layer (116) is heated when a voltage is applied between two separated points on the conductive layer (116).

16. The unit of any of the embodiments 1-15, wherein each of the heating elements (118) comprises a serpentine pattern.

17. The unit of any of the embodiments 1-16, wherein each of the through holes (122) defines a tactile pixel (124) area and is aligned with a heating element in the conductive layer (116) so that the heating element provides local heating of the polymer (104) membrane (102a).

18. The unit of any of the embodiments 1-17, wherein the rigid (106) membrane (102a) is laminated on the polymer (104) membrane (102a).

19. A refreshable tactile display (500), comprising:  
a plurality of tactile pixel (124)s each controlled by softening a surface (142) area of a polymer (104) membrane (102a), wherein the polymer (104) membrane (102a) is relatively

rigid (106) at ambient temperature and in a softened state (130, 134) at an elevated temperature;

a conductive layer (116) including a plurality of heating elements (118), each of the heating elements (118) coupled to a different one of the surface (142) areas of the polymer (104) membrane (102a); and

a rigid (106) membrane (102a) comprising through holes (122)holes (122), each of the through holes (122)holes (122) aligned with one of the heating elements (118), wherein:

the softening of the polymer (104) membrane (102a) is controlled by applying (100) a voltage across one or more of the heating elements (118), so as to heat one or more of the surface (142) areas of the polymer (104) membrane (102a) to the elevated temperature and into the softened state (130, 134);

the one or more surface (142) areas in the softened state (130, 134) are deformed out of a plane (132, 136) of the polymer (104) membrane (102a) into a deformed state (130, 134) by a fluidic pressure (112) generated using a fluidic pressure (112) source, such that part of the tactile pixel (124) coupled to the surface (142) area associated with the tactile pixel (124) is raised above a plane (132, 136) including the through holes (122)holes (122);

the deformed state (130, 134) is maintained at the ambient temperature; and

deformation (134a) in the deformed state (130, 134) is recovered by raising a temperature of the one or more surface (142) areas in the deformed state (130, 134) to above a softening temperature at which the polymer (104) membrane (102a) softens.

20. The refreshable tactile display (500) of embodiment 19, wherein the polymer (104) membrane (102a):

comprises a phase changing polymer (104) exhibiting a tensile modulus change by at least two orders of magnitude in a temperature range of less than 10°C;

possesses a tensile modulus of at least 100 MPa at room temperature to provide a high blocking force, and

becomes rubbery with tensile modulus less than to 1MPa at the elevated temperature; and

has a thickness T greater than 10 μm.

21. The refreshable tactile display (500) of embodiments 19 or 20, wherein:  
the conductive layer (116) comprises one or more conductive materials selected from the group of single walled carbon nanotube, multiwalled carbon nanotube, graphite power, graphene, metal nanowires, metal nanoparticles, thin coating of a metal or alloy, thin  
5 conducting polymer (104) coating, conducting polymer (104) nanofibers,  
each heating element covers one of the surface (142) areas comprising a circular area with diameter larger than 0.1 mm (34) but less than 10 mm (34),  
each heating element aligns with one of the through holes (122)holes (122), comprising a circular through hole, on the rigid (106) membrane (102a),  
10 the rigid (106) membrane (102a) comprises a chamber cover for a fluidic pressure (112) chamber connected to the fluidic pressure (112) source, the fluidic pressure (112) chamber transferring or applying (100) the fluidic pressure (112) to the polymer (104) membrane (102a).
- 15 22. The display (500) of embodiment 21, wherein the carbon nanotubes are embedded in a polymer (104) layer.
23. The display (500) of any of the embodiments 19-22, wherein each of the heating elements (118) comprise a serpentine pattern.
- 20 24. The display (500) of any of the embodiments 19-22, wherein the tactile pixel (124)s have a relatively flat surface (142).
- 25 25. The display (500) of embodiment 19, wherein the polymer (104) membrane (102a) comprises a combination of stearyl acrylate (SA), urethane diacrylate (UDA), acrylic acid (AA), trimethylolpropane triacrylate (TMPTA), 2,2-Dimethoxy-2- phenylacetophenone (DMPA), and benzophenone (BP).
- 30 26. The display (500) or unit of any of the embodiments 1-25, wherein deformation (134a) of the polymer (104) membrane (102a) actuates one or more pixels by displacing one or more pins (124a) in the one or more through holes (122)holes (122).



27. The display (500) or unit of any of the embodiments 1-26, wherein Joule heating of the conductive layer (116) softens the polymer (104) membrane (102a).

5 28. The display (500) or unit of any of the embodiments 1-27, wherein the polymer (104) layer and the conductive layer (116) form an interpenetrating composite (the polymer (104) layer and the conductive layer (116) interpenetrate).

29. A method of making the refreshable tactile display (500) (e.g., of any of the  
10 previous embodiments), comprising:

a) stretching a softened polymer (104) membrane (102a) and maintaining deformation (134a) of the softened polymer (104) membrane (102a) when the polymer (104) membrane (102a) is cooled to ambient temperature;

15 b) spraying a dispersion of carbon nanotubes (CNTs) in a solvent onto the deformed rigid (106) polymer (104) membrane (102a) through a shadow mask which has one or more serpentine shaped cutout pattern(s), so as to form a carbon nanotube coating on the deformed rigid (106) polymer (104) membrane (102a);

c) spraying a solution comprising a polymer (104) or polymer (104) precursor on top of the carbon nanotube coating; and

20 d) releasing the deformation (134a) of the stretched polymer (104) membrane (102a) at elevated temperature, and cooling down to ambient temperature.

30. A method of making a refreshable tactile display (500) (e.g., of any of the previous embodiments), comprising:

25 a) forming a coating of carbon nanotubes on a release substrate;

b) patterning the coating into serpentine shapes by laser ablation;

c) applying (100) a polymer (104) precursor layer over the coating;

d) curing the polymer (104) precursor layer, forming a cured polymer (104) layer; and

e) separating the cured polymer (104) layer from the release substrate.

30

31. A bistable electroactive polymer (104) (e.g., for use in any of the previous embodiments), comprising a combination of stearyl acrylate (SA), urethane diacrylate (UDA), acrylic acid (AA), trimethylolpropane triacrylate (TMPTA), 2,2-Dimethoxy-2-phenylacetophenone (DMPA), and benzophenone (BP).

5

32. A bistable electroactive polymer (104) (BSEP) (e.g., for use in any of the previous embodiments) comprising a combination of tert-butyl acrylate (TBA), urethane diacrylate (UDA), ethoxylated trimethylolpropane triacrylate (ETMPTA), and 2,2-Dimethoxy-2-phenylacetophenone (DMPA).

10 33. A PolyPad device of any of the previous embodiments fabricated to display  $5 \times 15$  Braille cells (450 Braille pins) and 1012 tactile graphic pixels in a relatively small area comparable to a smart phone screen, optionally further comprising a PCB board to individually switch the taxels is compact and thin, and optionally wherein the display is integrated with the pump and battery into a foldable phone case-like package with a total  
15 thickness of  $\sim 1$  cm, optionally with fully raised pin height to be 0.6 mm with height variation of  $<20\%$  among the 450 dots, and an intermediate height of 0.3 mm (for graphic display) with height variation of  $<20\%$ . In one or more examples, the power consumed for heating, pumping, refreshing and communicating, of about 0.8 W or less; a single phone battery will allow a use time of one day on a full charge.

20 34. The display of any of the previous embodiments, wherein the Joule heating electrode is patterned directly and only on the active taxel areas, the area being heated is only  $1.77 \text{ mm}^2$  per taxel pixel or less, and the polymer film is of  $90 \text{ }\mu\text{m}$  thickness or less, 30 V was applied to the S-CNT electrode of  $50 \text{ k}\Omega$  resistance takes 1 s to reach  $50^\circ\text{C}$ , the power consumption is calculated to be 18 mW.

25 35. The display of any of the previous embodiments, wherein for a smartphone screen-sized panel with  $48 \times 24$  taxels, roughly 50% of the dots are raised during content refreshing, so the total power consumption is 2.16 W or less, the device further comprising a switching circuit and a pneumatic pump consume about 1 W during operation, so that overall power consumption is thus 3.16 W which is within the feasible range for small or portable  
30 devices.

36. A method of reading a display of any of the previous embodiments, comprising a human feeling or sensing the pins, taxel, or tactile pixel using their fingertips, wherein the taxel, tactile pixels or pins are arranged according to Braille format so that the human reads, feels, or senses the Braille format using the fingertips.

5 37. The method or device of any of the previous examples, further comprising a computer (e.g., smartphone) modulating the pins, taxels, or tactile pixels using a voltage applied to the heating elements/conductive layer, the pins, taxels, or pixels modulated so that the Braille format represents information outputted from, or intended for display by, the computer.

10 38. The method or device of any of the previous examples, wherein the fluidic pressure comprises a constant or uniform pressure during the reading.

#### Advantages and Improvements

Many transducer technologies are under investigation for refreshable Braille displays. In addition to piezoelectrics [13], there are electromagnetic linear actuators, shape memory alloys (SMAs) [14] thermopneumatic actuators (TPAs) [15, 16] electrostrictive polymers [17], and dielectric elastomers (DEs) [18, 19]. These technologies all offer certain advantages, as well as limitations. Electromagnetic linear actuators are difficult to shrink to Braille dot size and require continuous power. SMAs require complex thermal management strategies to maintain reasonable actuation rates, which increases cost. TPAs suffer from slow response speed and high-power consumption, requiring periodic pulsing to maintain their actuated shape. Electrostrictive polymers and DEs have poor cycling lifetimes and high driving voltages (1-5 kV), and have only one stable state, requiring constant actuation to remain in the raised state. This causes major issues with regard to limited reliability, high power consumption, and safety concerns. Actuator configurations capable of bi-stability are possible, but are much more complex. Oscillatory operation modes also exist wherein active dots are oscillated between the up and down states while inactive dots remain in the down state [20]. While this method circumvents the need for bi-stability, the oscillating mode makes characters more difficult to read, and can accelerate actuator fatigue. As observed by Leonardis, et al. [11], none of these actuation technologies offer the compactness, flexibility, and low power consumption required by the proposed PolyPad devices illustrated herein.

Embodiments described herein, on the other hand, provide a high resolution refreshable tactile display that can exert large stroke and provide high blocking force. Embodiments of the device described herein have a compact structure and high actuator density with a single fluidic reservoir. In one or more examples, the tactile display described herein uses the bistable  
5 electroactive polymer (BSEP) thin film with highly stretchable Joule heating electrodes as the active layer that can perform stable actuation with low voltage supply (30V). Each actuator can be individually controlled by application of local heating and pneumatic pressure. An enabling element of this approach is the fabrication of a highly stretchable Joule heating electrode. The compliant heater can locally soften the BSEP film in a rapid and precise manner. Thus, while the  
10 activation of the BSEP transistor requires high voltage, a pneumatic tactile display according to embodiments of the present invention requires only a low voltage signal to achieve large stroke, high blocking force, and safe operation with fast response speed. Moreover, unlike other commercialized tactile devices, which have complex components and cost several thousand dollars, a pneumatic tactile display according to examples described herein possesses a compact  
15 form factor with extraordinary working performances, and can be produced at low cost.

The demonstrated refreshable tactile display should find a wide range of applications in recreation, entertainment, robotics, health care, and so on. Potential applications for such tactile display are numerous, such as reproducing surface topography, providing haptic feedback for human- machine interfaces, and electronic Braille readers.

20 In one or more examples, the unique combination of the VSP and pneumatic actuation results in a compact Braille technology that can be packaged into small convenient form factors with low production cost for broad adoption. The low driving voltage facilitates low-cost, energy-efficient, and compact circuitry. The bistable VSP membrane ensures long-term durability. A serpentine patterned (e.g., AgNW) network embedded in the VSP membrane  
25 enables fast and reliable display refreshing. Materials and device architecture is adaptable for Braille add-on to various devices including, but not limited to, the iPhone®, iPad®, and Kindle®, with high tactile pixel resolution, compact form factors, light weight, and fast display refresh.

### References

30 The following references are incorporated by reference herein.

1. Dang, T., Annaswamy, T. M. & Srinivasan, M. A. Development and evaluation

of an epidural injection simulator with force feedback for medical training. *Stud. Health Technol. Inform.* 81, 97–102 (2001).

2. Langrana, N. A., Burdea, G., Lange, K., Gomez, D. & Deshpande, S. Dynamic force feedback in a virtual knee palpation. *Artif. Intell. Med.* 6, 321–333 (1994).

5 3. Vining, D. J., Liu, K., Choplin, R. H. & Haponik, E. F. Virtual bronchoscopy: Relationships of virtual reality endobronchial simulations to actual bronchoscopic findings. *Chest* 109, 549–553

4. Maisto, M. et al. Evaluation of wearable haptic systems for the fingers in Augmented Reality applications. *IEEE Trans. Haptics XX*, 1–1 (2017).

10 5. Bouzit, M., Burdea, G., Popescu, G. & Boian, R. The Rutgers Master II - New design force- feedback glove. *IEEE/ASME Trans. Mechatronics* 7, 256–263 (2002).

6. Cortesao, R., Park, J. & Khatib, O. Real-time adaptive control for haptic manipulation with Active Observers. *Proc. 2003 IEEE/RSJ Int. Conf. Intell. Robot. Syst. (IROS 2003)* (Cat. No.03CH37453) 3, 2938–2943 (2003).

15 7. Turner, M. L., Gomez, D. H., Tremblay, M. R., Cutkosky, M. R. & Alto, P. Preliminary Tests of an Arm-Grounded Haptic Feedback Device in Telemanipulation. *Proc. ASME IMECE Haptics Symp.* 1–6 (1998).

8. Choi, H. R. et al. Tactile display as a Braille display for the visually disabled. *2004 IEEE/RSJ Int. Conf. Intell. Robot. Syst. (IEEE Cat. No.04CH37566)* 2, 1985–1990  
20 (2004).

9. King, H. H., Donlin, R. & Hannaford, B. Perceptual thresholds for single vs. multi-finger haptic interaction. *2010 IEEE Haptics Symp. HAPTICS 2010* 95–99 (2010). doi:10.1109/HAPTIC.2010.5444670

10. Motto Ros, P. et al. A new dynamic tactile display for reconfigurable braille:  
25 implementation and tests. *Front. Neuroeng.* 7, 6 (2014).

11. Summers, I. R. & Chanter, C. M. A broadband tactile array on the fingertip. *J. Acoust. Soc. Am.* 112, 2118–2126 (2002).

12. Wagner, C. ., Lederman, S. J. & Howe, R. D. Design and performance of a tactile shape display. *Haptics-e* 6 (2004).

30 13. Velazquez, R., Pissaloux, E. E., Hafez, M. & Szewczyk, J. Tactile rendering

with shape-memory- alloy pin-matrix. *IEEE Trans. Instrum. Meas.* 57, 1051–1057 (2008).

14. Lee, J. S. & Lucyszyn, S. A micromachined refreshable Braille cell. *J. Microelectromechanical Syst.* 14, 673–682 (2005).

15. Kwon, H. J., Lee, S. W. & Lee, S. S. Braille dot display module with a PDMS membrane driven by a thermopneumatic actuator. *Sensors Actuators, A Phys.* 154, 238–246 (2009).

16. Koo, I. M. et al. Development of soft-actuator-based wearable tactile display. *IEEE Trans. Robot.* 24, 549–558 (2008).

17. Matysek, M., Lotz, P., Winterstein, T. & Schlaak, H. F. Dielectric elastomer actuators for tactile displays. *Proc. - 3rd Jt. EuroHaptics Conf. Symp. Haptic Interfaces Virtual Environ. Teleoperator Syst. World Haptics 2009* 290–295 (2009). doi:10.1109/WHC.2009.4810822

18. Jungmann, M. & Schlaak, H. F. Miniaturised electrostatic tactile display with high structural compliance. *Proc. Conf. Eurohaptics* 12–17 (2002).

19. De Rossi, D., Carpi, F., Carbonaro, N., Tognetti, A. & Scilingo, E. P. Electroactive polymer patches for wearable haptic interfaces. *Proc. Annu. Int. Conf. IEEE Eng. Med. Biol. Soc. EMBS* 8369–8372 (2011). doi:10.1109/IEMBS.2011.6092064

20. Lee, H. S. et al. Design analysis and fabrication of arrayed tactile display based on dielectric elastomer actuator. *Sensors Actuators, A Phys.* 205, 191–198 (2014).

21. Phung, H. et al. Tactile display with rigid coupling based on soft actuator. *Meccanica* 50, 2825–2837 (2015).

22. Yu, Z. et al. Large-strain, rigid-to-rigid deformation of bistable electroactive polymers. *Appl. Phys. Lett.* 95, 21–24 (2009).

23. Wu, X., Kim, S. H., Zhu, H., Ji, C. H. & Allen, M. G. A refreshable braille cell based on pneumatic microbubble actuators. *J. Microelectromechanical Syst.* 21, 908–916 (2012).

24. Yobas, L., Huff, M. A., Lisy, F. J. & Durand, D. M. A novel bulk-micromachined electrostatic microvalve with a curved-compliant structure applicable for a pneumatic tactile display. *J. Microelectromechanical Syst.* 10, 187–196 (2001).

25. Besse, N., Rosset, S., Zarate, J. J. & Shea, H. Flexible Active Skin: Large Reconfigurable Arrays of Individually Addressed Shape Memory Polymer Actuators. *Adv.*

Mater. Technol. 1700102, 1700102 (2017).

26. Ren, Z. et al. Phase-Changing Bistable Electroactive Polymer Exhibiting Sharp Rigid-to-Rubbery Transition. *Macromolecules* 49, 134–140 (2016).

27. Yuan, W. et al. Fault-tolerant dielectric elastomer actuators using single-walled  
5 carbon nanotube electrodes. *Adv. Mater.* 20, 621–625 (2008).

28. Yamada, T. et al. A stretchable carbon nanotube strain sensor for human-motion detection. *Nat. Nanotechnol.* 6, 296–301 (2011).

29. Niu, X. et al. Bistable large-strain actuation of interpenetrating polymer networks. *Adv. Mater.* 24, 6513–6519 (2012).

10 30. Dong, J., Ozaki, Y. & Nakashima, K. Infrared, Raman, and Near-Infrared Spectroscopic Evidence for the Coexistence of Various Hydrogen-Bond Forms in Poly(acrylic acid). *Macromolecules* 30, 1111–1117 (1997).

31. Sun, J.-Y. et al. Highly stretchable and tough hydrogels. *Nature* 489, 133–136 (2012).

15 32. Haque, M. A., Kurokawa, T., Kamita, G. & Gong, J. P. Lamellar bilayers as reversible sacrificial bonds to toughen hydrogel: Hysteresis, self-recovery, fatigue resistance, and crack blunting. *Macromolecules* 44, 8916–8924 (2011).

33. Tuncaboylu, D. C., Sari, M., Oppermann, W. & Okay, O. Tough and self-healing hydrogels formed via hydrophobic interactions. *Macromolecules* 44, 4997–5005  
20 (2011).

34. Runyan, N. H. & Carpi, F. Seeking the 'holy braille' display: might electromechanically active polymers be the solution? *Expert Rev. Med. Devices* 8, 529–532 (2011).

35. McCoul, D., Hu, W., Gao, M., Mehta, V. & Pei, Q. Recent Advances in  
25 Stretchable and Transparent Electronic Materials. *Adv. Electron. Mater.* 2, 1500407 (2016).

36. Trung, T. Q. & Lee, N. E. Recent Progress on Stretchable Electronic Devices with Intrinsically Stretchable Components. *Adv. Mater.* 29, (2017).

37. Bauer, S. et al. 25th anniversary article: A soft future: From robots and sensor skin to energy harvesters. *Adv. Mater.* 26, 149–162 (2014).

30 38. Zhang, Y. et al. Buckling in serpentine microstructures and applications in elastomer-supported ultra-stretchable electronics with high areal coverage. *Soft Matter* 9, 8062

(2013).

39. Li, T., Suo, Z., Lacour, S. P. & Wagner, S. Compliant thin film patterns of stiff materials as platforms for stretchable electronics. *J. Mater. Res.* 20, 3274–3277 (2005).

40. Gonzalez, M. et al. Design of metal interconnects for stretchable electronic  
5 circuits. *Microelectron. Reliab.* 48, 825–832 (2008).

41. Lu, N., Lu, C., Yang, S. & Rogers, J. Highly sensitive skin-mountable strain gauges based entirely on elastomers. *Adv. Funct. Mater.* 22, 4044–4050 (2012).

42. Gutruf, P., Walia, S., Nur Ali, M., Sriram, S. & Bhaskaran, M. Strain response of stretchable micro-electrodes: Controlling sensitivity with serpentine designs and  
10 encapsulation. *Appl. Phys. Lett.* 104, 1–5 (2014).

43. Hu, H. et al. Determination of the acidic sites of purified single-walled carbon nanotubes by acid-base titration. *Chem. Phys. Lett.* 345, 25–28 (2001).

44. Li, Y. et al. A smart, stretchable resistive heater textile. *J. Mater. Chem. C* 5, 41–46 (2017).

15 45. Kang, J. et al. High-Performance Graphene-Based Transparent Flexible Heaters. *Nano Lett.* 11, 5154–5158 (2011). doi:10.1021/nl202311v

46. Li, Y. Q. et al. Multifunctional Wearable Device Based on Flexible and Conductive Carbon Sponge/Polydimethylsiloxane Composite. *ACS Appl. Mater. Interfaces* 8, 33189–33196 (2016).

20 47. Zhou, R., Li, P., Fan, Z., Du, D. & Ouyang, J. Stretchable heaters with composites of an intrinsically conductive polymer, reduced graphene oxide and an elastomer for wearable thermotherapy. *J. Mater. Chem. C* 5, 1544–1551 (2017).

48. Yoon, S. S. & Khang, D. Y. Facile patterning of Ag nanowires network by micro-contact printing of siloxane. *ACS Appl. Mater. Interfaces* 8, 23236–23243 (2016).

25 49. Hong, S. et al. Highly Stretchable and Transparent Metal Nanowire Heater for Wearable Electronics Applications. *Adv. Mater.* 27, 4744–4751 (2015).

50. Hu, H. et al. Substrateless Welding of Self-Assembled Silver Nanowires at Air/Water Interface. *ACS Appl. Mater. Interfaces* 8, 20483–20490 (2016).

30 51. Choi, S. et al. Stretchable Heater Using Ligand-Exchanged Silver Nanowire Nanocomposite for Wearable Articular Thermotherapy. *ACS Nano* 9, 6626–6633 (2015).

52. Ko, E.-H., Kim, H.-J., Lee, S.-M., Kim, T.-W. & Kim, H.-K. Stretchable Ag



electrodes with mechanically tunable optical transmittance on wavy-patterned PDMS substrates. *Sci. Rep.* 7, 46739 (2017).

53. Jo, H. S. et al. Highly flexible, stretchable, patternable, transparent copper fiber heater on a complex 3D surface. *NPG Asia Mater.* 9, e347 (2017).

54. Li, P., Ma, J., Xu, H., Xue, X. & Liu, Y. Highly stable copper wire/alumina/polyimide composite films for stretchable and transparent heaters. *J. Mater. Chem. C* 4, 3581–3591 (2016).

55. Ding, S. et al. One-Step Fabrication of Stretchable Copper Nanowire Conductors by a Fast Photonic Sintering Technique and Its Application in Wearable Devices. *ACS Appl. Mater. Interfaces* 8, 6190–6199 (2016).

56. An, B. W. et al. Stretchable, Transparent Electrodes as Wearable Heaters Using Nanotrough Networks of Metallic Glasses with Superior Mechanical Properties and Thermal Stability. *Nano Lett.* 16, 471–478 (2016).

57. Yeon, C., Kim, G., Lim, J. W. & Yun, S. J. Highly conductive PEDOT:PSS treated by sodium dodecyl sulfate for stretchable fabric heaters. *RSC Adv.* 7, 5888–5897 (2017).

58. Refreshable Tactile Display Based on a Bistable Electroactive Polymer and a Stretchable Serpentine Joule Heating Electrode. Yu Qiu, Zhiyun Lu, and Qibing Pei. *ACS Appl. Mater. Interfaces* 2018, 10, 24807–24815, including supplementary information.

59. Meng, Y.; Jiang, J.; Anthamatten, M. Body Temperature Triggered Shape-Memory Polymers with High Elastic Energy Storage Capacity. *J. Polym. Sci., Part B: Polym. Phys.* 2016, 54, 1397–1404.

60. Hu, X.; Zhou, J.; Vatankhah-Varnosfaderani, M.; Daniel, W. F. M.; Li, Q.; Zhushma, A. P.; Dobrynin, A. V.; Sheiko, S. S. Programming Temporal Shapeshifting. *Nat. Commun.* 2016, 7, 12919.

61. Dong, J.; Ozaki, Y.; Nakashima, K. Infrared, Raman, and Near- Infrared Spectroscopic Evidence for the Coexistence of Various Hydrogen-Bond Forms in Poly(Acrylic Acid). *Macromolecules* 1997, 30, 1111–1117.

62. Sun, J.-Y.; Zhao, X.; Illeperuma, W. R. K.; Chaudhuri, O.; Oh, K. H.; Mooney, D. J.; Vlassak, J. J.; Suo, Z. Highly Stretchable and Tough Hydrogels. *Nature* 2012, 489, 133–136.

63. Haque, M. A.; Kurokawa, T.; Kamita, G.; Gong, J. P. Lamellar Bilayers as

Reversible Sacrificial Bonds to Toughen Hydrogel: Hysteresis, Self-Recovery, Fatigue Resistance, and Crack Blunting. *Macromolecules* 2011, *44*, 8916–8924.

64. Tuncaboylu, D. C.; Sari, M.; Oppermann, W.; Okay, O. Tough and Self-Healing Hydrogels Formed via Hydrophobic Interactions. *Macromolecules* 2011, *44*, 4997–5005.

5 65. McCoul, D.; Hu, W.; Gao, M.; Mehta, V.; Pei, Q. Recent Advances in Stretchable and Transparent Electronic Materials. *Adv. Electron. Mater.* 2016, *2*, 1500407.

66. Trung, T. Q.; Lee, N.-E. Recent Progress on Stretchable Electronic Devices with Intrinsically Stretchable Components. *Adv. Mater.* 2017, *29*, 1603167.

67. Bauer, S.; Bauer-Gogonea, S.; Graz, I.; Kaltenbrunner, M.; Keplinger, C.; Schwödiauer, R. 25th Anniversary Article: A Soft Future: From Robots and Sensor Skin to Energy Harvesters. *Adv. Mater.* 2014, *26*, 149–162.

68. Hu, H.; Bhowmik, P.; Zhao, B.; Hamon, M. A.; Itkis, M. E.; Haddon, R. C. Determination of the Acidic Sites of Purified Single-Walled Carbon Nanotubes by Acid-Base Titration. *Chem. Phys. Lett.* 2001, *345*, 25–28.

15 69. Zhang, Y.; Xu, S.; Fu, H.; Lee, J.; Su, J.; Hwang, K.-C.; Rogers, J. A.; Huang, Y. Buckling in Serpentine Microstructures and Applications in Elastomer-Supported Ultra-Stretchable Electronics with High Areal Coverage. *Soft Matter* 2013, *9*, 8062.

70. Li, T.; Suo, Z.; Lacour, S. P.; Wagner, S. Compliant Thin Film Patterns of Stiff Materials as Platforms for Stretchable Electronics. *J. Mater. Res.* 2005, *20*, 3274–3277.

20

### Conclusion

This concludes the description of the preferred embodiment of the present invention. The foregoing description of one or more embodiments of the invention has been presented for 25 the purposes of illustration and description. It is not intended to be exhaustive or to limit the invention to the precise form disclosed. Many modifications and variations are possible in light of the above teaching. It is intended that the scope of the invention be limited not by this detailed description, but rather by the claims appended hereto.

30

WHAT IS CLAIMED IS:

1. A refreshable tactile display unit comprising:

5 a) a polymer membrane comprising a polymer which is relatively rigid at an ambient temperature and in a rubbery state at an elevated temperature, wherein a rigid-to-soft transition of the polymer occurs within a temperature range narrower than 10 °C;

b) a fluidic pressure chamber, wherein the fluidic pressure chamber applies fluidic pressure, generated from a fluidic pressure source, to the polymer membrane;

10 d) a conductive layer including one or more heating elements coupled to the polymer membrane; and

e) a rigid membrane comprising one or more through holes, wherein:  
the polymer membrane deforms through the one or more through holes in response to:

15 one or more of the heating elements heating the polymer membrane to the elevated temperature so as to form a softened polymer membrane in the rubbery state, and

the fluidic pressure source applying the fluidic pressure to the softened polymer membrane so as to deform the polymer membrane.

20

2. The unit of claim 1, wherein the polymer is the bistable electroactive polymer (BSEP) comprising a combination of stearyl acrylate (SA), urethane diacrylate (UDA), acrylic acid (AA), trimethylolpropane triacrylate (TMPTA), 2,2-Dimethoxy-2- phenylacetophenone (DMPA), and benzophenone (BP).

25

3. The unit of claim 1, wherein the polymer is the bistable electroactive polymer (BSEP) comprising 80 parts of stearyl acrylate (SA) by weight, 20 parts of UDA by weight, 5 parts of acrylic acid (AA) by weight, 1.5 parts of trimethylolpropane triacrylate (TMPTA) by weight, 0.25 parts of 2,2-Dimethoxy-2- phenylacetophenone  
30 (DMPA) by weight, and 0.125 parts of benzophenone (BP) by weight.

4. The unit of claim 1, wherein the polymer is a bistable electroactive polymer (BSEP) comprising 40-80 parts of stearyl acrylate (SA) by weight, 20-60 parts of UDA by weight, 5-15 parts of acrylic acid (AA) by weight, 0.25-1.5 parts of trimethylolpropane triacrylate (TMPTA) by weight, 0.125-0.75 parts of 2,2-Dimethoxy-2- phenylacetophenone (DMPA) by weight, and 0.0075-0.2 parts of benzophenone (BP) by weight.

5. The unit of claim 1, wherein the polymer is a bistable electroactive polymer (BSEP) comprising a combination of tert-butyl acrylate (TBA), urethane diacrylate (UDA), ethoxylated trimethylolpropane triacrylate (ETMPTA), and 2,2-Dimethoxy-2- phenylacetophenone (DMPA).

6. The unit of claim 1, wherein the polymer is a bistable electroactive polymer (BSEP) comprising 90-110 parts of tert-butyl acrylate (TBA) by weight, 5-25 parts urethane diacrylate (UDA) by weight, 1-5 parts ethoxylated trimethylolpropane triacrylate (ETMPTA) by weight, and 0.25-1.5 parts 2,2-Dimethoxy-2- phenylacetophenone (DMPA) by weight.

7. The unit of any of the claims 1-6, wherein the polymer membrane:  
has a tensile modulus greater than 100 megapascals (MPa) but less than 10 gigapascals (GPa) at the ambient temperature; and  
has a tensile modulus of greater than 10 kPa but less than 10 MPa at the elevated temperature.

8. The unit of any of the claims 1-7, wherein the polymer membrane has a rigid-to-soft transition temperature higher than 40°C but lower than 70°C.

9. The unit of any of the claims 1-8, wherein the fluidic pressure comprises pneumatic pressure caused by compressed gas, a pneumatic pump, or compressed vapor due to liquid evaporation.

10. The unit of any of the claims 1-8, wherein the fluidic pressure comprises liquidous pressure caused by compressed liquid, a liquid pump, or a liquid volume change due to a phase change or a temperature change.

5 11. The unit of any of the claims 1-10, wherein the fluidic pressure chamber is rigid.

12. The unit of any of the claims 1-10, wherein the fluidic pressure chamber is flexible.

10

13. The unit of any of the claims 1-12, wherein the conductive layer is a coating on the polymer membrane.

14. The unit of any of the claims 1-13, wherein the conductive layer is  
15 deposited by printing, spraying, or casting.

15. The unit of any of the claims 1-14, wherein the conductive layer is heated when a voltage is applied between two separated points on the conductive layer.

20

16. The unit of any of the claims 1-15, wherein each of the heating elements comprises a serpentine pattern.

17. The unit of any of the claims 1-16, wherein each of the through holes  
25 defines a tactile pixel area and is aligned with a heating element in the conductive layer so that the heating element provides local heating of the polymer membrane.

18. The unit of any of the claims 1-17, wherein the rigid membrane is laminated on the polymer membrane.

30

19. A refreshable tactile display, comprising:

a plurality of tactile pixels each controlled by softening a surface area of a polymer membrane, wherein the polymer membrane is relatively rigid at ambient temperature and in a softened state at an elevated temperature;

5 a conductive layer including a plurality of heating elements, each of the heating elements coupled to a different one of the surface areas of the polymer membrane; and

a rigid membrane comprising through holes, each of the through holes aligned with one of the heating elements, wherein:

10 the softening of the polymer membrane is controlled by applying a voltage across one or more of the heating elements, so as to heat one or more of the surface areas of the polymer membrane to the elevated temperature and into the softened state;

15 the one or more surface areas in the softened state are deformed out of a plane of the polymer membrane into a deformed state by a fluidic pressure generated using a fluidic pressure source, such that part of the tactile pixel coupled to the surface area associated with the tactile pixel is raised above a plane including the through holes;

the deformed state is maintained at the ambient temperature; and

20 deformation in the deformed state is recovered by raising a temperature of the one or more surface areas in the deformed state to above a softening temperature at which the polymer membrane softens.

20. The refreshable tactile display of claim 19, wherein the polymer membrane:

25 comprises a phase changing polymer exhibiting a tensile modulus change by at least two orders of magnitude in a temperature range of less than 10°C;

possesses a tensile modulus of at least 100 MPa at room temperature to provide a high blocking force, and

30 becomes rubbery with tensile modulus less than 1MPa at the elevated temperature; and

has a thickness greater than 10  $\mu\text{m}$ .

21. The refreshable tactile display of claims 19 or 20, wherein:  
the conductive layer comprises one or more conductive materials selected  
from the group of single walled carbon nanotube, multiwalled carbon nanotube,  
5 graphite powder, graphene, metal nanowires, metal nanoparticles, thin coating of a  
metal or alloy, thin conducting polymer coating, conducting polymer nanofibers,  
each heating element covers one of the surface areas comprising a circular  
area with diameter larger than 0.1 mm but less than 10 mm,  
each heating element aligns with one of the through holes, comprising a  
10 circular through hole, on the rigid membrane,  
the rigid membrane comprises a chamber cover for a fluidic pressure  
chamber connected to the fluidic pressure source, the fluidic pressure chamber  
transferring or applying the fluidic pressure to the polymer membrane.

15 22. The display of claim 21, wherein the carbon nanotubes are embedded  
in a polymer layer.

23. The display of any of the claims 19-22, wherein each of the heating  
elements comprise a serpentine pattern.

20 24. The display of any of the claims 19-22, wherein the tactile pixels have  
a relatively flat surface.

25 25. The display of claim 19, wherein the polymer membrane comprises a  
combination of stearyl acrylate (SA), urethane diacrylate (UDA), acrylic acid (AA),  
trimethylolpropane triacrylate (TMPTA), 2,2-Dimethoxy-2- phenylacetophenone  
(DMPA), and benzophenone (BP).

30 26. The display or unit of any of the claims 1-25, wherein deformation of  
the polymer membrane actuates one or more pixels by displacing one or more pins  
in the one or more through holes.

27. The display or unit of any of the claims 1-26, wherein Joule heating of the conductive layer softens the polymer membrane.

5 28. The display or unit of any of the claims 1-27, wherein the polymer layer and the conductive layer form a interpenetrating composite (the polymer layer and the conductive layer interpenetrate).

29. A method of making the refreshable tactile display, comprising:

10 a) stretching a softened polymer membrane and maintaining deformation of the softened polymer membrane when the polymer membrane is cooled to ambient temperature;

15 b) spraying a dispersion of carbon nanotubes (CNTs) in a solvent onto the deformed rigid polymer membrane through a shadow mask which has one or more serpentine shaped cutout pattern(s), so as to form a carbon nanotube coating on the deformed rigid polymer membrane;

c) spraying a solution comprising a polymer or polymer precursor on top of the carbon nanotube coating; and

20 d) ) releasing the deformation of the stretched polymer membrane at elevated temperature, and cooling down to ambient temperature.

30. A method of making a refreshable tactile display, comprising:

a) forming a coating of carbon nanotubes on a release substrate;

b) patterning the coating into serpentine shapes by laser ablation;

25 c) applying a polymer precursor layer over the coating;

d) curing the polymer precursor layer, forming a cured polymer layer; and

e) separating the cured polymer layer from the release substrate.

31. A bistable electroactive polymer, comprising a combination of stearyl acrylate (SA), urethane diacrylate (UDA), acrylic acid (AA), trimethylolpropane

30



triacrylate (TMPTA), 2,2-Dimethoxy-2- phenylacetophenone (DMPA), and benzophenone (BP).

32. A bistable electroactive polymer (BSEP) comprising a combination of  
5 tert-butyl acrylate (TBA), urethane diacrylate (UDA), ethoxylated trimethylolpropane triacrylate (ETMPTA), and 2,2-Dimethoxy-2- phenylacetophenone (DMPA).

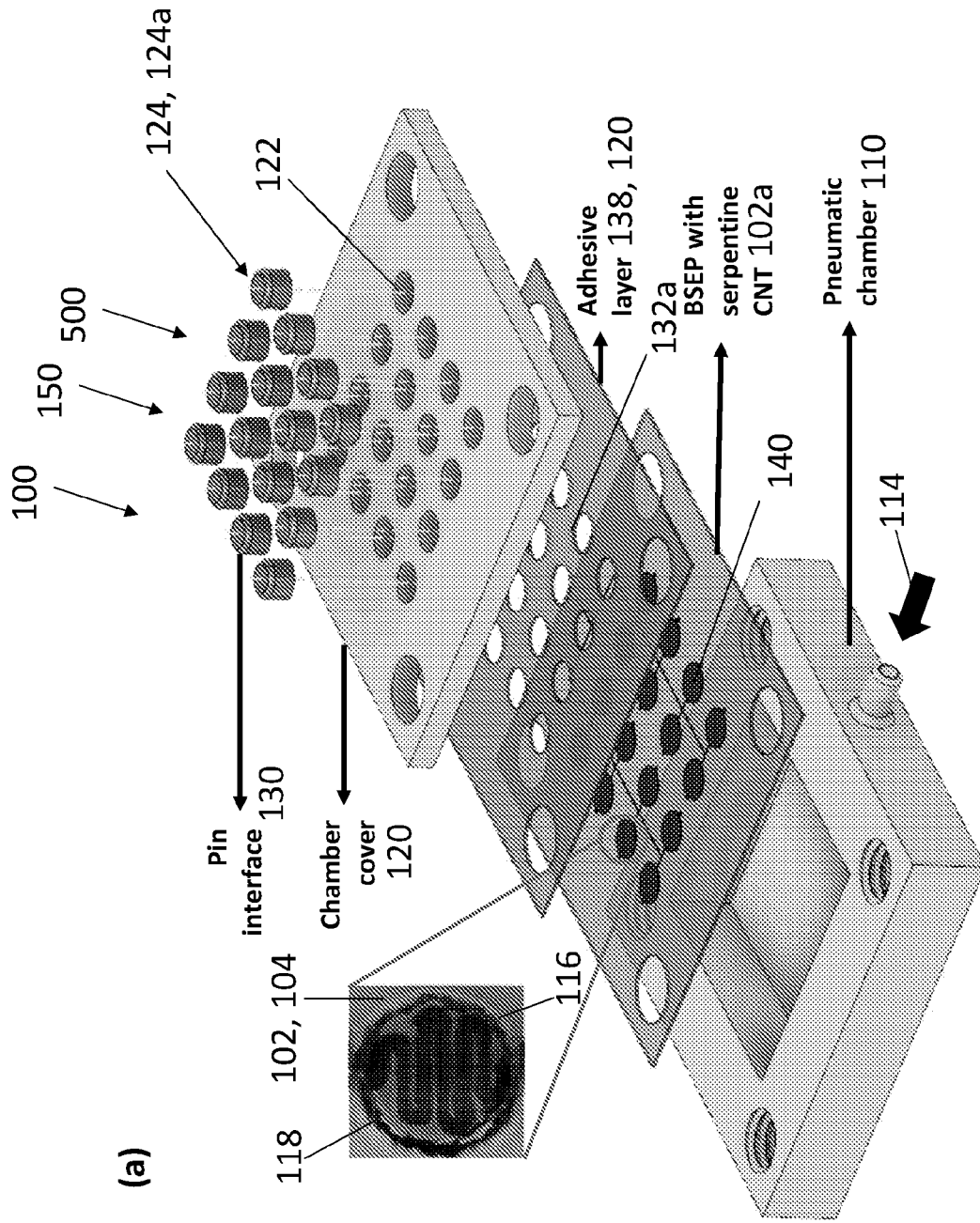


FIG. 1A

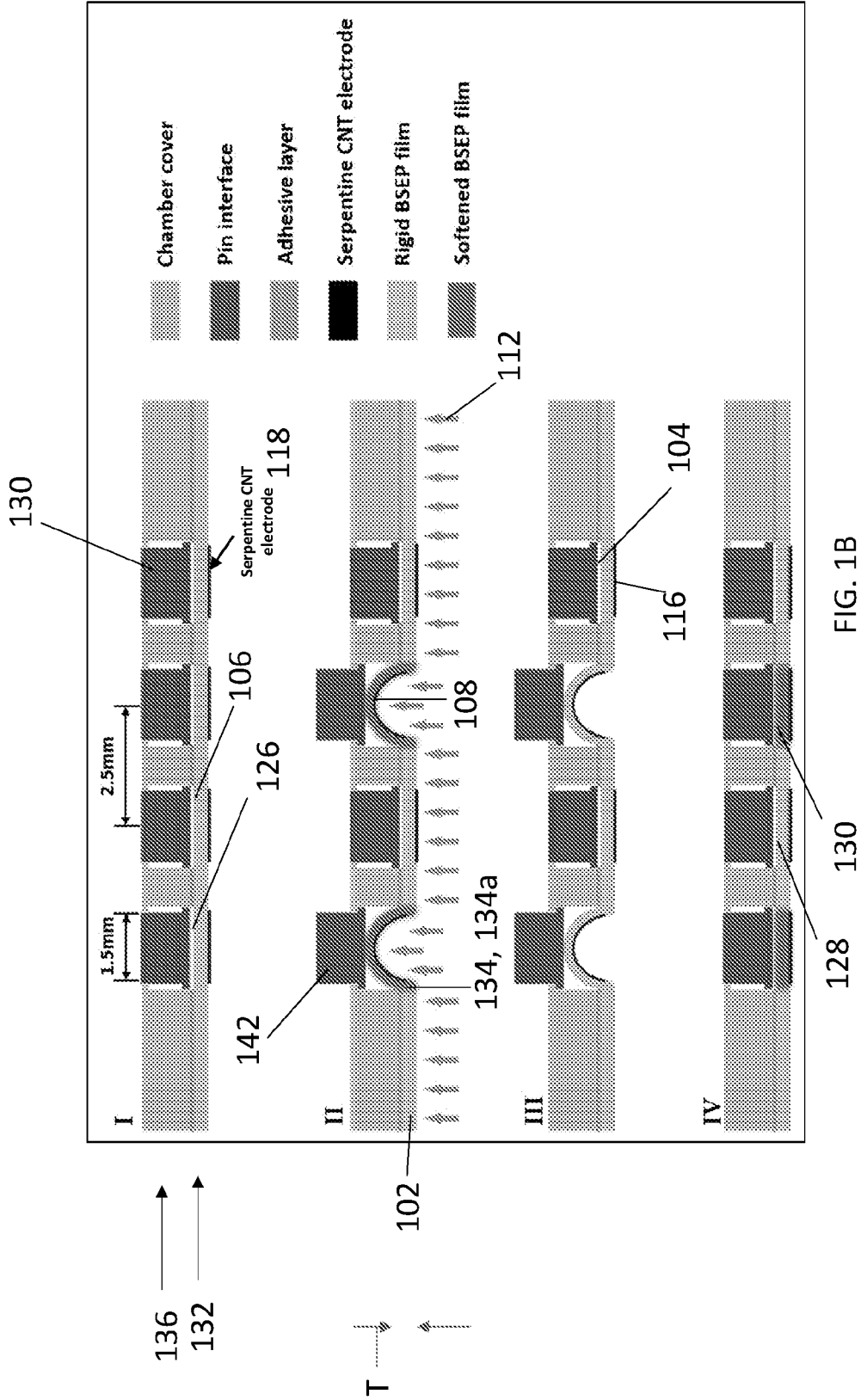


FIG. 1B

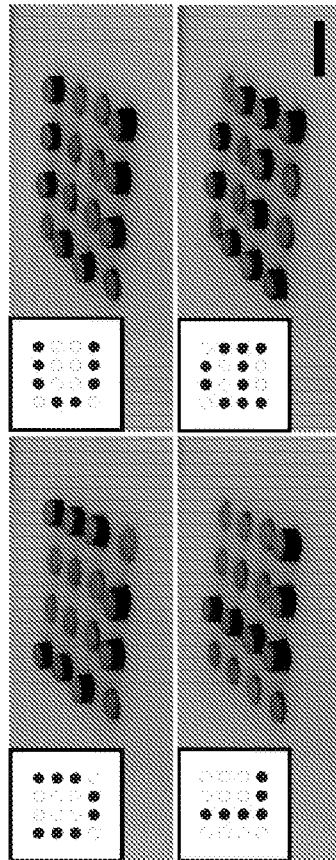


FIG. 1C

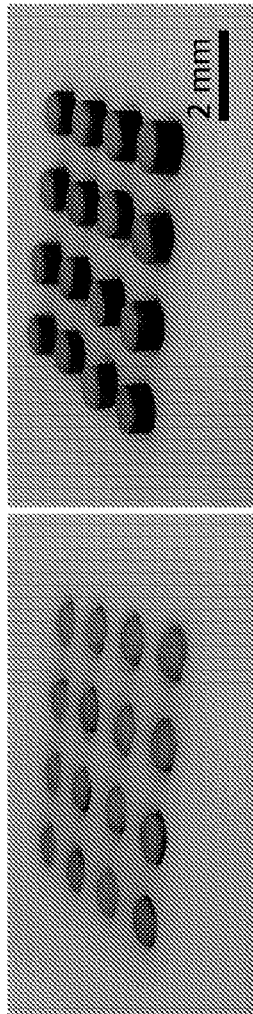
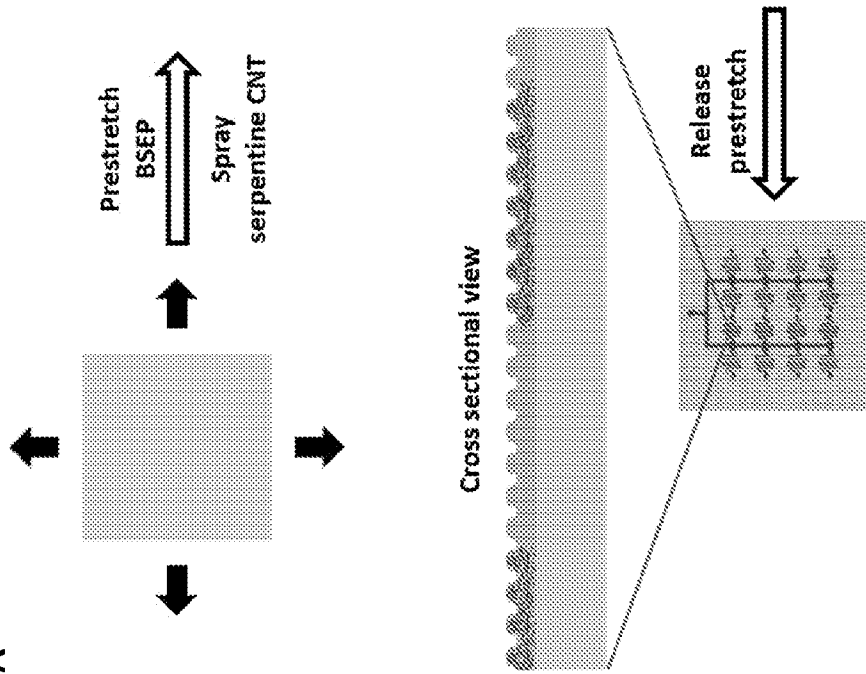
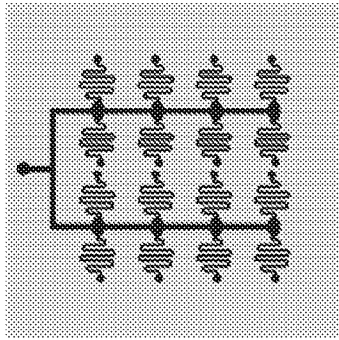


FIG. 1D

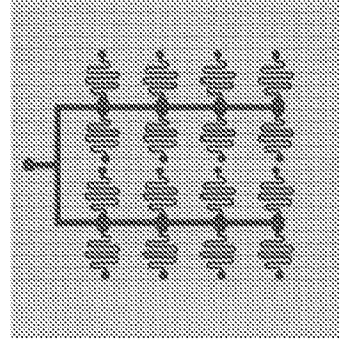
FIG. 1. Prestretch  
2A



II. Pattern

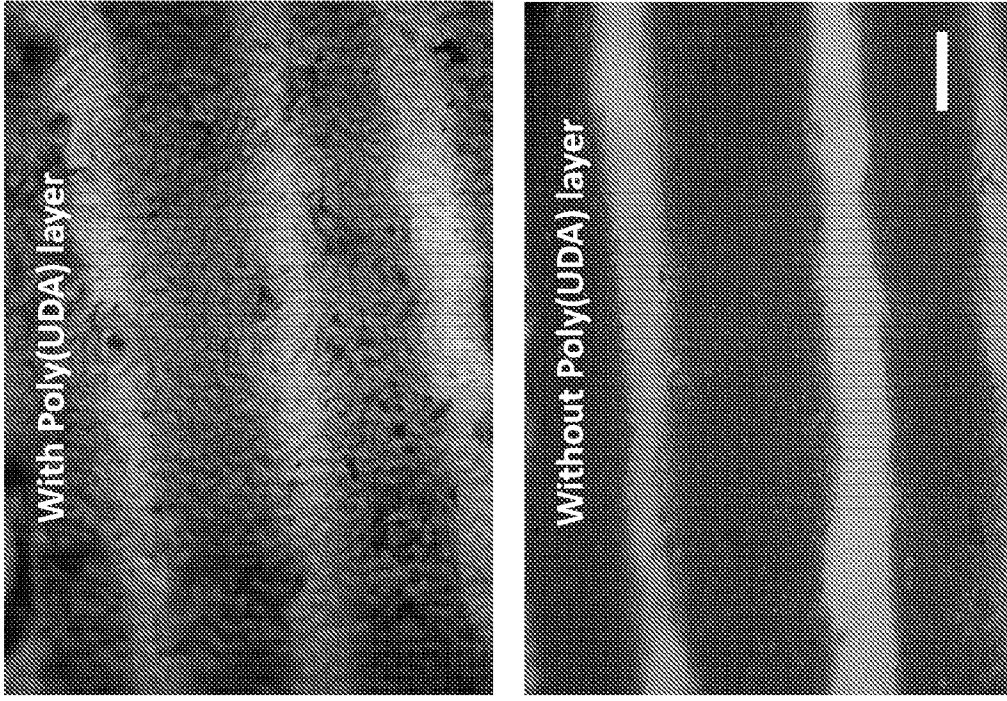


Spray UDA solution and cure



III. Protect

FIG. 2B



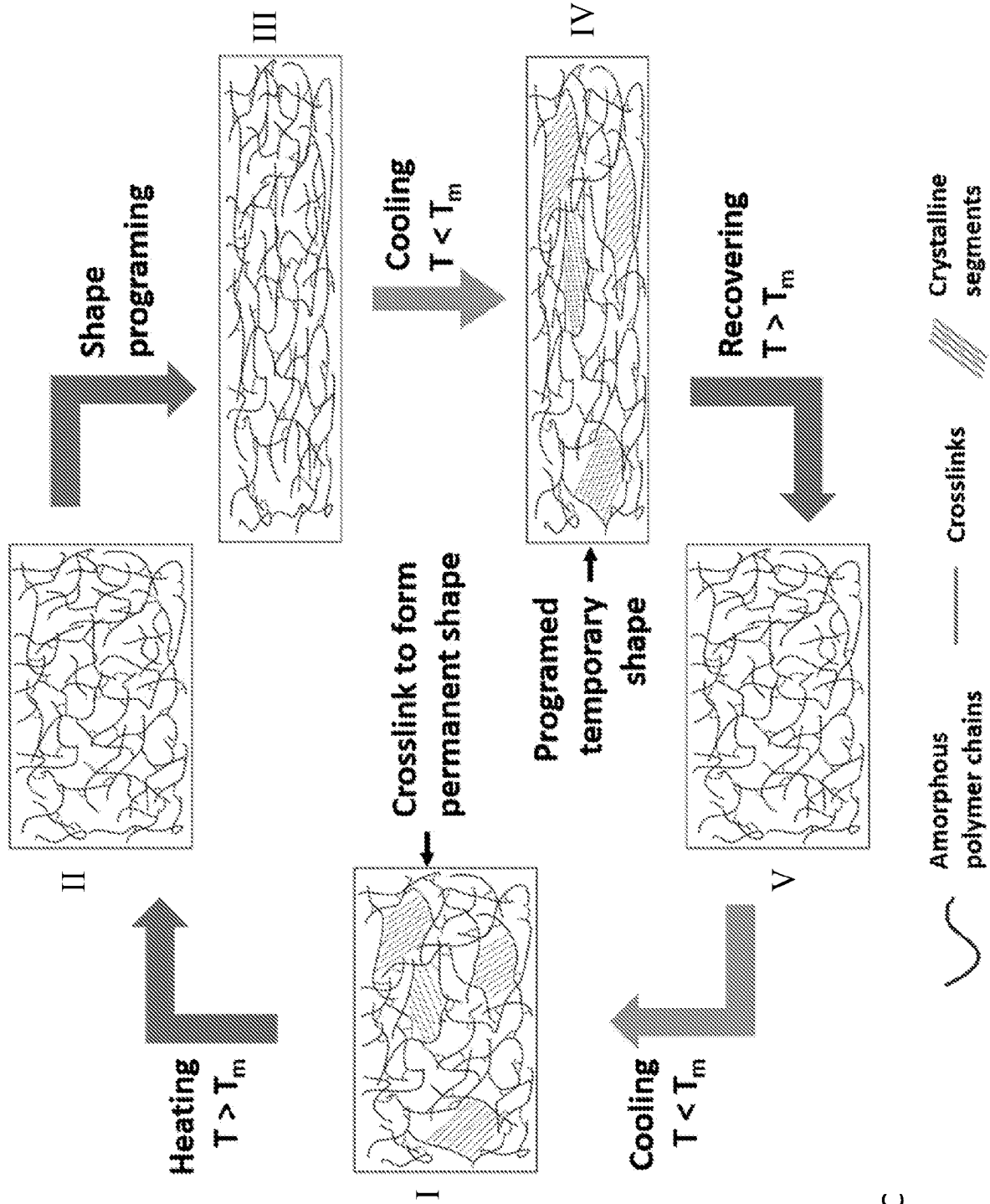
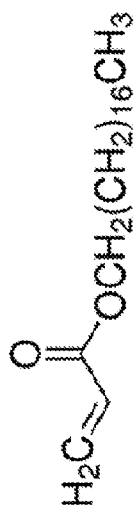


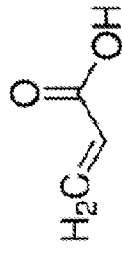
FIG. 2C



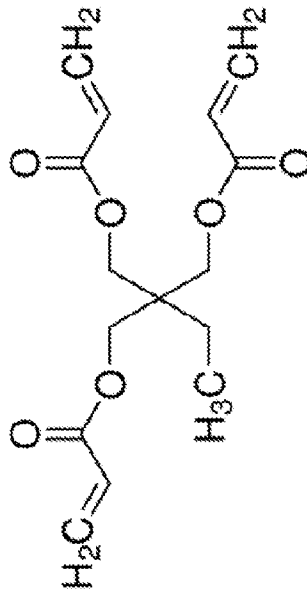
Stearyl acrylate (SA)



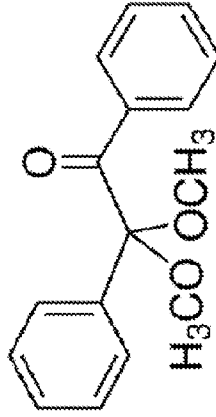
UDA



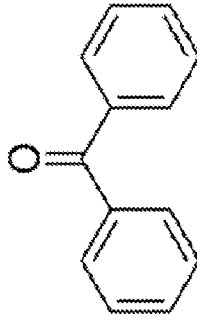
Acrylic acid (AA)



TMPTA



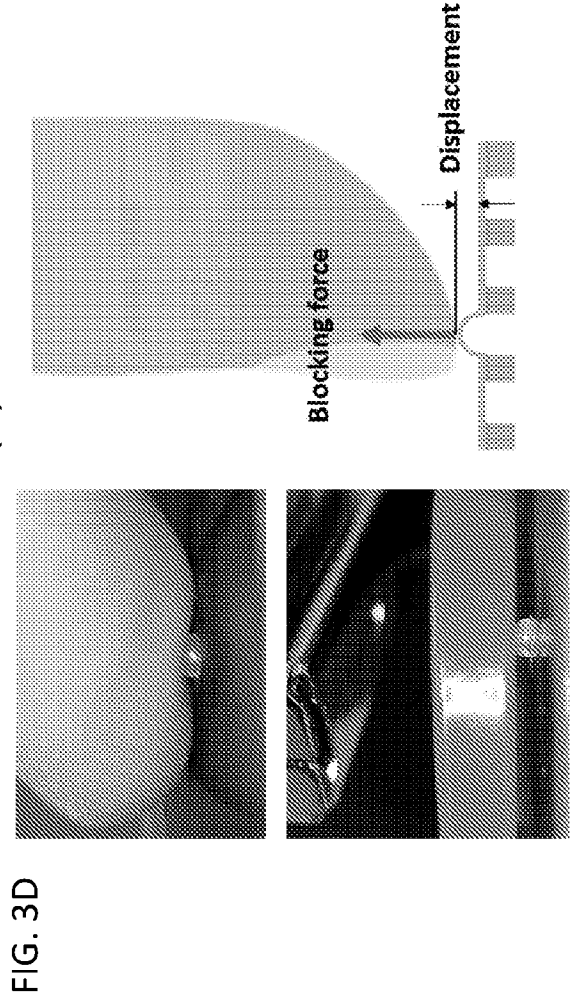
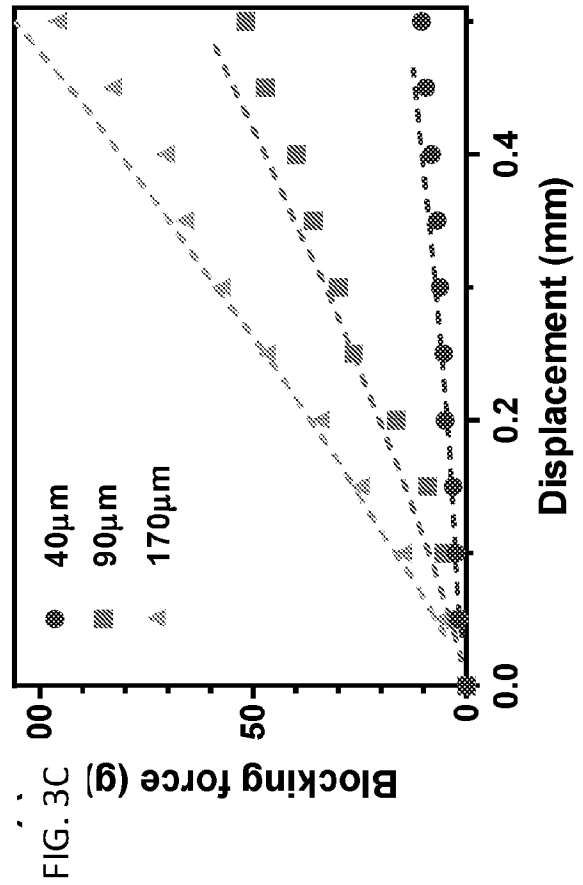
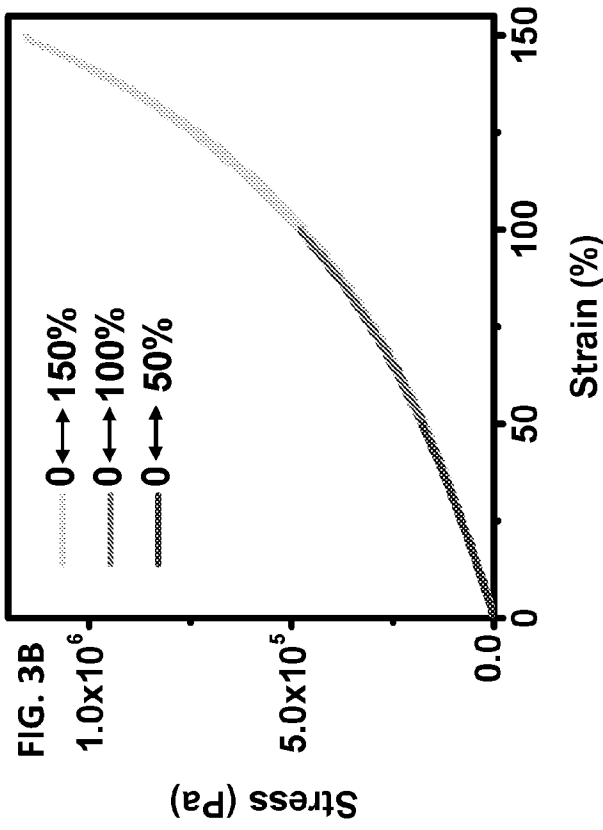
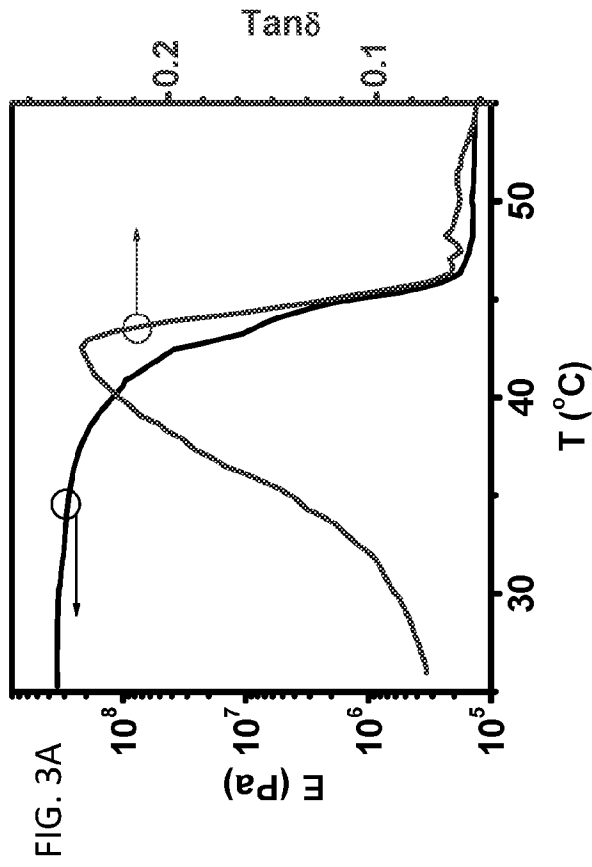
DMPA



BP

FIG 2D





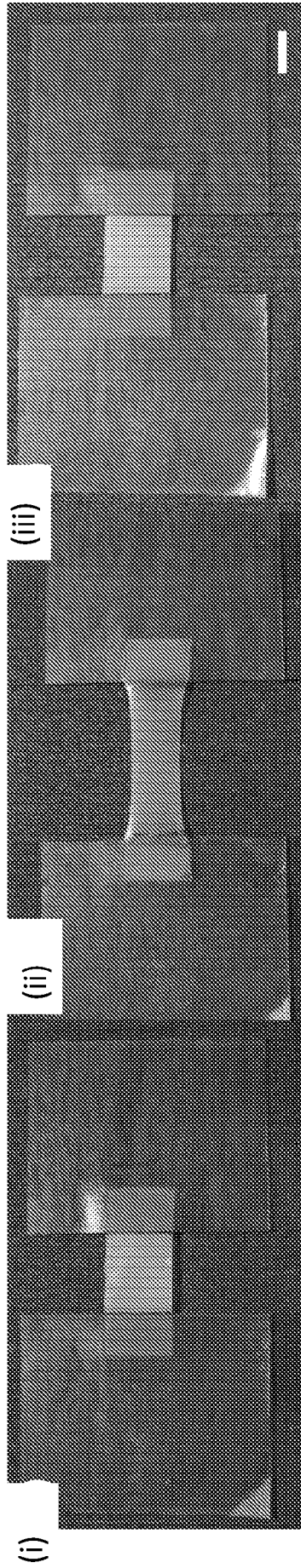


FIG. 3E

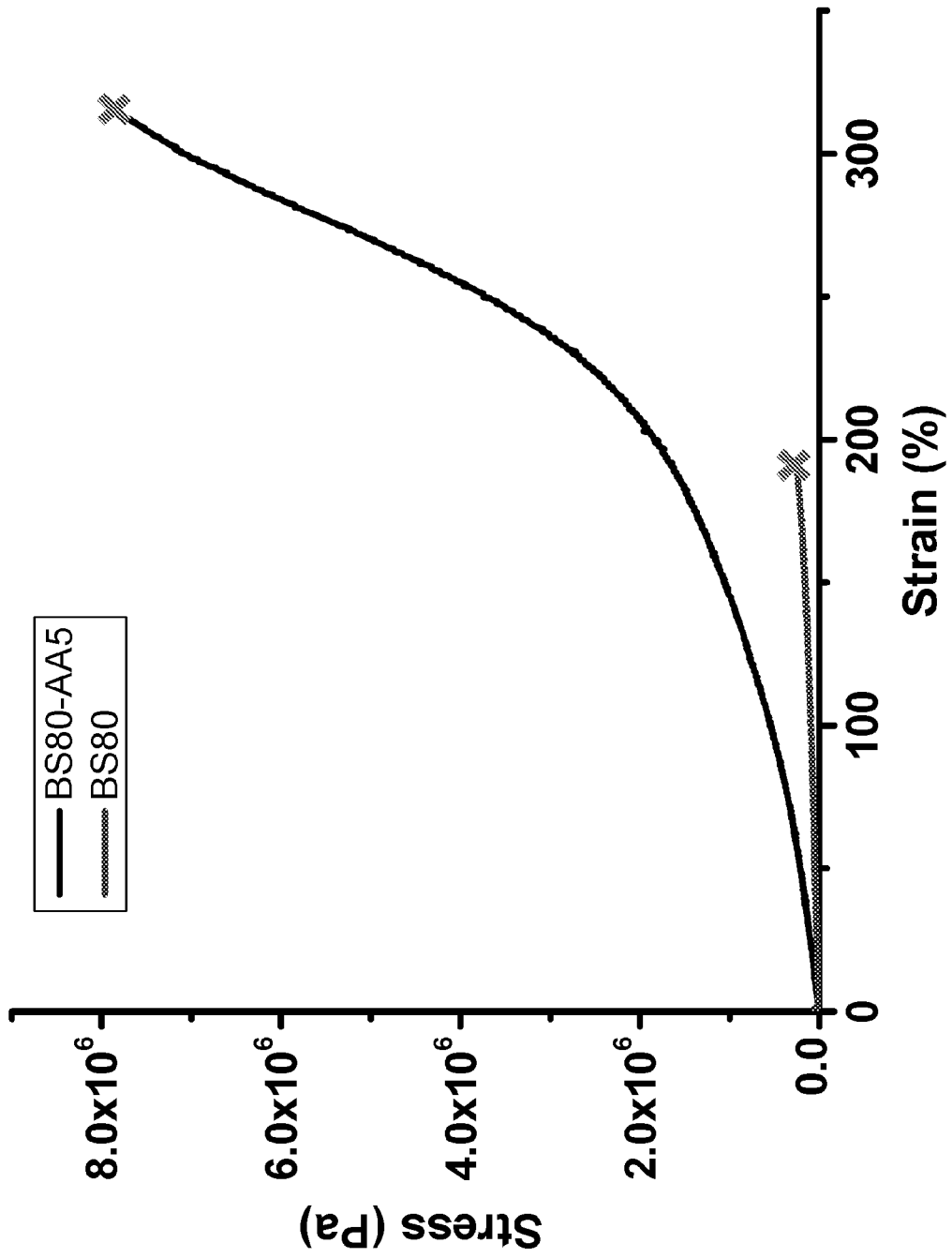


FIG. 3F

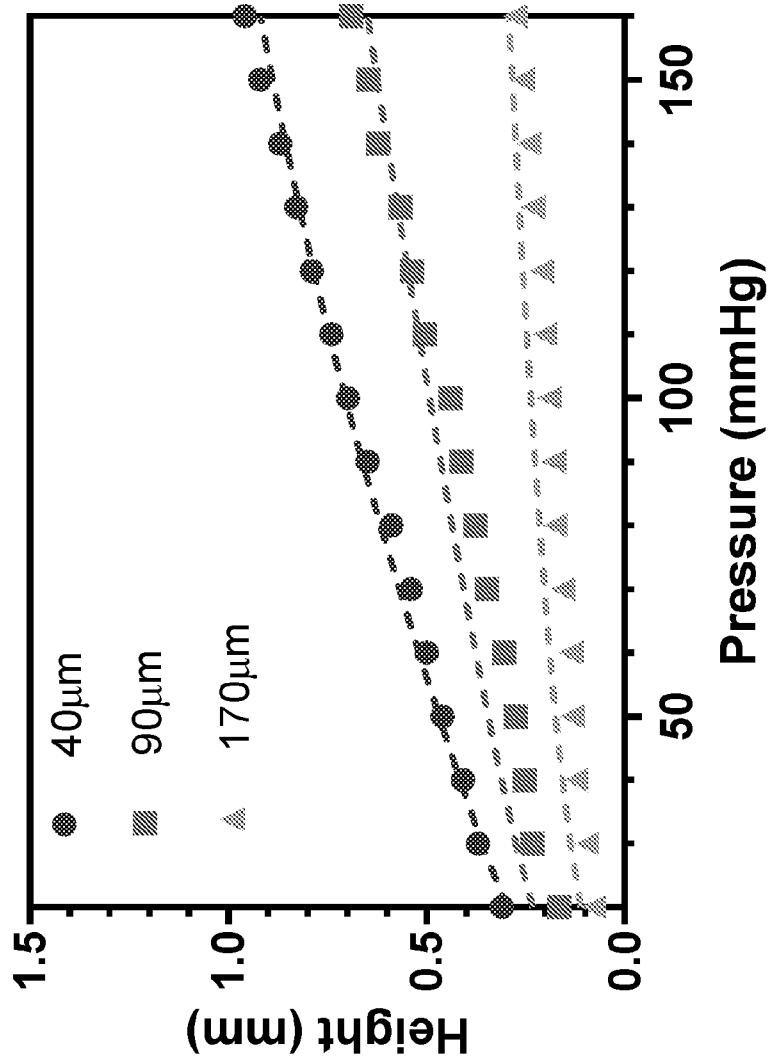


FIG. 3G

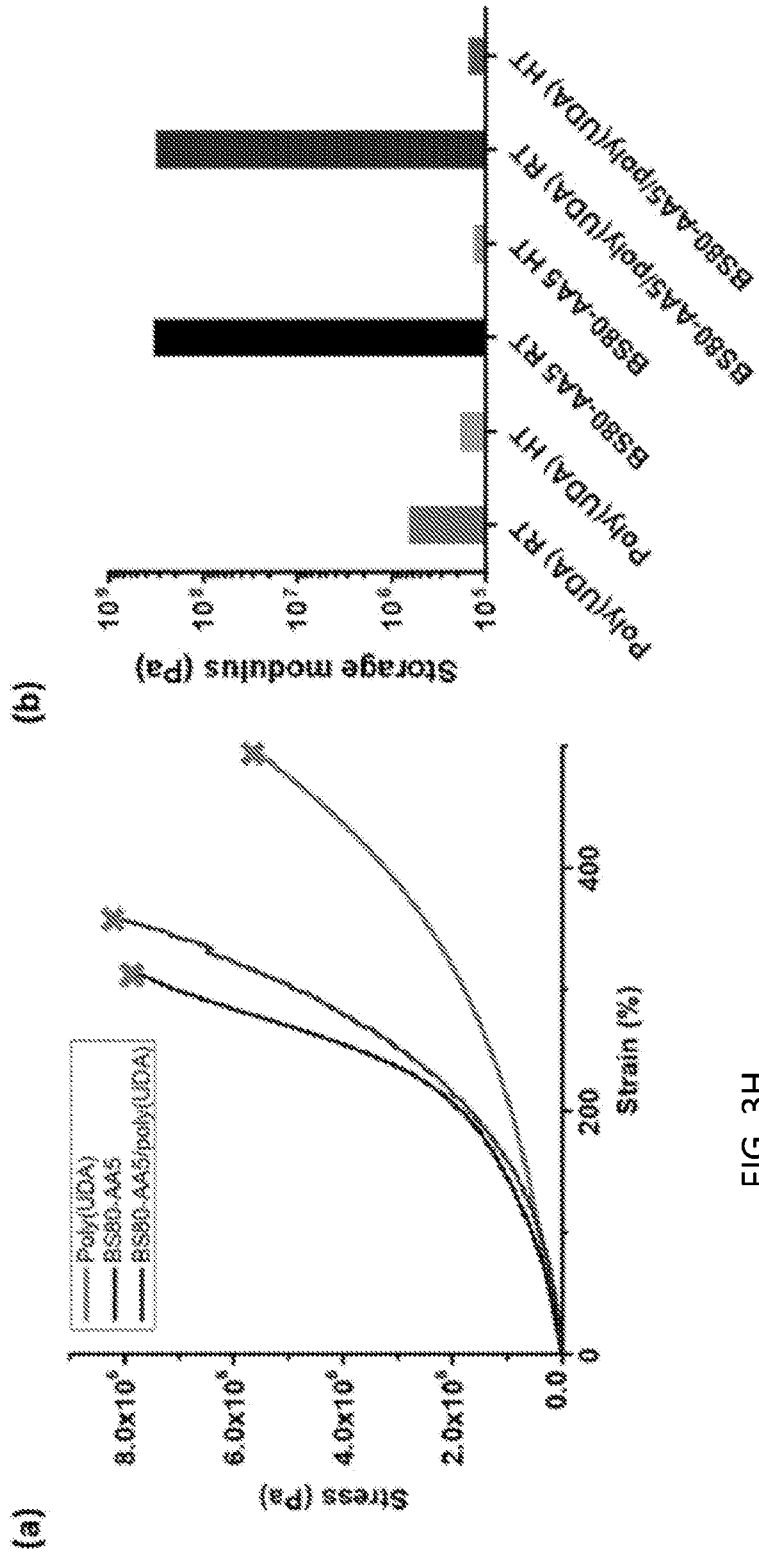


FIG. 3I

FIG. 3H

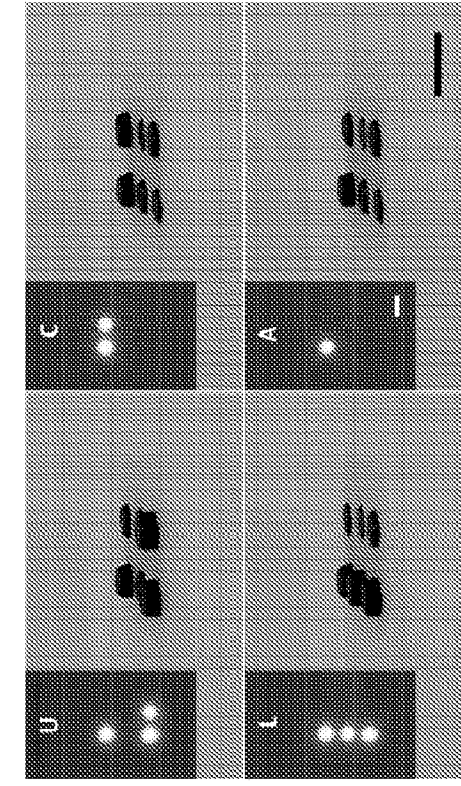
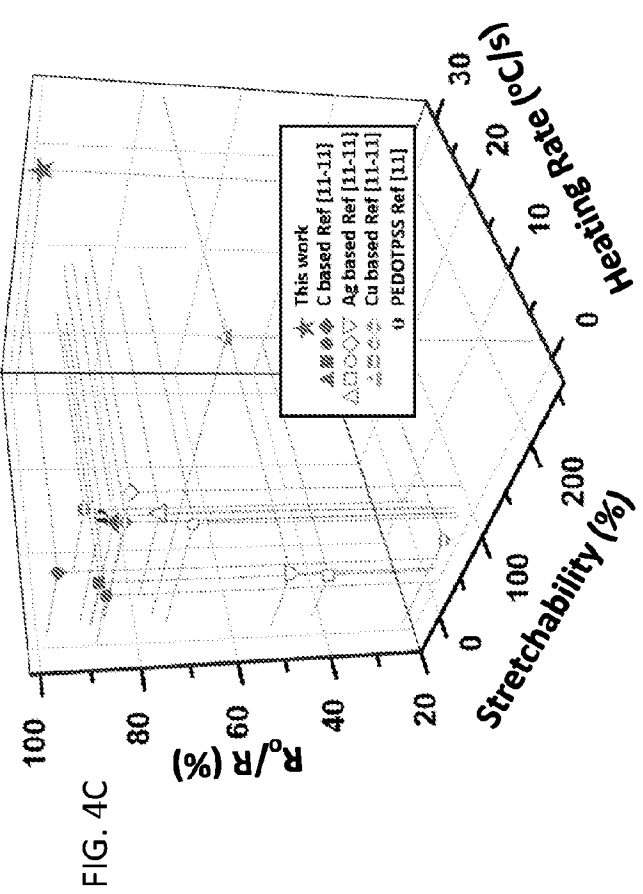
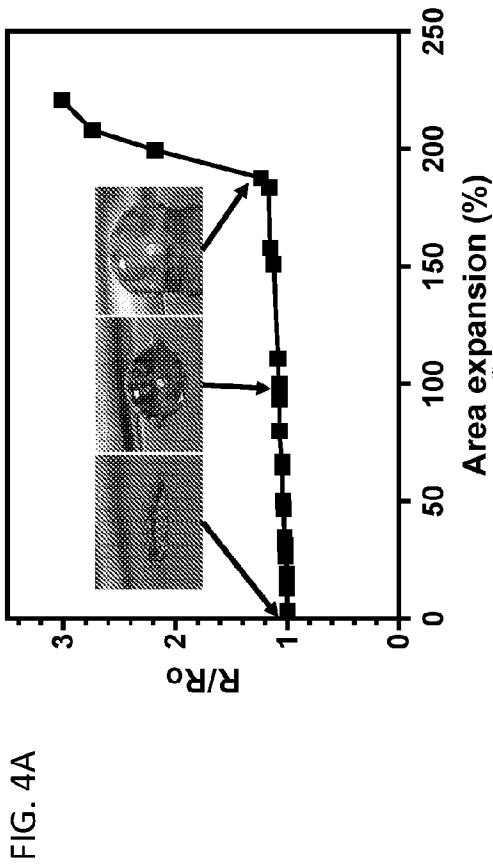
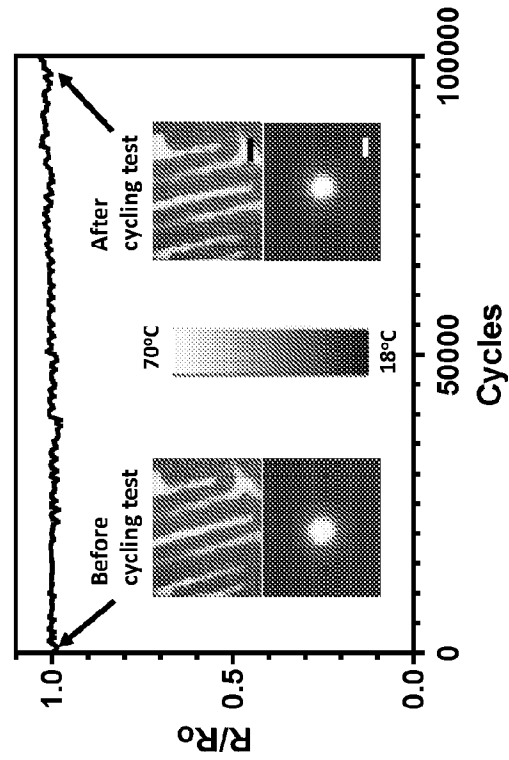


FIG. 4D

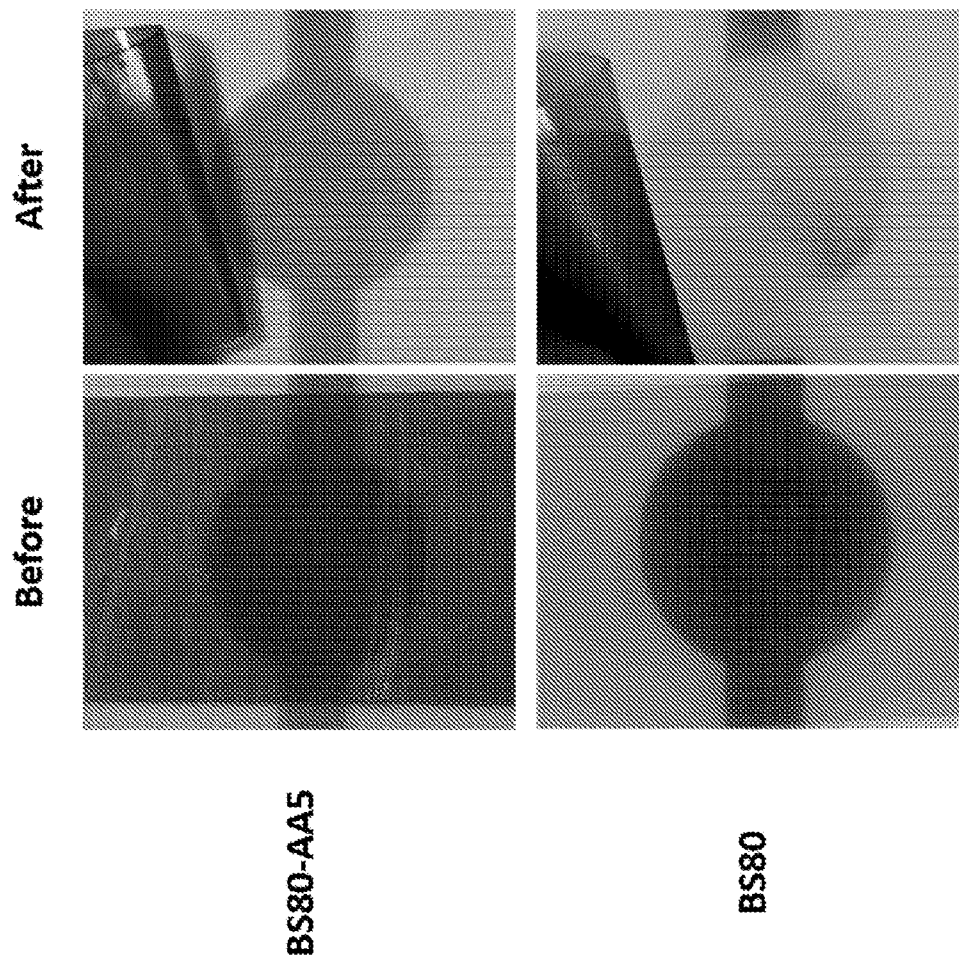


FIG. 4E

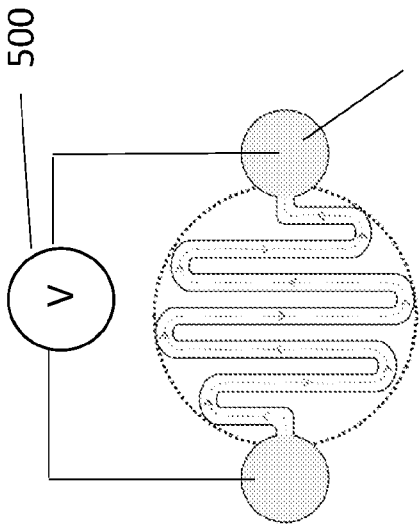


FIG. 5A

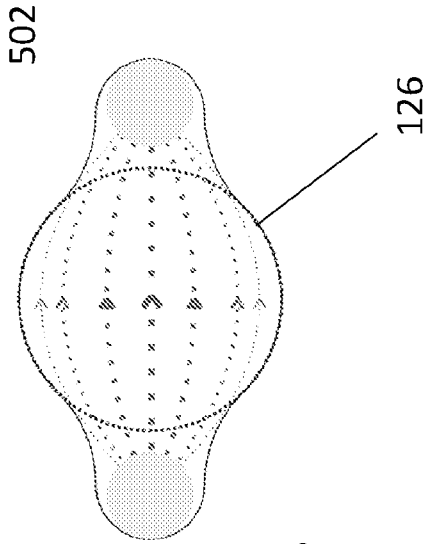


FIG. 5B



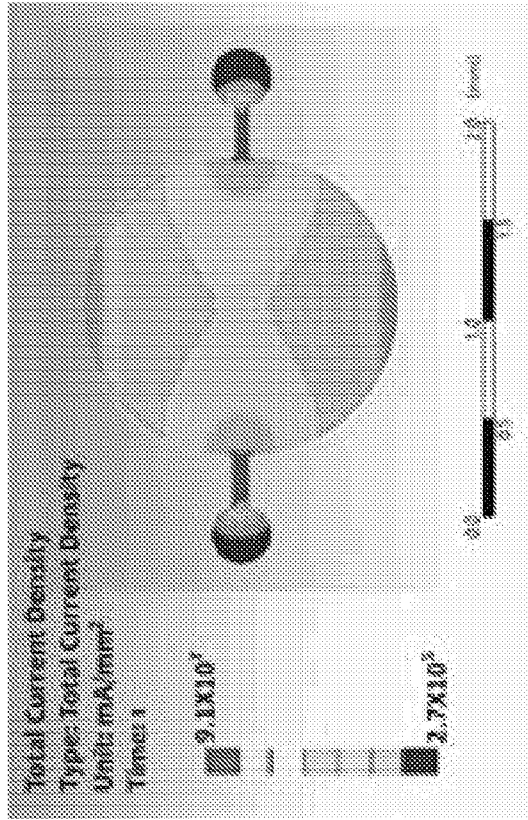


FIG. 5D

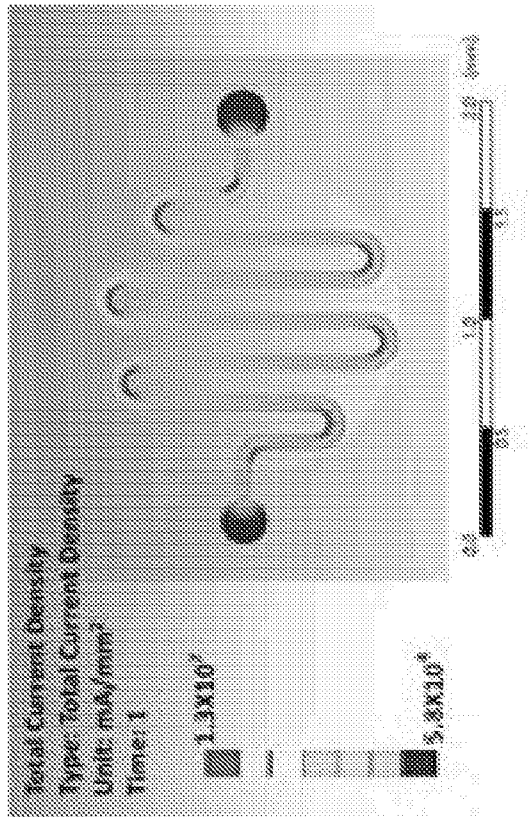


FIG. 5C

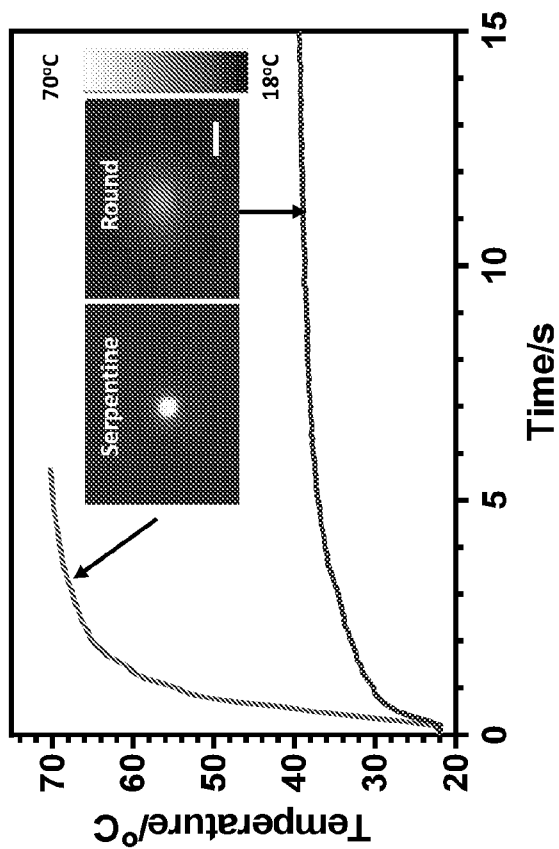


FIG. 5E

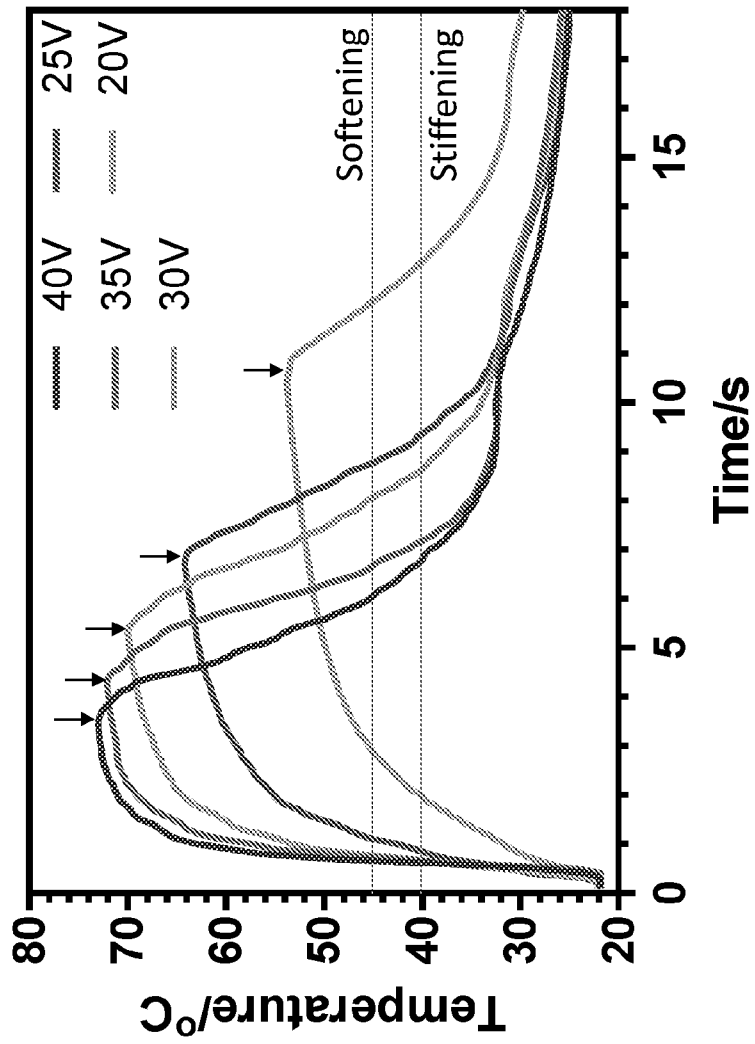


FIG. 6A

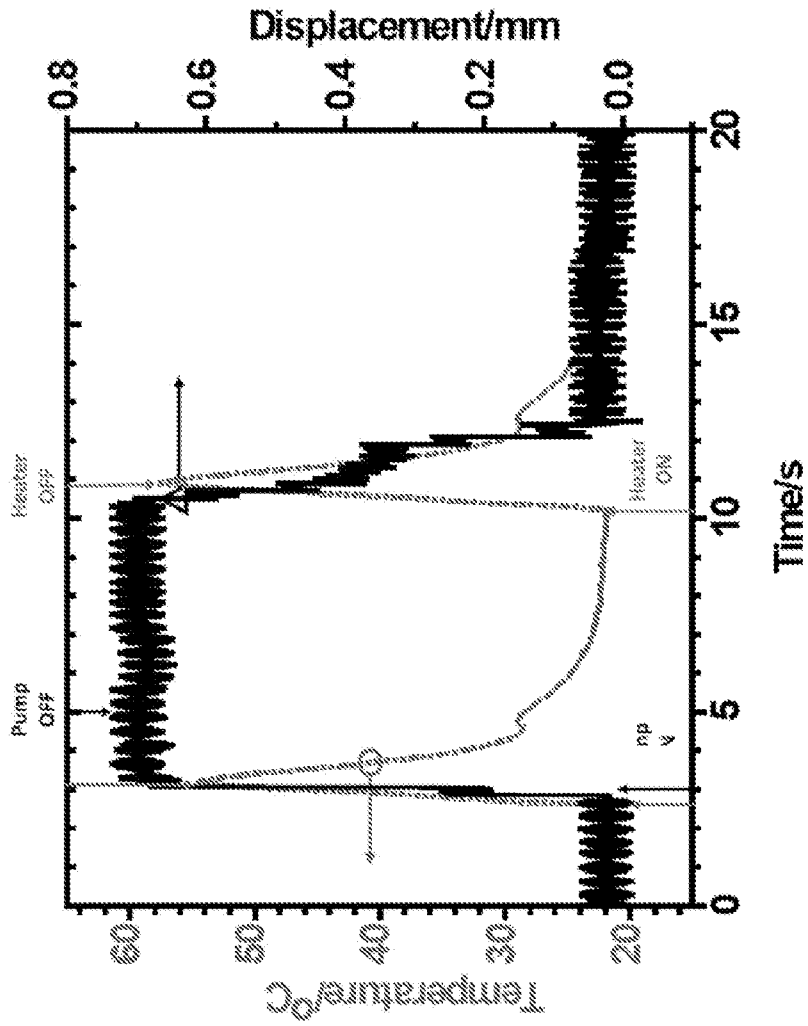


FIG. 6B

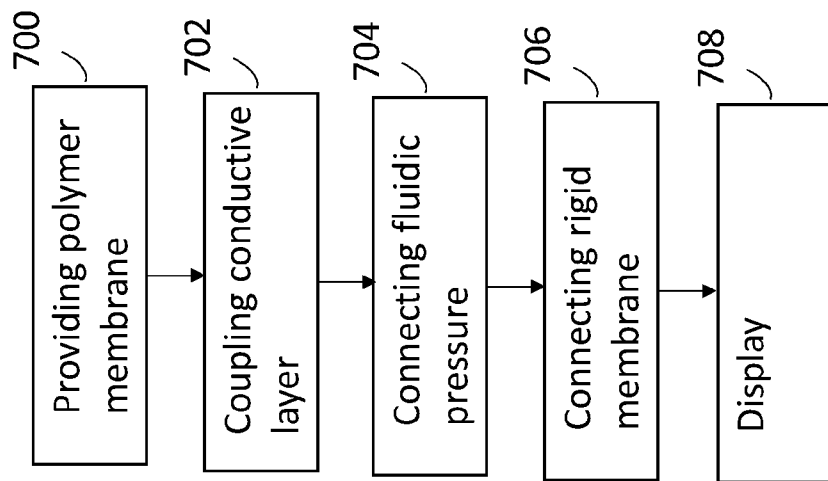


FIG. 7A

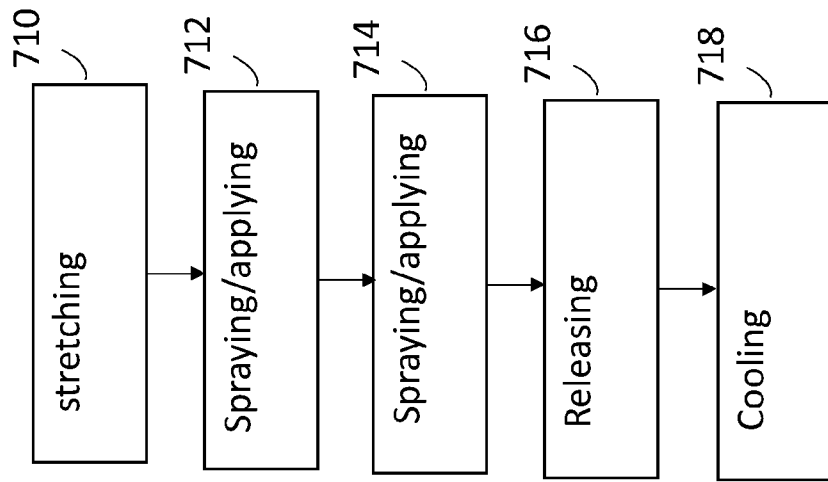


FIG. 7B

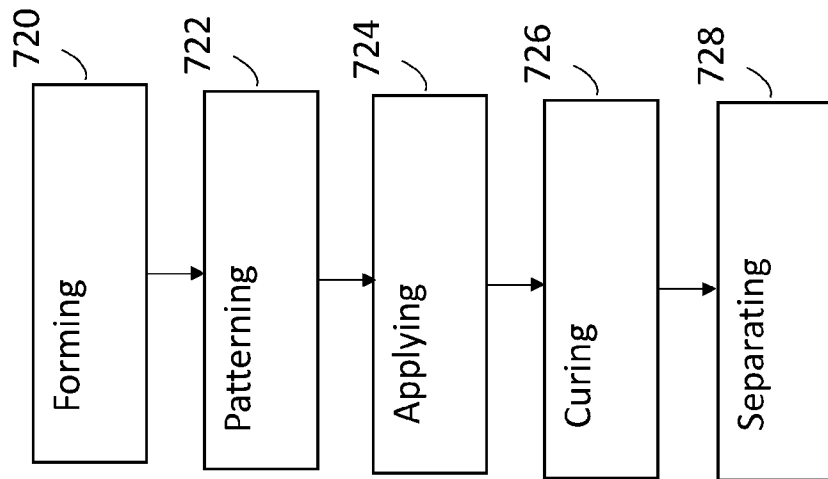


FIG. 7C

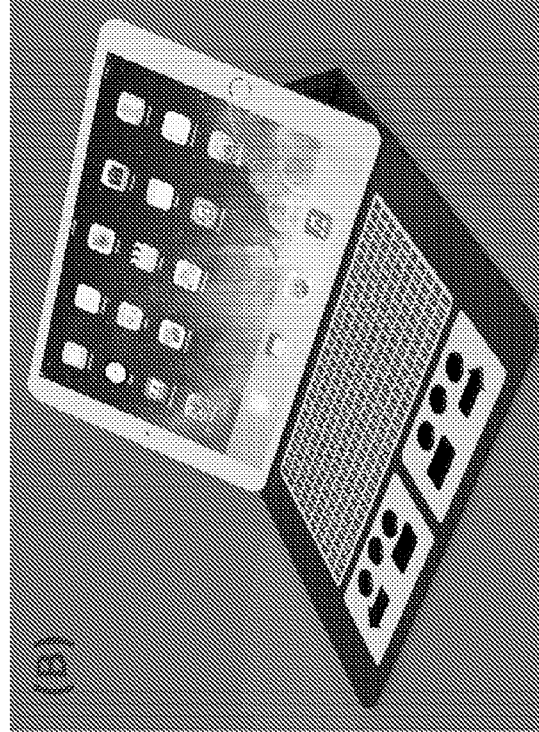


FIG. 8B



FIG. 8A

500



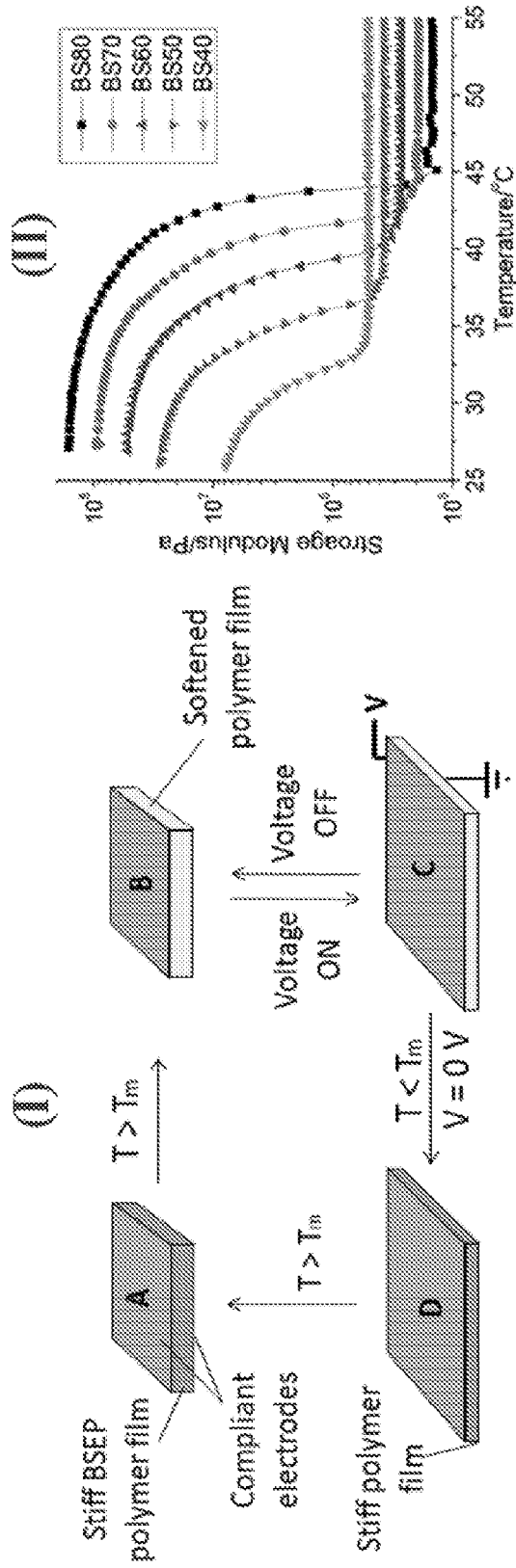


FIG. 9B

FIG. 9A

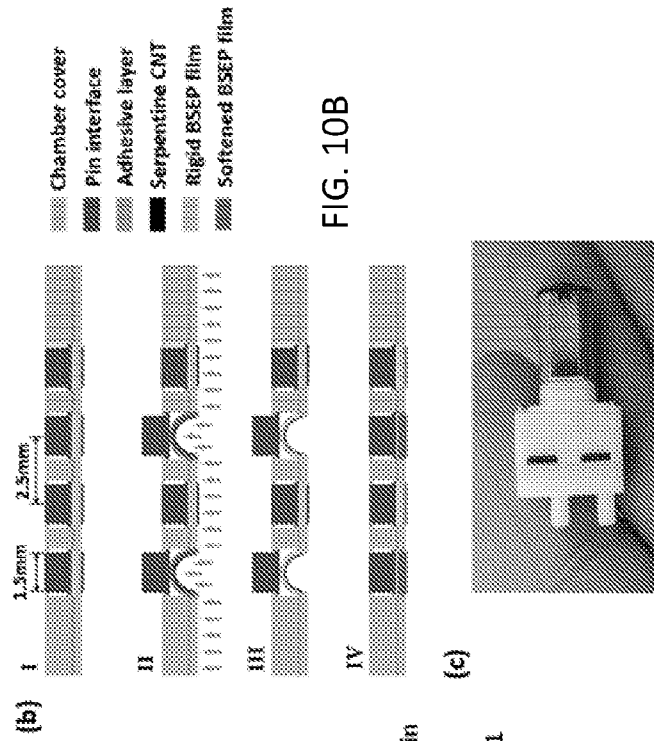


FIG. 10B

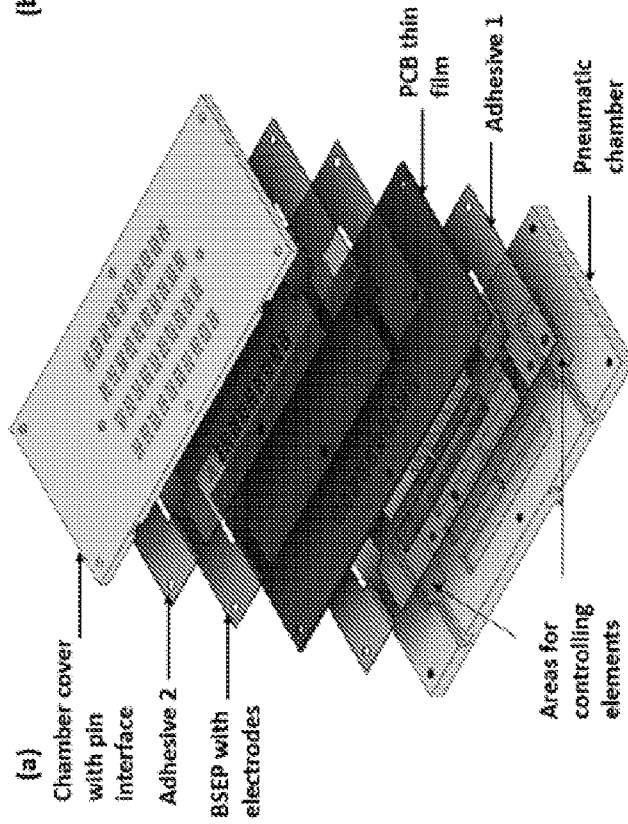


FIG. 10A

FIG. 10C

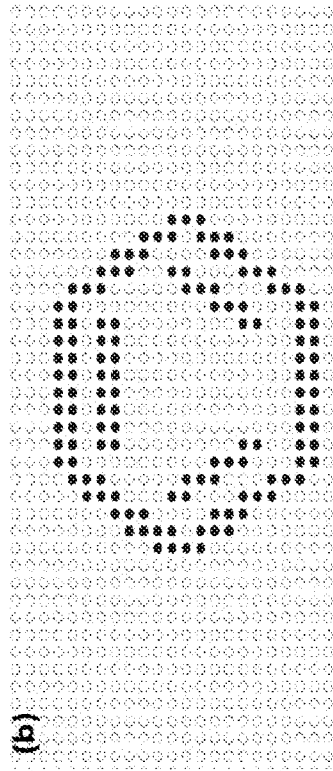


FIG. 11A

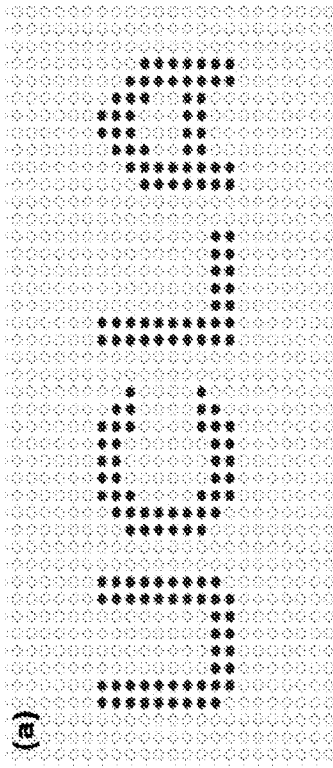


FIG. 11B

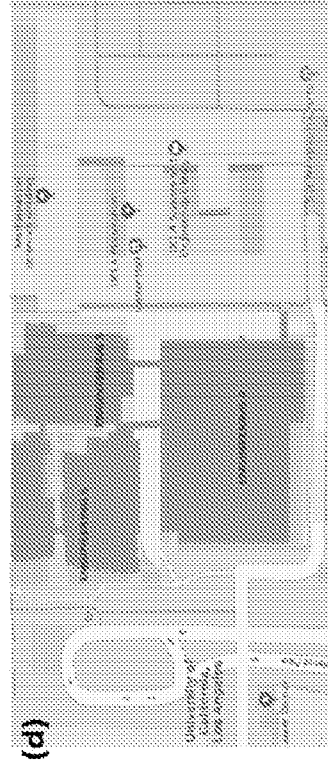


FIG. 11C

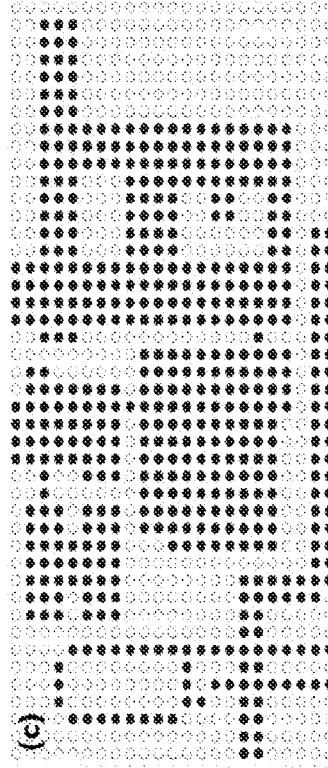


FIG. 11D

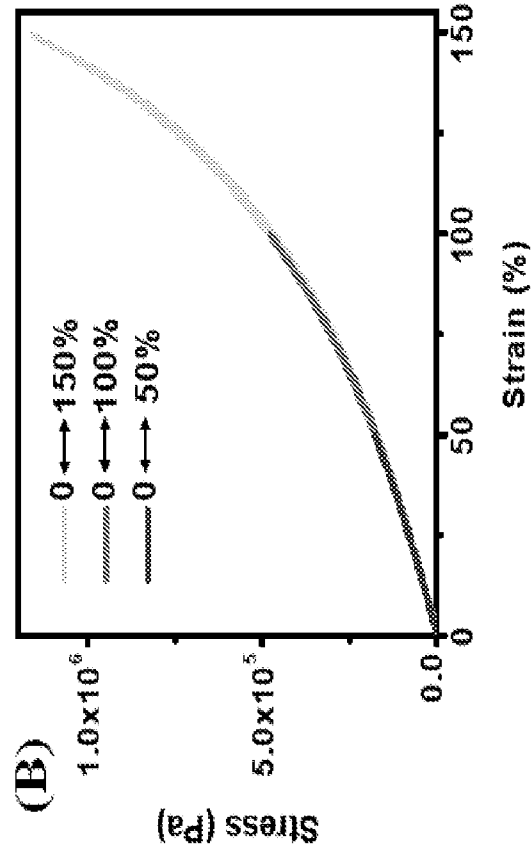


FIG. 12B

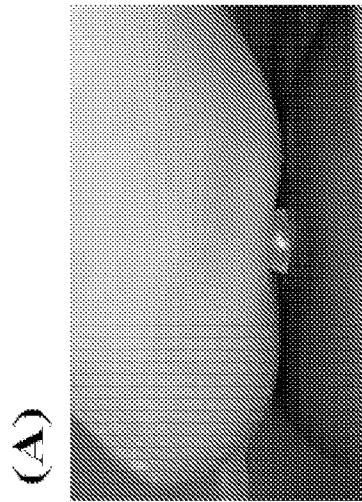


FIG. 12A

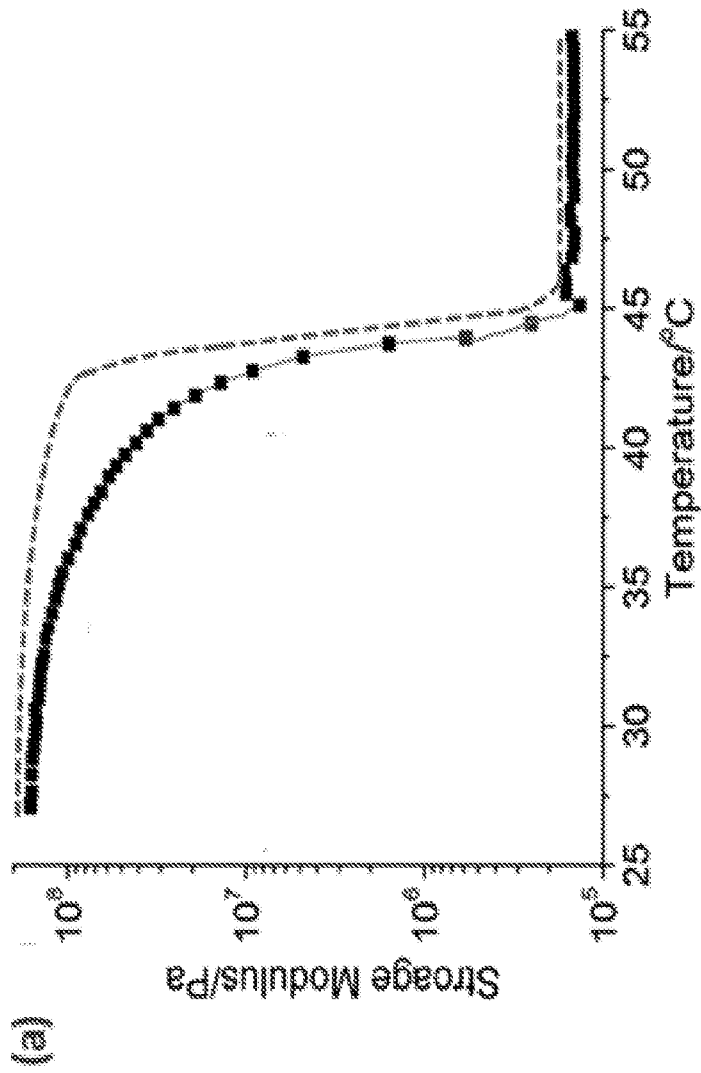


FIG. 13A



FIG. 13B

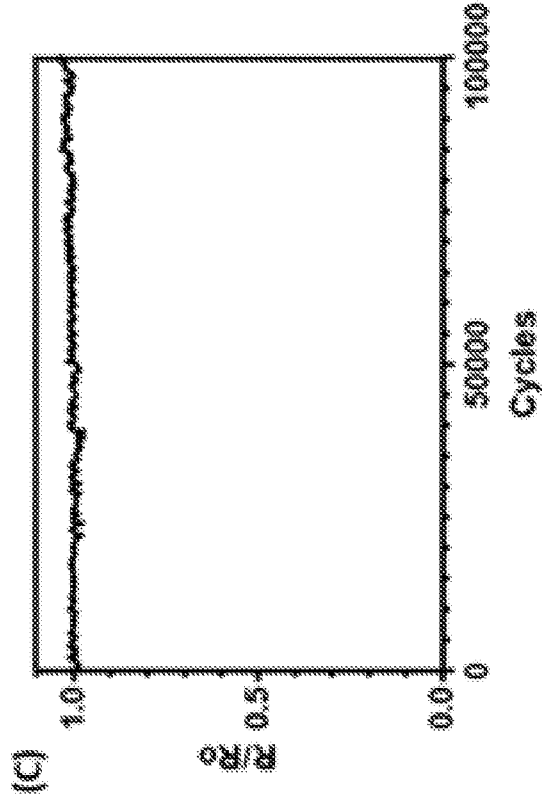
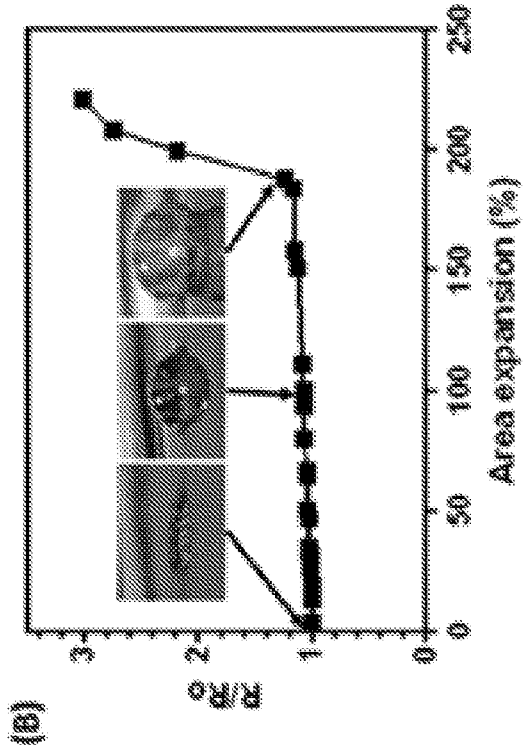
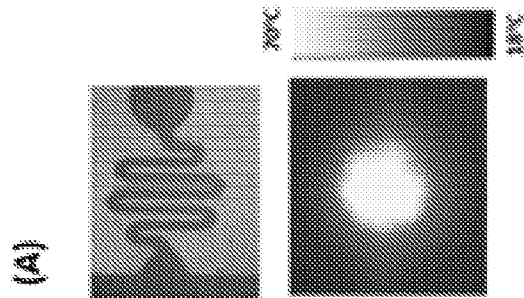


FIG. 14A

FIG. 14B

FIG. 14C

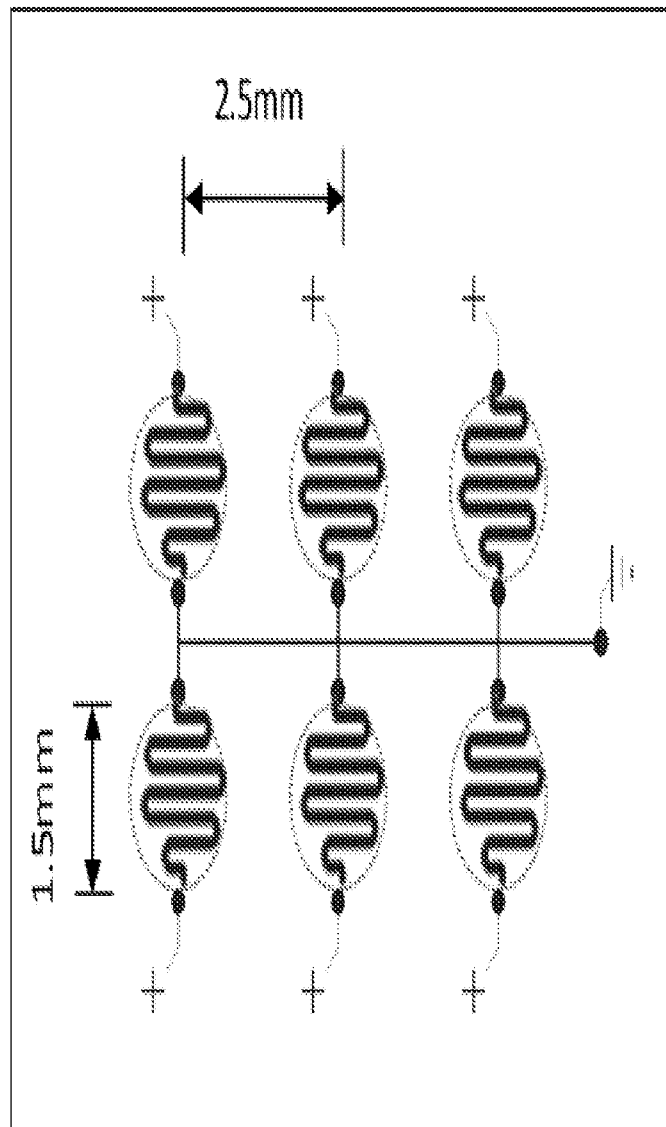


FIG. 15

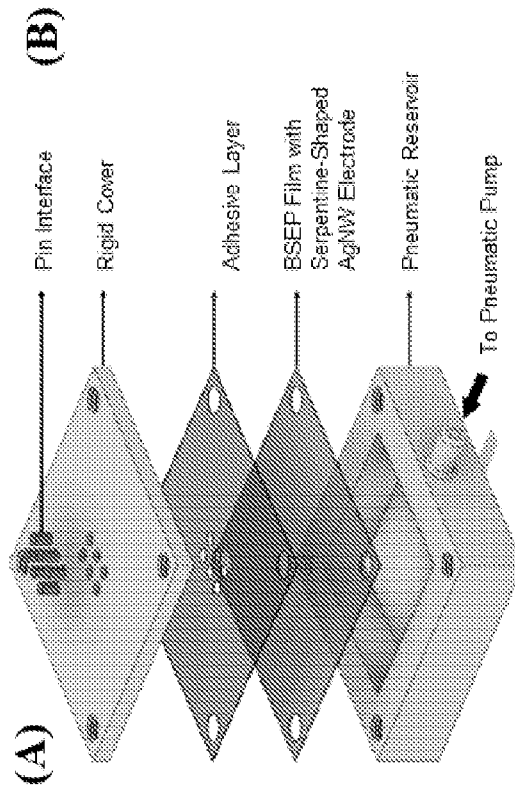


FIG. 16A

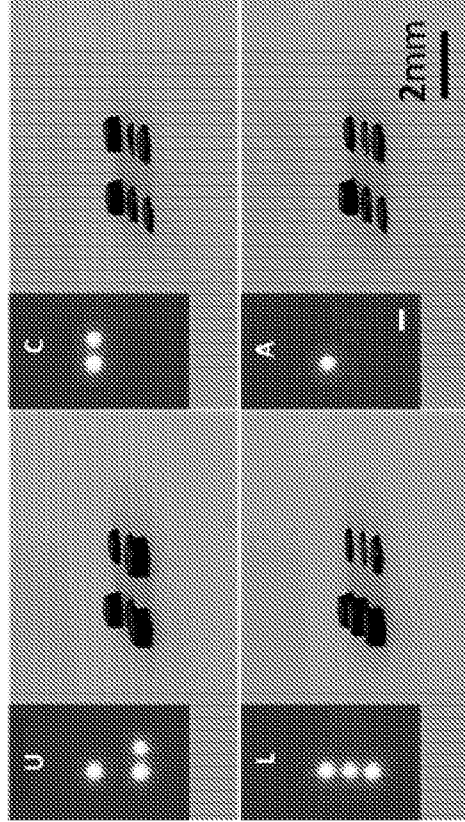


FIG. 16B



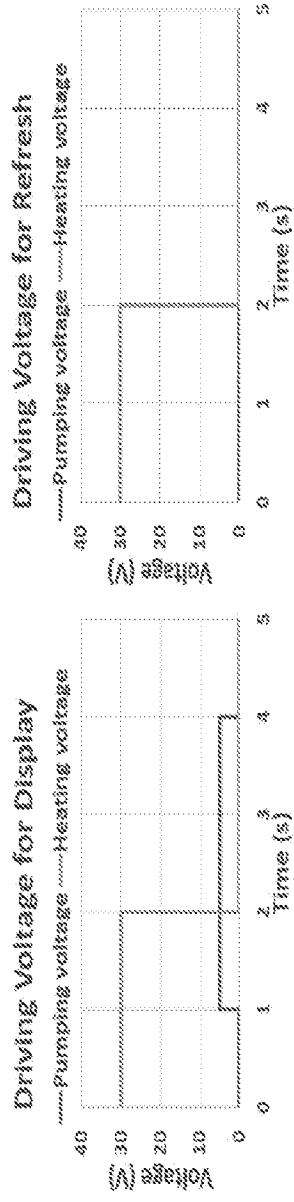


FIG. 17A

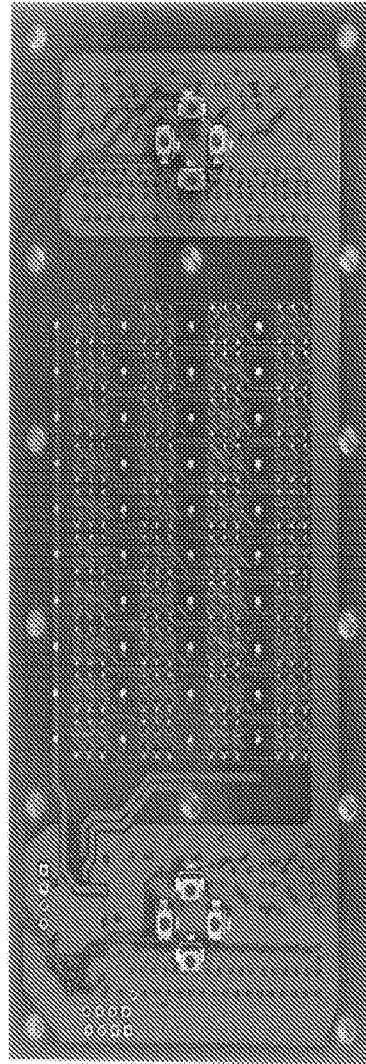


FIG. 17B

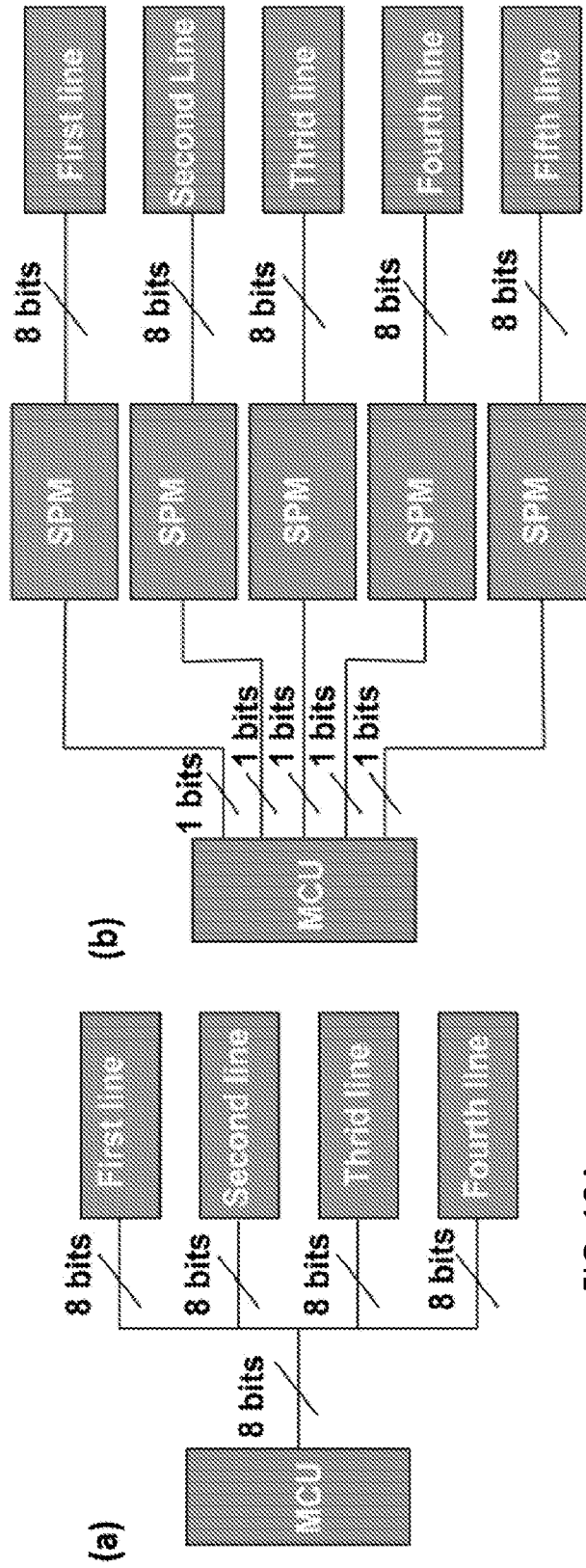


FIG. 18A

FIG. 18B